

UNIVERSIDAD NACIONAL AUTONOMA DE MEXICO

RECTOR
Dr. Jorge Carpizo

SECRETARIO GENERAL
Dr. José Narro Robles

SECRETARIO GENERAL ACADEMICO
Lic. Abelardo Villegas

SECRETARIO GENERAL ADMINISTRATIVO
C.P. José Romo Díaz

ABOGADO GENERAL
Lic. Manuel Barquín Alvarez

COORDINADOR DE LA
INVESTIGACION CIENTIFICA
Dr. José Sarukhán Kermez

INSTITUTO DE GEOLOGIA
Ciudad Universitaria
04510 México, D. F.

DIRECTOR
Dr. José C. Guerrero

EDITORA
Magdalena Alcayde

CO-EDITORES CIENTIFICOS
Dr. Zoltan de Cserna Dr. Fernando Ortega-Gutiérrez



26 ENE 2012

ISSN 0185-5530

UNIVERSIDAD NACIONAL AUTONOMA DE MEXICO

INSTITUTO DE GEOLOGIA

Boletín 102



CONTRIBUTIONS TO THE STRATIGRAPHY OF THE
SIERRA MADRE LIMESTONE (CRETACEOUS)
OF CHIAPAS

Part 1. Physical stratigraphy and petrology of the Cretaceous
Sierra Madre Limestone, west-central Chiapas

by

DAVID R. STEELE

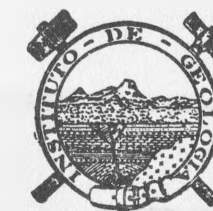
26 ENE 2012

Part 2. Biostratigraphy and paleoenvironmental analysis of
the Sierra Madre Limestone (Cretaceous), Chiapas

by

LOWELL E. WAITE

Studies completed within the framework of an agreement for
mutual scientific collaboration with the University of Texas
at Arlington



MEXICO, D. F.
1985 (1986)

CONTENTS

	<i>Page</i>
Presentación	v
Presentation	vi
Part 1. Physical stratigraphy and petrology of the Cretaceous Sierra Madre Limestone, west-central Chiapas, by <i>David R. Steele</i>	1
Part 2. Biostratigraphy and paleoenvironmental analysis of the Sierra Madre Limestone (Cretaceous, Chiapas, by <i>Lowell E. Waite</i>	103

DR © 1985 Universidad Nacional Autónoma de México
Ciudad Universitaria, México, D. F.

Impreso y hecho en México
DIRECCION GENERAL DE PUBLICACIONES

ISSN 0185-5530

PRESENTACION

El presente número del Boletín del Instituto de Geología, de la Universidad Nacional Autónoma de México, contiene los resultados de dos proyectos de investigación, cada uno desarrollado como tesis para optar por el grado de Maestro en Ciencias en la Facultad de Postgrado de la Universidad de Texas en Arlington. Ambos estudios, que se complementan, versan sobre diversos aspectos de la estratigrafía de la potente secuencia carbonatada del Cretácico que aflora en Chiapas y es conocida como la Caliza Sierra Madre. Estas rocas han sido identificadas más al norte sólo en el subsuelo en pozos perforados por Petróleos Mexicanos, donde constituyen las rocas almacenadoras de la riqueza extraordinariamente alta de los hidrocarburos.

Los datos que se presentan servirán a los geólogos de PEMEX y de la Comisión Federal de Electricidad en sus quehaceres rutinarios como datos de referencia o de comparación, y a los científicos en los estudios tendientes a refinar y detallar el marco paleogeográfico y paleotectónico del sureste de México que, a su vez, pudieran contribuir en forma eficaz para la localización de otros blancos con fines económicos.

Al publicar estos estudios en nuestro Boletín, el Instituto de Geología presenta una vez más el testimonio de su interés en promover y apoyar proyectos de investigaciones científicas de alta calidad y difundir los resultados que se desarrollen sobre diversos temas de la geología de México, tanto de investigadores nacionales como extranjeros, para profundizar así en el conocimiento de la constitución geológica de nuestro país.

Ciudad Universitaria, D. F., 10 de diciembre de 1984

Dr. José C. Guerrero
Director del Instituto de Geología

Part 1

PHYSICAL STRATIGRAPHY AND PETROLOGY OF THE
CRETACEOUS SIERRA MADRE LIMESTONE,
WEST-CENTRAL CHIAPAS

by

DAVID R. STEELE

Shell Development Company
Houston, Texas

Study completed within the framework of an agreement for mutual scientific
collaboration of the University of Texas at Arlington with Instituto de Geología
of Universidad Nacional Autónoma de México

TABLE OF CONTENTS

	<i>Page</i>
SUMARIO	6
ABSTRACT	9
INTRODUCTION	10
Purpose and location of study	10
Methods of study	11
Acknowledgments	13
Geologic setting	13
Previous work	19

PRESENTATION

The present number of the Boletín del Instituto de Geología, of the Universidad Nacional Autónoma de México, contains the results of two research projects which were carried out as theses for obtaining the degree of Master of Science at the Faculty of the Graduate School of the University of Texas at Arlington. Both papers, which mutually complement each other, refer to different aspects of the stratigraphy of the thick Cretaceous carbonate sequence which crops out in Chiapas and is known as the Sierra Madre Limestone. These rocks, farther to the north have been identified only at subsurface in wells drilled by Petróleos Mexicanos where they form the reservoir rocks of the extraordinary wealth of hydrocarbons.

The data here presented would contribute to geologists of Petróleos Mexicanos and Comisión Federal de Electricidad in their daily routine work as reference or comparative material, and also to scientists in their studies aimed at the refining and detailing of the paleogeographic and paleotectonic framework of southeastern Mexico which, in turn, could also contribute in an expedite way to the locating of other targets of economic importance.

By publishing these studies in our Boletín, the Instituto de Geología once more attests its interest to promote and support high quality scientific research and to publish its results, which are carried out on different subjects of the geology of Mexico, either by national or foreign scientists in order to contribute to the advancement of the knowledge of the geological constitution of our country.

Ciudad Universitaria, D. F., December 10, 1984

Dr. José C. Guerrero
Director of Instituto de Geología

TABLE OF CONTENTS (continued)

	Page
DESCRIPTION OF LITHOFACIES	22
Unit 1: Dolomite and collapse breccia	22
Unit 2: Lime mudstone; dolomite; and miliolid, pellet and requieniid lime wackestone	25
Unit 3: Undescribed interval	25
Unit 4: Spicular lime mudstone to wackestone	26
Unit 5: Planktonic foraminifer-bearing mollusk fragment lime wackestone ...	26
Unit 6: Planktonic foraminifer lime mudstone to wackestone	26
Unit 7: Planktonic foraminifer-bearing oyster, mollusk fragment lime wackestone	27
Unit 8: Worn skeletal fragment, ooid lime grainstone	27
Unit 9: Lime mudstone; pellet lime packstone; and laminated lime mudstone	28
Unit 10: Undescribed interval	28
Unit 11: Pellet-intraclast lime packstone; radiolitid fragment lime packstone; and stromatolites	28
Unit 12: Planktonic foraminifer-bearing radiolitid and pellet lime wackestone ..	29
Unit 13: Pellet-intraclast lime packstone; radiolitid fragment lime packstone and stromatolites	29
Unit 14: Lime mudstone; miliolid and requieniid lime wackestone and stromatolites	30
Unit 15: Nodular mollusk lime wackestone and fossiliferous marl	31
Unit 16: Worn skeletal fragment, ooid lime grainstone	32
Unit 17: Lime mudstone and laminated lime mudstone	32
Unit 18: Radiolitid fragment lime packstone and wackestone; pellet-intraclast lime packstone; and stromatolites	32
Unit 19: Lime mudstone and pellet lime wackestone	33
Unit 20: Nodular <i>Dicyclina</i> bearing, pellet lime wackestone with planktonic foraminifers and chert nodules	34
Unit 21: Whole radiolitid, pellet lime wackestones and whole radiolitid biostromes	35
ENVIRONMENTAL INTERPRETATION OF LITHOFACIES	36
Dolomite and collapse breccia lithofacies: the hypersaline platform interior environment	39

TABLE OF CONTENTS (continued)

	Page
Lime mudstone; pellet, miliolid and requieniid rudist lime wackestone lithofacies: the platform interior lime mud environment	39
Lime mudstone and laminated lime mudstone lithofacies: the tidal mudflat environment	44
Worn skeletal fragment, ooid lime grainstone lithofacies: the ooid sand shoal environment	44
Radiolitid lime wackestone and packstone and pellet-intraclast lime packstone lithofacies: lagoonal environments	48
Planktonic foraminifer bearing nodular mollusk lime wackestone lithofacies: the open marine environment	55
Planktonic foraminifer lime mudstone lithofacies: the basinal open marine environment	57
GEOLOGIC INTERPRETATIONS OF SEQUENTIAL LITHOFACIES AND ENVIRONMENTS	58
CONCLUSIONS	65
REFERENCES CITED	66
APPENDIX. Thickness of unmeasured intervals as computed by the method of Mandelbaum and Sanford (1952)	71

ILLUSTRATIONS

FIGURE 1.—Geologic map of the study area in west-central Chiapas with the localities of measured sections and sampling localities	12
—— 2.—Outcrop pattern and distribution of the depositional environments in the Sierra Madre Limestone and equivalent formations in southern Mexico and Guatemala	15
—— 3.—Stratigraphic relationships of formations in west-central Chiapas and Guatemala	16
—— 4.—Generalized graphic section of the Sierra Madre Limestone, west-central Chiapas	23
—— 5.—Generalized graphic section with lithofacies and depositional environments in the Sierra Madre Limestone, west-central Chiapas	37
—— 6.—Subenvironments interpretable on the basis of allochem composition, texture, grain size, and primary sedimentary structures in the ooid, worn skeletal fragment grainstone lithofacies represented by unit 16	46

ILLUSTRATIONS (continued)

	<i>Page</i>
—— 7.—Contrast in the distribution of depositional textures in representative units of open lagoonal deposits (units 12, 18) versus restricted lagoonal deposits (units 11, 13)	50
—— 8.—The three dimensional depositional model inferred from the succession of lithofacies in the Sierra Madre Limestone of west-central Chiapas	60
—— 9.—Illustration of the predictable and orderly time-transgressive succession of lithofacies and depositional environments interpreted from the lithologic units of the Sierra Madre Limestone composite measured section, west-central Chiapas	61
PLATE 1.—Map of field localities and composite measured section of the Sierra Madre Limestone, west-central Chiapas	in pocket
—— 2.—Field exposures and characteristic textures of the basal collapse breccia and dolomite lithofacies	74
—— 3.—Channel deposits and dolomite textures characteristic of the collapse breccia and dolomite facies	76
—— 4.—Algal stromatolites and sedimentary structures characteristic of the upper interval in the collapse breccia and dolomite lithofacies	78
—— 5.—Field exposures of section V and lithologic features characteristic of the lime mudstone, and pellet, miliolid, requieniid rudist lime wackestone lithofacies	80
—— 6.—Fenestral fabrics	82
—— 7.—Representative lithologic textures of unit 4 and the lime mudstone and laminated lime mudstone lithofacies	84
—— 8.—Fauna and lithologic textures of the planktonic foraminifer-bearing nodular mollusk lime wackestone lithofacies and planktonic foraminifer lime mudstone lithofacies	86
—— 9.—Textural features in the worn skeletal fragment, ooid lime grainstone lithofacies	88
—— 10.—Cementation fabrics and diagenetic features primarily in the worn skeletal fragment, ooid lime grainstone lithofacies	90
—— 11.—Textural features and fauna representative of the radiolitid lime wackestone and packstone and pellet-intraclast lime packstone lithofacies ...	92
—— 12.—Surface exposures of storm deposits and radiolitid thickets and clusters characteristic of the lagoonal environment and radiolitid lime wackestone and packstone and pellet intraclast lime packstone lithofacies	94

ILLUSTRATIONS (continued)

	<i>Page</i>
—— 13.—Algal stromatolites and associated supratidal early diagenetic features in the radiolitid lime wackestone and packstone and pellet-intraclast lime packstone lithofacies	96
—— 14.—Field exposures of sections XI and VI	98
—— 15.—Field exposures and depositional textures of unit 21 in section X and unit 19 in section XI	100

SUMARIO

La Caliza Sierra Madre, tal como fue medida y descrita en el área del presente estudio al surponiente de Ocozucua en la parte centro-occidental del Estado de Chiapas, tiene 2,575 m¹ de espesor y una edad albiano-santoniana pudiendo, sin embargo, extenderse su límite inferior en forma discutible hasta el Barremiano. La sección estratigráfica compuesta y medida se dividió en 21 unidades correspondientes a ocho litofacies cíclicas mayores. Esta secuencia representa por lo menos cuatro períodos de acumulación prolongada sobre una plataforma, interrumpidos por tres períodos cortos de inundación marina. Las inundaciones marinas tuvieron lugar durante el Cenomaniano medio, Cenomaniano tardío y Coniaciano.

Las ocho litofacies mayores identificadas en las 19 unidades litológicas descritas (no se tuvo acceso a las unidades 3 y 10, o estuvieron cubiertas por lo que no fueron descritas), junto con los ambientes interpretados de depósito, son los siguientes: la litofacies de dolomita y brecha de colapso, representando el ambiente de la parte interna hipersalina de la plataforma (unidad 1); la litofacies de *lime mudstone* y *lime wackestone* de pellas y miliólidos y la litofacies de requiñidos (unidades 2 y 14), representando la parte interna de la plataforma; la litofacies de *lime mudstone* y de *lime mudstone* de estructura laminar (unidades 9 y 17), representando el ambiente de llanura fangosa de intermareas; la litofacies de *grainstone* de ooides y fragmentos esqueléticos abrasionados (unidades 8 y 16), representando el ambiente de banco arenoso ooidal; la litofacies de *lime packstone* de pellas e intraclastos y de *lime packstone* de radiolíticos (unidades 11 y 13), representando el ambiente lagunar interno restringido; la litofacies de *lime mudstone-wackestone* de foraminíferos planctónicos y de *lime packstone* de radiolíticos (unidades 12, 18, 19 y 21), representando el ambiente lagunar interno abierto; la litofacies de *lime wackestone* nodular de foraminíferos planctónicos y moluscos (unidades 5, 7, 15 y 20), representando el ambiente de una plataforma marina abierta; y la litofacies de *lime mudstone-wackestone* de foraminíferos planctónicos (unidad 6), representando el ambiente de una cuenca desarrollada sobre una plataforma marina abierta y profunda.

La parte basal de la Caliza Sierra Madre comprende una secuencia transgresiva del Barremiano(?) - Albiano, formada por la litofacies (unidad 1) de dolomita y brecha de colapso, que está cubierta por la litofacies (unidad 2) parcialmente dolomitizada de *lime mudstones* y *wackestones* de pellas, miliólidos y requiñidos. Las brechas de colapso de la unidad 1 indican la presencia antaño de evaporitas y se cree que sobreyacen concordantemente a la Formación San Ricardo, implicando una edad barremiana. Sin embargo, Castro-Mora y colaboradores (1975) abogan en favor de una edad albiana para la parte basal de la Caliza Sierra Madre, implicando así la falta de los estratos aptianos y barremianos por discordancia.

Las brechas de colapso por disolución de las evaporitas, la estructura fenestral estromatolítica, las laminaciones finas y las superficies de disecación y canales de

¹ Ver nota de pie en la p. 11.

intermareas con remanentes de litoclastos y de gasterópodos indican un depósito que se efectuó principalmente en ambientes someros de sub o supramareas en la parte interna hipersalina de la plataforma. Se destaca la presencia de dos generaciones primarias de dolomita. La dolomita finamente cristalina se presenta principalmente asociada con rasgos de depósito de intermarea y supramarea y está interpretada como penecontemporánea. Se considera que la dolomita de cristalinidad gruesa, textura sucrosica y aspecto pervasivo con mosaicos cristalinos anhedrales y rombos euhedrales con zoneamiento, se formó durante la diagénesis tardía como resultado probable de sepultamiento profundo.

La litofacies de *lime mudstone* y *wackestone* de pellas, miliólidos y requiñidos se acumuló en un ambiente de baja energía en la parte interna de la plataforma, siendo probablemente parcialmente equivalente al ambiente de la parte interna hipersalina de la plataforma. Esta litofacies, que sobreyace a la litofacies de dolomita, indica una transgresión albiana.

La unidad 3 representa una falta importante en la sección medida entre dos localidades en el campo. Los estudios recientes de Guillermo Moreno, estudiante de postgrado de la Universidad de Texas en Arlington, indican que las estimaciones previas en cuanto al espesor de este intervalo no medido han sido muy bajas, ya que la sección medida compuesta alcanza los 3,450 m. Tiene importancia también la presencia de un intervalo marino abierto debajo del Cenomaniano medio.

La inundación marina del Cenomaniano medio está representada por la litofacies de *lime wackestone* nodular de foraminíferos planctónicos y moluscos (unidades 5 y 7). Un conjunto abundante y diverso de pelecípodos, gasterópodos, ostras, algas rojas y fragmentos de equinoides, dentro de una matriz de pellas, calciesferas y foraminíferos planctónicos, indica condiciones de plataforma abierta. La estratificación nodular es resultado de bioturbación completa.

La litofacies de *lime mudstone* de foraminíferos planctónicos (unidad 6) se depositó durante la transgresión máxima del Cenomaniano medio en aguas con profundidades mayores a los 100 m. La ausencia de macrofósiles y la conservación de la laminación indican actividad bentónica mínima durante ese evento.

Estos estratos de mar abierto sobreyacen en forma abrupta la litofacies de *lime mudstone* con miliólidos, pellas, espículas de esponjas extraordinariamente abundantes y fenestras tubulares rellenas de calcita espática (unidad 4). En ausencia de otros indicadores batimétricos, este conjunto probablemente indica una acumulación en el ambiente lagunar interno.

Un borde de plataforma de relieve bajo progradó rápidamente a través de la plataforma inundada, a medida que las profundidades del agua se volvían más someras y se incrementaba la producción de carbonatos. El borde progradacional de la plataforma está representado por la litofacies de *grainstone* de ooides y fragmentos esqueléticos abrasionados (unidad 8). La secuencia en esta litofacies es característica de los ambientes de bancos arenosos. Las *packstones* altamente bioturbadas y formadas por fragmentos esqueléticos de corales, radiolíticos, moluscos y equinoides permiten definir el ambiente como de banco situado a barlovento. Las *grainstones* con diastratificación en canal definen una faja arenosa móvil, mientras que las *packstones* formadas por ooides, *grapestones* y por gasterópodos cubiertos oncolíticamente representan el ambiente de la llanura arenosa estabilizada hacia el sotavento.

La litofacies de *lime mudstone* y de *lime mudstone* de estructura laminar (unidad 9) sobreyace a la litofacies de *grainstone* y representa el ambiente de llanura fangosa de intermareas, detrás del complejo del banco arenoso. Su fauna está formada principalmente por ostrácodos, oncolitos de gasterópodos y estromatolitos.

La unidad 10 corresponde a un intervalo de 25 m de espesor, que no fue descrito por falta de acceso, localizado entre dos caminamientos de afloramientos continuos.

Las litofacies de *lime packstone* de pellas e intraclastos y de *lime wackestone* y *packstone* de radiolíticos (unidades 11, 12 y 13) representan el depósito en el ambiente de laguna amplia dentro de la secuencia progradacional, que se encontraba detrás del complejo formado por el banco ooidal y la llanura fangosa. La unidad 12 fue reconocida como tal por la predominancia de las texturas de *wackestone* y por la presencia común de foraminíferos planctónicos, habiendo indicadores de la presencia de aguas ligeramente más profundas y con mejor circulación.

Estos estratos lagunares representan las litofacies más características de la Caliza Sierra Madre en la región de Ocozocuautila. Los radiolíticos, que constituyen la fauna dominante, se encuentran raras veces en posición de crecimiento. Se presentan típicamente en estratos que poseen laminación burda con la disminución de su granulometría hacia arriba; sus bases muestran los efectos de acarreo por las tempestades de antaño. La presencia de estromatolitos, así como la micritización eminente y las incrustaciones por algas azul-verdes y rojas indican que la laguna tenía aguas muy someras.

La sección medida de afloramientos continuos se interrumpió al llegar a un anticlinal modificado por una cabalgadura, cuyo flanco meridional es vertical mientras que el septentrional está ligeramente inclinado. Así, la sección medida continuó junto al eje de este anticlinal, siguiendo hacia abajo sobre el flanco septentrional, estimándose que sólo muy poco de la secuencia quedó así perdido.

La secuencia de las unidades 14 a la 18 inclusive encima de la cabalgadura es muy semejante a las unidades 4 a la 13 inclusive debajo de la cabalgadura. Encima de la cabalgadura, la litofacies de la plataforma interna formada por miliólidos, pellas y requiñidos está cubierta por la litofacies de mar abierto de *lime wackestone* nodular y marga con foraminíferos planctónicos y moluscos (unidad 15). La fauna variada y particularmente los abundantes pelecípodos, gasterópodos, equinoides irregulares y foraminíferos planctónicos, que están muy bien conservados en la unidad 15, la colocan en la Zona de *Rotalipora cushmani* del Cenomaniano superior. Una secuencia completa de plataforma progradacional sobreyace los estratos de mar abierto. Esta secuencia progradacional está formada en su base por *lime grainstones* de ooides y fragmentos esqueletales abrasionados (unidad 16), por *lime mudstones* de llanura fangosa de intermareas y *lime mudstones* dolomíticas con estructura laminar (unidad 17), *lime packstones* de pellas e intraclastos y *lime packstones* y *wackestones* de radiolíticos (unidad 18) y *lime mudstone* de pellas y *wackestone* de la parte interna de la plataforma (unidad 18).

El estudio paleontológico de las muestras no pudo establecer la diferencia en tiempo que pudiera existir entre los dos conjuntos de microfauna casi idénticos de los intervalos de mar abierto de las unidades 5 al 17 y de la unidad 15. A pesar de que se consideran las semejanzas de espesores, de la fauna y de la secuencia litológica que fueron controladas por los procesos de depósito, existe la posibilidad de que las unidades 14 al 18 en

parte representen la repetición por cabalgamiento de la sección formada por las unidades 4 al 13.

El proceso de progradación de la plataforma estable y el depósito continuaron durante el Turoniano, después de la transgresión del Cenomaniano tardío. Durante el final del Turoniano o el Coniaciano la plataforma carbonatada fue inundada de nuevo. Este intervalo de mar abierto se caracteriza también por la litofacies de *lime wackestone* nodular de foraminíferos planctónicos y moluscos (unidad 20). Son particularmente abundantes en esta litofacies las calciesferas, los nódulos de pedernal azul y el foraminífero bentónico grande, *Dicyclina schlumbergeri*.

Las *lime wackestones* nodulares de mar abierto de la unidad 20 cambian hacia arriba en estratos más masivos de *lime wackestones* de pellas con grandes radiolíticos enteros (unidad 21). En contraste con los radiolíticos pequeños retrabajados del ambiente lagunar, estos radiolíticos son miembros grandes y robustos de la Subfamilia Sauvagesiinae y se presentan en asociaciones sueltas o en grupos en posición de crecimiento, a los que rodean abundantes escombros de rudistas. Tanto la transición gradacional entre las unidades 20 y 21, como la ausencia de una litofacies de *grainstone* de ooides y un conjunto mezclado de faunas de aguas someras y abiertas indican más bien que el depósito se efectuó sobre un perfil de rampa y no sobre un perfil de plataforma carbonatada de alta energía.

ABSTRACT

A 2,575¹ m thick composite stratigraphic section of the Sierra Madre Limestone was measured southwest of Ocozocuautila, Chiapas. The formation is believed to be Neocomian to Santonian in age although biostratigraphic control is poor. Eight major lithofacies were identified representing four periods of carbonate platform deposition interrupted by three major marine inundations. The lithofacies occur in predictable vertical stratigraphic sequences interpretable as facies tracts of analogous modern environments. The lithofacies represent deposition in a hypersaline evaporite platform interior, carbonate platform interior, open interior lagoon, restricted interior lagoon, tidal mudflat, ooid sand shoal, open marine, and basinal open marine environments.

The dolomite and collapse breccia lithofacies represents deposition in a hypersaline platform interior environment. Collapse breccias indicate the former presence of evaporites. Petrographic evidence and field relationships indicate two primary generations of dolomite. Finely crystalline dolomite associated with the former evaporites is interpreted as penecontemporaneous. Coarsely-crystalline sucrosic dolomite exhibiting anhedral crystalline mosaics and zones of euhedral rhombs is interpreted as the result of pervasive deep burial dolomitization. The unit is believed to conformably overlie the San Ricardo Formation although stratigraphic and faunal evidence is inconclusive.

The lime mudstone, pellet, miliolid lime wackestone and requieniid lime wackestone lithofacies was deposited in a quiet, shallow, low energy platform interior environment. The environment was laterally equivalent to the hypersaline platform interior environment

¹ See foot note on p. 11.

and was also established subsequently following periods of rapid platform progradation after marine inundations.

The ooid and abraded skeletal fragment grainstone lithofacies was deposited in an ooid sand shoal environment marginal to the prograding platform edge. The ooids are small (less than 0.2 mm mean diameter) and exhibit radial rather than concentric layering. The structure implies a relatively low energy depositional environment for ooid formation possibly a result of diminished wave and current energy on the shallow open shelf. The shelf slope between the platform and the open marine environment was very gentle. A platform margin was established southwest of Ocozocuaula only during periods of tectonic instability or maximum global eustatic rises in sea level when the precipitous platform margin in the Reforma area was submerged.

Lime mudstones, requeniid wackestones and thinly-laminated dolomitic lime mudstones were deposited in a low energy sublittoral and tidal flat environment directly leeward of the ooid sand shoal complex. Desiccation features and birdseye structures are common. The rapid lithologic change reflects a rapid energy change resulting from early lithification in the ooid sand shoal complex which formed an effective although discontinuous barrier to open marine circulation.

The whole to fragmented radiolitic lime packstone to wackestone and pellet-intraclast lime packstone to wackestone lithofacies was deposited in a broad gently circulated interior lagoon environment seaward of the platform interior environment and leeward of the ooid sand shoal complex and tidal mud flat environments. Planktonic foraminifers and echinoids are characteristic of the lithofacies in areas of the lagoon with more direct contact with open marine circulation and normal marine salinity. Better circulation and salinity probably was the result of lateral discontinuities in the ooid sand shoal barrier. The restricted lagoon environment was characterized by the absence of planktonic foraminifers and echinoids. Thinly-laminated lime mudstones and stromatolites were deposited on supratidal exposures which restricted circulation in parts of the lagoon. Requeniid rudist lime wackestones are common in the restricted areas.

The fossiliferous marl and nodular mollusk lime wackestone lithofacies was deposited in the open marine shelf environment seaward of ooid sand shoal environment. Planktonic foraminifers, echinoids, calcispheres, and sponge spicules are common. An open marine shelf environment resulted when the carbonate platform submerged as a result of rapid rises in global sea level or rapid subsidence associated with tectonism and the influx of terrigenous clay. The carbonate platform was inundated during the mid-Cenomanian, late Cenomanian and Coniacian. The maximum inundation occurred during the mid-Cenomanian when the planktonic foraminifer lime mudstone to wackestone lithofacies was deposited in a basinal open marine environment.

INTRODUCTION

PURPOSE AND LOCATION OF STUDY

The purpose of the research reported herein was to document and interpret the shelf and carbonate platform facies sequences in the massive Cretaceous

Sierra Madre Limestone in west-central Chiapas, Mexico. This research represents the initial stages of a regional study undertaken by faculty members at the University of Texas at Arlington, within the framework of an agreement for mutual scientific collaboration with the Instituto de Geología, Universidad Nacional Autónoma de México, to understand Mesozoic tectonics and basin formation in southern Mexico. Localities in the area south and west of the town of Ocozocuaula were selected for compilation of the reference section because of their accessibility and relatively continuous exposure (Figure 1).

The field work and sample preparation for this study were accomplished as a cooperative project with fellow graduate student L. E. Waite from The University of Texas at Arlington. Waite (Part 2, this Boletín) describes the paleontology and biostratigraphy of the reference section. Hopefully, these publications will provide a firm basis for continuing research concerning the Cretaceous carbonate platform development in southern Mexico.

METHODS OF STUDY

Field work in the study area was conducted during 10 weeks of the summer of 1980. Much of the time was spent in obtaining maps and in reconnaissance of potential sections for measurement. Topographic maps and aerial photographs were generously supplied by the Comisión Federal de Electricidad and the Consejo de Recursos Minerales. The location of all sections measured is shown in Figure 1 and in Plate 1. A total of 10 of the 13 localities shown was used in constructing the 2,575 m thick composite measured section¹. A 384 m thick stratigraphic interval outcropping between areas A and B (Figure 1, Plate 1) was not described because of inaccessible exposures and poor exposures along Federal Highway 190. The thickness of the described section was measured using a Jacob staff and Brunton compass. The thickness of uniformly dipping strata in inaccessible areas was estimated by the method described by Mandelbaum and Sanford (1952). Samples were collected at regular 3 m intervals with additional lithologic and faunal samples taken as necessary. All 647 samples collected were slabbed, polished and etched with dilute hydrochloric acid. Thin sections were prepared from 489 of the samples. A petrographic description of slabs and thin sections combined with other

¹ Subsequent work in the area south of Río Venta and directly across the river from measured section X (Figure 1, Plate 1) by Guillermo Moreno (The University of Texas at Arlington graduate student) has demonstrated that the combined thickness of units 1, 2, and 3 (Figure 4, and Plate 1) is 2,140 m and not 1,286 m as estimated during the course of this investigation. Thus the total thickness of the Sierra Madre in this area would be 3,429 m.

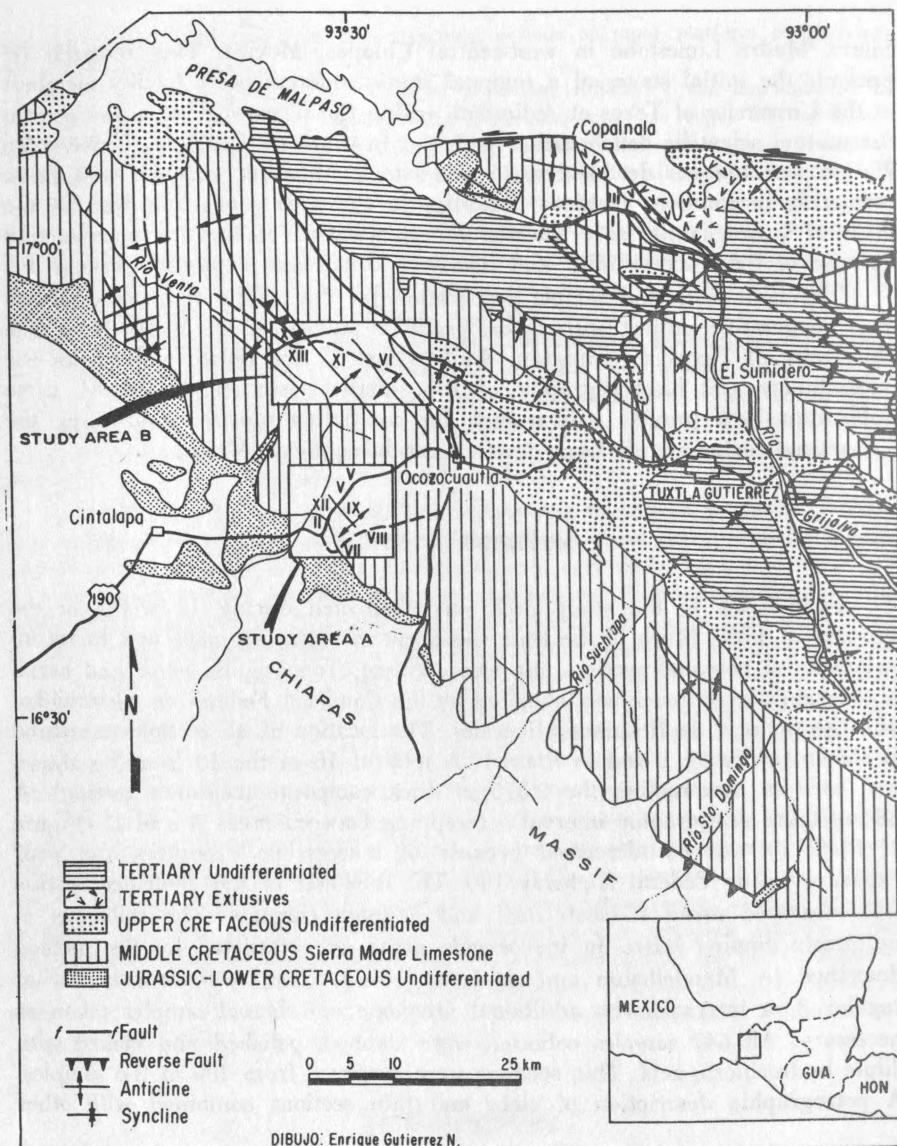


FIGURE 1.—Geologic map of study area in west-central Chiapas with the locations of measured sections and sampling localities (cf. Plate 1). Geology from López-Ramos (1975); reverse fault along the Chiapas massif from Moravec (1983).

depositional features is available in Appendix III of the author's (Steele, 1982) M. S. thesis. The thesis may be obtained from or consulted in the libraries of The University of Texas at Arlington or of the Instituto de Geología of the Universidad Nacional Autónoma de México in Mexico City. The classification of Dunham (1962, p. 117) was used to classify the samples according to their depositional texture. The percentage of the allochems in the samples was estimated using the "Charts for Estimating Particle Percentages" by Swanson (1981, 12.2-12.33). To determine the presence of dolomite, samples were stained with Alizarine Red as described by Friedman (1959). The residue from several washed marl samples from section XI, unit 15, was digested in dilute hydrochloric acid to examine the insoluble residue for noncarbonate minerals.

ACKNOWLEDGMENTS

This publication is the result of M. S. thesis research completed at The University of Texas at Arlington under the directions of Dr. C. I. Smith. The author wishes to express his appreciation to Dr. Smith and to the thesis committee members, Drs. Burke Burkart, B. F. Perkins and D. A. Kotila, for their assistance with the research and preparation of this manuscript.

Lowell E. Waite, fellow graduate student, field partner, and friend, equally contributed toward the completion of a measured section of the Sierra Madre Limestone and laboratory preparation of the 647 samples collected.

The writer is especially grateful for the assistance, field support, maps and aerial photographs generously offered by Ingenieros Luis Lozano and Jaime García of the Comisión Federal de Electricidad and Ing. Enrique Montesinos H., of the Consejo de Recursos Minerales. Special appreciation goes to Ing. José Luis Hernández-Bielma of the Comisión Federal de Electricidad for his friendship and personal assistance in the field.

The United States Geological Survey, through a grant to The University of Texas at Arlington financed the field, laboratory and manuscript preparation expenses.

GEOLOGIC SETTING

The Sierra Madre Limestone is a massive Neocomian(?)—Santonian carbonate platform sequence in southern Mexico and northern Guatemala. It is exposed in a narrow northwest trending homocline paralleling the Chiapas massif in Chiapas, Veracruz, and eastern Oaxaca; along the northeast and

southwest flanks of the Chiapas Central Depression or synclinorium; and in cores of anticlinal folds of the Sierra Madre Oriental in northeastern Chiapas (Figure 2). In Guatemala, the lithologic equivalents of the Sierra Madre Limestone, the Ixcoy and Coban Limestones (Figure 3), are exposed in the Sierra de los Cuchumatanes and southward to the Polochic-Motagua fault system (Figure 2).

More than 3,400 m of primarily shallow water platform carbonates, comprising the Sierra Madre Limestone and equivalent formations were deposited in a rapidly subsiding tectonic basin. The broad carbonate platform covered an area including: all of Chiapas northeast of the Chiapas massif; the Yucatán Peninsula; all of Guatemala north of the Polochic-Motagua fault system; and a narrow band extending northward to Veracruz (Viniegra-Osorio, 1981; Bishop, 1980, fig. 4).

Mesozoic basin development in southern Mexico was probably initiated by the formation of grabens in response to Jurassic rifting in the Gulf of Mexico region as described by Buffler and coworkers (1980). A thick Callovian(?)–Oxfordian salt sequence was deposited in these early basins between the Yucatán tectonic block and the Chiapas massif (Viniegra-Osorio, 1971, 1981; Figure 2). The Todos Santos Formation (Sapper, 1894) is believed to be laterally equivalent to the basinward salt sequence and also overlies the salt in the subsurface (Figure 3). The Todos Santos Formation is a thick continental red bed sequence comprised of conglomerate and sandstone deposited as coalescing alluvial fans and braided streams (Blair, 1981) during the Late Jurassic to Neocomian (Ver Wiebe, 1925; Müllerried, 1936; Roberts and Irving, 1957; Chubb, 1959; Vinson, 1962). Andesite to dacite volcanics, probably associated with the formation of grabens and initial deposition of the Todos Santos Formation, were radiometrically (K/Ar) age dated as 148 ± 6 Ma (earliest Callovian) by Castro-Mora and coworkers (1975). The Todos Santos Formation lies nonconformably on the Chiapas massif in west-central Chiapas (Richards, 1963) and nonconformably overlies the crystalline basement or slightly metamorphosed late Paleozoic Santa Rosa Group in southern Chiapas and Guatemala (Walper, 1960; Richards, 1963; Burkart and Clemons, 1972; Anderson *et al.*, 1973; López-Ramos, 1975).

Continued basinal subsidence and increased marine circulation from Tithonian through Neocomian time led to a vertical facies change throughout northern Central America from Todos Santos red terrigenous clastics to marginal marine deposits of fine to coarse grained sandstone, siltstone, and some limestone and gypsum. Richards (1963) proposed the name San Ricardo Formation for these deposits exposed above the Todos Santos at its type section near Ventosa, Guatemala (Vinson, 1962) and in a Todos Santos reference section near Cintalapa, Chiapas (Figure 3). The San Ricardo Formation is

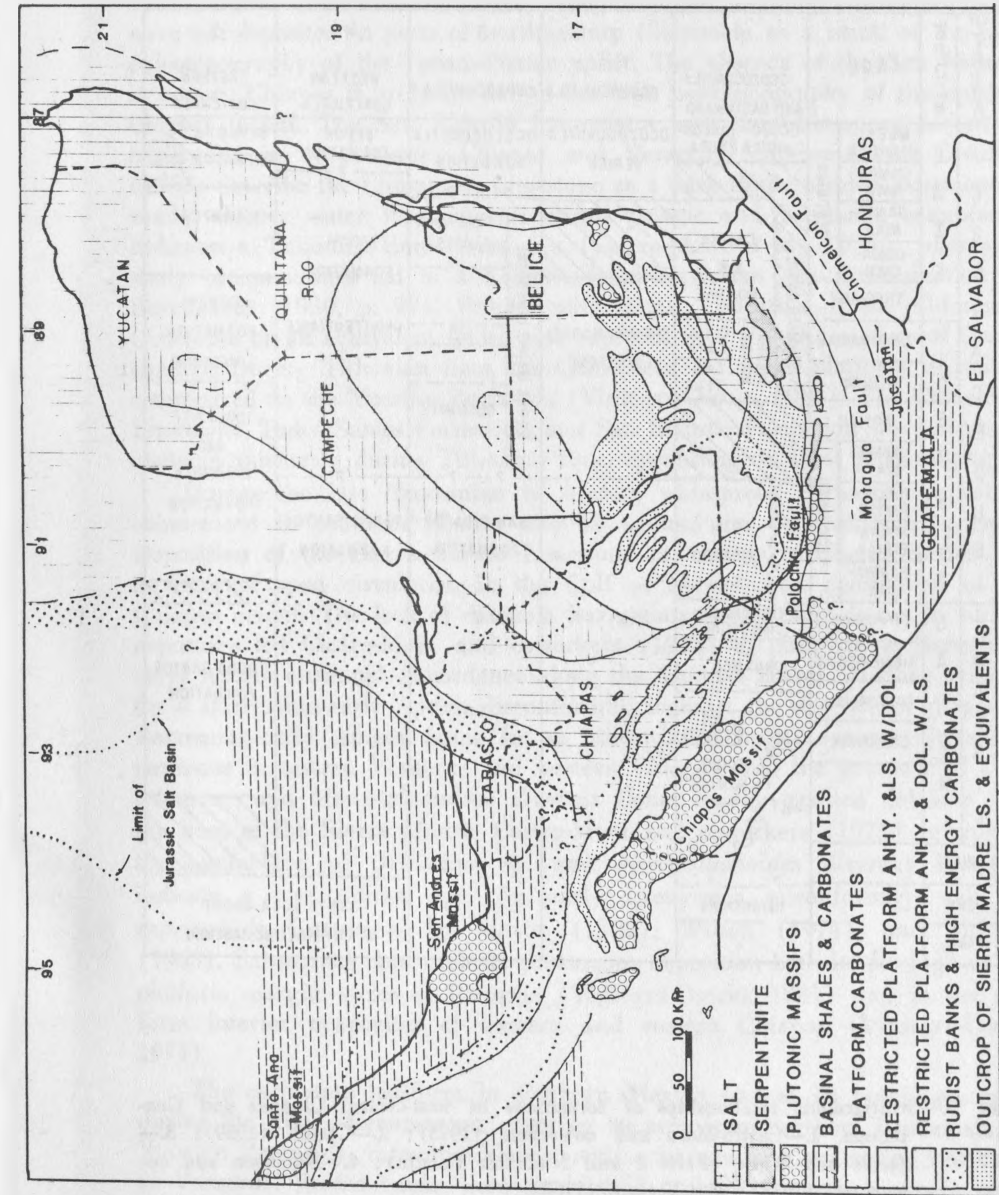


FIGURE 2.—Outcrop pattern and distribution of the depositional environments in the Sierra Madre Limestone and equivalent formations in southern Mexico and Guatemala. Lithofacies and depositional environments from Viniegra-Osorio (1971 and 1981).

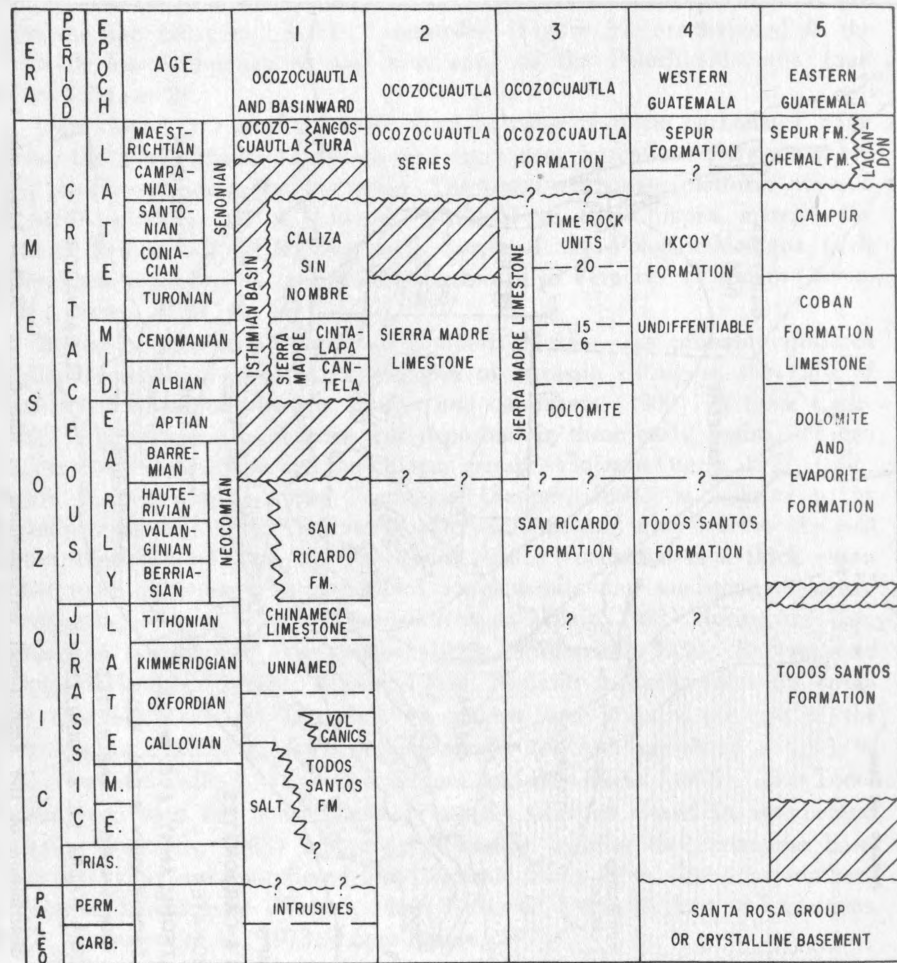


FIGURE 3.—Stratigraphic relationships of formations in west-central Chiapas and Guatemala. 1.—Castro-Mora and coworkers (1975); 2.—Chubb (1959); 3.—Steele and Waite (Parts 1 and 2 of this Boletín); 4.—Anderson and coworkers (1973); 5.—Vinson (1962).

not present above the Todos Santos everywhere in eastern Chiapas and northwestern Guatemala (Blair, 1981; Castro-Mora *et al.*, 1975; Burkart and Clemons, 1972). Burkart and Clemons (1972) recognized that marginal marine sediments were not deposited in parts of northwestern Guatemala as a result of the high paleotopography of the Tenam-Poxlac uplift. The absence of the San Ricardo in eastern Chiapas is probably due to the high paleotopography of the uplifted Chiapas massif. The San Ricardo intercalates with the Chinameca Limestone basinward in northwestern Chiapas and Veracruz. Contreras and Castellón (1968) describe the Chinameca Limestone as a dark thinly-bedded, occasionally sandy, deeper water limestone. A mixed pelagic and benthonic microfauna indicates a Tithonian-Hauterivian age (Castro-Mora *et al.*, 1975), whereas a study of ammonites led to a Kimmeridgian-Berriasian age determination by Burckhardt (1930, p. 97). Pelagic microfauna, indicative of the Chinameca Limestone or an equivalent facies, was reported in a PEMEX well near Ocozocaucla. During Tithonian time, the Chinameca carbonate platform deposition commenced on the Yucatán Peninsula (Viniegra-Osorio, 1981). The Chinameca Limestone, Todos Santos Formation, and San Ricardo Formation were deposited contemporaneously during Tithonian time, depending on local paleogeography.

During the late Neocomian to Aptian, widespread carbonate deposition commenced in southern Mexico and all around the Gulf of Mexico basin. Deposition of the Sierra Madre Limestone throughout southern Mexico was a result of open circulation in the Gulf of Mexico and denudation of the Chiapas massif. The lack of dateable Barremian-early Aptian fauna in surface exposures led Castro-Mora and coworkers (1975) to postulate a Barremian-early Aptian erosional discordance along the Chiapas massif. Further evidence for a Barremian-early Aptian disconformity includes the absence of diagnostic Barremian-early Aptian fauna in an otherwise complete Jurassic-Neocomian sequence in eastern Veracruz and western Chiapas, and the presence of *Orbitolina* sp. and *Microcalamoides diversus* Bonet in fine-grained dolomite near the base of the Sierra Madre. Castro-Mora and coworkers (1975) interpreted the assemblage of *Orbitolina* sp. and *Microcalamoides diversus* Bonet to indicate a late Albian age. An early Cretaceous unconformity was also reported in Guatemala by Vinson (1962), Wilson (1974), and Richards (1963). Subsurface data indicate continuous deposition both in the high energy platform margin facies at Reforma (Viniegra-Osorio, 1981) and in the platform interior evaporites of western and eastern Chiapas (Viniegra-Osorio, 1971).

The carbonate platform in southern Mexico was at its maximum extent during the Albian-Cenomanian, covering an area from northern Guatemala, the Yucatán Peninsula, through Chiapas, with a narrow arm extending northward to Veracruz. Rudist banks were established around the entire margin of the

platform, while deposition in the platform interior was predominately evaporitic-anhydrite and dolomite (Viniegra-Osorio, 1981). The platform through central Guatemala (Figure 3) is less well defined than in the northern Reforma area. In the Chiantla Quadrangle, Guatemala, Blount and Moore (1969) described a section of the Ixcoy Limestone (a Sierra Madre equivalent; Figure 3) comprised of more than 500 m of lithoclast packstone. The lithoclasts were predominately rudist debris, angular fragments of rudists, angular chert fragments, and a "significant quantity of grainstone clasts". Blount and Moore (1969) attributed the sequence "to uplift caused by faulting and subsequent erosion of a previously deposited well-lithified carbonate sequence" or from erosion of large massive rudist bioherms with steep submarine scarps. The latter interpretation was not favored for several reasons, including: relatively small size of the rudist fragments; lack of large blocks of unabraded rudists, and the great thickness of the deposit would necessitate a bank of gigantic proportions. The sequence may indicate a tectonically active southern platform margin as evidenced by the intrusion of serpentinites, the high quantity of grainstones (absent in the platform interior sediments), a facies change in the northern Chiantla Quadrangle to platform interior lime packstone and wackestones (Blount and Moore, 1969), and a southward facies change to basinal thin-bedded graywacke, shale, and radiolarian limestone. The radiolarian limestone comprises the Río Las Vacas Formation (Wilson, 1974) and is exposed northeast of Guatemala City in southern Guatemala. Wilson (1974) interpreted the Río Las Vacas Formation to be deposited at bathyal depths primarily by turbidites.

Turonian to Santonian age strata deposited on the carbonate platform extending across most of northern Central America are characterized by gray to tan, thick-bedded, large rudistid lime wackestone and biostromal limestone interbedded with thin to thick-bedded micrite and biomicrite. The strata may contain minor amounts of dolomite, shale or sandstone. The sequence is named the Campur Formation (Vinson, 1962) in eastern Guatemala, the San Cristóbal Formation (Ver Wiebe, 1925) in southeastern Chiapas, and the "Caliza Sin Nombre" (Unnamed Limestone) in western Chiapas (Figure 3). It is not a differentiable unit in western Guatemala (Clemons *et al.*, 1974).

Initial Laramide orogenic pulses destroyed carbonate platform deposition in Chiapas and northern Guatemala during the Campanian and Maastrichtian. Castro-Mora and coworkers (1975) show a Campanian erosional unconformity along the entire Chiapas massif. A Campanian disconformity is also reported in eastern Guatemala by Vinson (1962) and in the subsurface by Viniegra-Osorio (1971). Clastics derived from the reworked Todos Santos and the uplifted Chiapas massif comprise the Ocozocuautila series (Chubb, 1959) in Chiapas and the time and facies equivalent Sepur Formation (Sapper, 1899) in Guatemala. The Ocozocuautila series is most commonly referred to as the

Ocozocuautila Formation by Mexican geologists and other workers. Subsurface data from the wells Turiphache I, Caiba II, Lomas Tristes I-A, Chacamax-2A, and La Pita I show that the clastics of the Ocozocuautila Formation change facies northward into dolomite and limestone (Viniegra-Osorio, 1971). The Verapaz Group (Vinson, 1962) in northeastern Guatemala is equivalent to the Sepur Formation and to the Ocozocuautila Formation. The Lacandón Formation (Vinson, 1962) has no lithologic equivalent in Mexico and is comprised of detrital calcarenites derived from the uplift of the Maya Mountains and subsequent erosion of the Coban and Campur Limestones (Vinson, 1962). The Lomas Tristes Breccia and Méndez Formation are basinal deposits, unconformably overlying carbonate platform facies in northern and southern Chiapas (Castro-Mora *et al.*, 1975; Figure 3) where the carbonate platform was evidently down-faulted or subsided rapidly. The Méndez Formation is a dark basinal shale with pelagic microfauna. The Lomas Tristes Breccia is a calcarenite breccia probably deposited as basinal mass debris flows and interbedded with the Méndez Formation. At La Angostura in central Chiapas, Sánchez-Montes de Oca (1969) described a lateral facies change of the Ocozocuautila Formation clastics into platform carbonate deposits of micrite and biomicrite with "reefal" rudists and minor corals comprising the La Angostura Formation.

PREVIOUS WORK

The Sierra Madre Limestone was named by Gutiérrez-Gil (1956) for a thick sequence of Cretaceous limestones exposed throughout much of Chiapas and underlain by the Todos Santos Formation and overlain by the Ocozocuautila Formation. Previous investigations of the formation were primarily on the reconnaissance level. Although the formation is mentioned in numerous articles, no more than a half-dozen significant publications are readily accessible.

Early workers primarily concentrated on establishing the age of deposition for the Sierra Madre Limestone. Böse (1905) ascribed a middle Cretaceous age to the Sierra Madre based on *Ostrea (Chondrodonta) munsoni* Hill, similar to *Ostrea* sp. in the Edwards Formation (middle Albian) of Texas. Ver Wiebe (1925) referred to the Sierra Madre Limestone as the San Cristóbal Formation and considered it to be Comanchean (Albian-Cenomanian) in age. Müllerried (1936) treated the Sierra Madre to be as old as Aptian and in part as young as Turonian. Gutiérrez-Gil (1956) also regarded the lower Sierra Madre to be Aptian and believed the upper 159 m, exposed along the Sumidero Canyon-Tuxtla Gutiérrez highway, to be Turonian based on *Coralliochama* sp. (upper Senonian; and probably misidentified as reported by Chubb, 1959), *Radiolites* sp. (Turonian-Campanian) and *Nerinea* sp. (mid-Jurassic-Maastrichtian).

Apparently Gutiérrez-Gil (1956) assigned a Turonian age to the assemblage based solely on the presence of *Radiolites* sp., although it is not clear why a younger age range was not interpreted. *Caprina* sp. and *Toucasia* sp. were reported in the lower Sierra Madre by Gutiérrez-Gil (1956). Chubb (1959) concurred with Gutiérrez-Gil that the upper 150 m of Sierra Madre Limestone were Turonian and cited as further evidence: *Distefanella lombricalis* d'Orbigny; *Sauvagesia da rio Catullo* or *Sauvagesia acutocostata* Adkins; a species between *Durania nicholasi* Whitefield and *Durania austinensis* Roemer; and other *Durania* species. Other fossils reported by Chubb (1959) were *Actaeonella*, *Ostrea vesicularis* Lamarck, an echinoid resembling *Pseudopyrina clarki* Böse, and *Archaeolithothamnium provinciale* Pfender. The fauna collected by Chubb was outside the area of the present study from localities including the Tuxtla-Sumidero Canyon road, Suchiapa-Villa Flores road, and in the Berriozábal area. Bronnimann (in Chubb, 1959) collected *Nummoloculina heimi* Bonet, *Cuneolina*, and *Quinqueloculina* in the lowest fossiliferous horizon above a thick dolomite section at Km 1039.1 along the Pan American Highway (section V in this study). He interpreted the environment of deposition as "back reef". J. P. Beckmann (personal communication, 1980) determined an Albian-Cenomanian age, with a slight preference toward the Cenomanian, from samples collected at the site studied by Bronnimann. He also identified *Valvulammina* sp., *Spirolina?* sp., and the algae *Thaumatoporella parvovesiculifero* Raineri and *Aeolisaccus* sp. from probable Cenomanian strata above those studied by Bronnimann.

PEMEX geologists began regional structural and stratigraphic mapping of the Sierra Madre Limestone several years ago in the process of evaluating southern Mexico's petroleum potential. Gutiérrez-Gil (1956) measured the first composite section (2,450 m) of the Sierra Madre Limestone along the Tuxtla Gutiérrez-Sumidero Canyon highway. A brief description of the lithology, fauna and structural geology was included. Zavala-Moreno (1971) reported that the section in the Sumidero Canyon region was informally divided into a lower Cantela member and an upper Cintalapa member. The Cantela member is a 400 to 900 m thick lower Albian dolomite and miliolid biomicrite unit, interpreted by Zavala-Moreno as a low-energy platform interior deposit. The Cintalapa member is a 750 m thick lower Albian-Cenomanian rudistid wackestone-packstone unit with interbedded biosparite and pelsparite; no environmental interpretation was given.

Castro-Mora and coworkers (1975), geologists of the Instituto Mexicano del Petróleo, conducted a regional study of the Cretaceous stratigraphy and microfacies of Chiapas. They divided the Sierra Madre Limestone into six units: 22, 23, 24, 25, 26, and 27. Unit 22 is principally dolomite and was interpreted to disconformably overlie the San Ricardo or Todos Santos For-

mations. It was dated as of late Albian age by the presence of *Orbitolina* sp. and *Microcalamoides diversus* Bonet, collected southeast of Suchiapa. Unit 23 is principally miliolid biomicrite intercalated with fossil-bearing micrite, micrite and dolomitic micrite deposited in very shallow water. It was considered upper Albian by the presence of *Nummoloculina heimi* Bonet, *Triloculina* and *Quinqueloculina*. Units 24 and 25 consist of pelmicrite, biomicrite with both benthonic and planktonic microfauna, micrite, dolomitic micrite and some chert. They are Cenomanian in age as determined by *Planomalina buxtorfi* Gandolfi (Unit 24), *Rotalipora appenninica* O. Renz, and *Praeglobotruncana stephani* Gandolfi. Units 26 and 27 comprise the "Caliza sin Nombre" formation which is distinguished from the Sierra Madre Limestone on the basis of distinctive fauna. Unit 26 is Turonian, dated by *Globotruncana sigali* Reichel, *Praeglobotruncana stephani* Gandolfi, *Globotruncana angusticarinata* Gandolfi. Unit 26 is primarily biomicrite and was interpreted to be deposited in water depths varying from shallow to bathyal. Unit 27 is lithologically similar to units 24 and 25, but contains abundant, large, radiolitid rudists. It was considered Coniacian to Santonian in age based on the assemblage of *Dicyclina schlumbergeri* Munier-Chalmas, *Pseudoittonella reicheli* Marie, *Valvulammina picardi* Henson, *Spiroloculina* sp. and the calcispheres *Calcisphaerula* and *Pithonella*. The Maastrichtian Ocozocuaula Formation was reported to disconformably overlie unit 27, with Campanian strata removed by erosion.

The nature of the contacts of the Sierra Madre Limestone to the underlying and overlying formations in the study area is controversial. Richards (1963) stated that the contact between the San Ricardo Formation and the overlying Sierra Madre Limestone was conformable in the Cintalapa-Ocozocuaula region. Castro-Mora and coworkers (1975) concluded that the contact was disconformable in the same region as previously discussed. Chubb (1959) stated that the contact between the Sierra Madre Limestone and the overlying Ocozocuaula series appeared conformable, except in the region of Bajucú and in southern Chiapas. However, he concluded that Coniacian and Santonian age strata were absent, implying that the Campanian-Maastrichtian age Ocozocuaula Formation disconformably overlies the Turonian age Sierra Madre Limestone. Castro-Mora and coworkers (1975) considered the upper 150 m of Sierra Madre Limestone, or "Caliza Sin Nombre", to be Turonian to Santonian age and disconformably overlain by the Maastrichtian age Ocozocuaula Formation, with Campanian age strata absent by erosion.

Estimates of the regional thickness of the Sierra Madre Limestone vary. As previously mentioned, Gutiérrez-Gil (1956) measured a 2,450 m section of Sierra Madre Limestone along the Tuxtla Gutiérrez-Sumidero Canyon highway. Viniegra-Osorio (1971, p. 485) shows a 2,040 m thick section measured along the Cintalapa-Ocozocuaula highway. Anderson and coworkers (1973) estimated

the Ixcoy Limestone to be 2,500 m thick along the southern flank of the Cuchumatanes in Guatemala.

DESCRIPTION OF LITHOFACIES

The composite stratigraphic section measured in the study area was subdivided into 21 units which include both lithologic units and covered or inaccessible intervals. The units are identifiable in the field on the basis of lithology, depositional texture, macrofauna, early diagenetic features, bedding and other sedimentary features. A detailed graphic section is given on Plate 1 and a generalized section on Figure 4. Locality maps for the described sections are provided on Plate 1. Sections VI, X, XI, and XIII are shown on the map labeled Study Area A, and sections II, IV, V, VII, VIII, IX and XII on the Study Area B map. Sections I and III (Figure 1) are on the Grijalva River north of Tuxtla Gutiérrez and are not included in this report.

UNIT 1: DOLOMITE AND COLLAPSE BRECCIA

Unit 1 (Figure 4) consists of 828 to 895 m of gray and tan dolomite (see Appendix for an explanation of range in the thickness of the unit). The contact with the underlying San Ricardo Formation appears conformable and is best exposed along the Pan American Highway at section II of Study Area B (Figure 1, Plate 1). The uppermost beds of the San Ricardo Formation are largely comprised of lime mudstone to wackestone with angular fine quartz sand and micritized shell fragments. The upper contact of unit 1 is gradational into alternating lime mudstone, miliolid lime wackestone, and dolomite of unit 2, exposed at section V of Study Area B (Figure 1, Plate 1). The exposures of unit 1 are poor throughout the study area and are characterized by karst topography and heavy vegetation.

The basal 50 m of unit 1 are a laterally extensive evaporite solution collapse breccia, sampled at sections II and VII, and observed at two other localities in the field area. Collapse breccias, 4-20 m thick, are common throughout the lower 355 m of the Sierra Madre Limestone along the Pan American Highway 190. The breccias (Plate 2, A-C) are characterized by grain-supported textures, apparent lateral continuity, and often include large collapse blocks up to 10 m thick. Beds throughout the lower 355 m interval are structurally disturbed due to slumping over collapse breccias. Breccia clasts are angular to subround, pebble to boulder size, lithologically similar to the overlying and underlying beds, and commonly have an iron oxide rim. Breccia clasts in the basal 50 m have numerous near-vertical fractures. The breccia matrix is

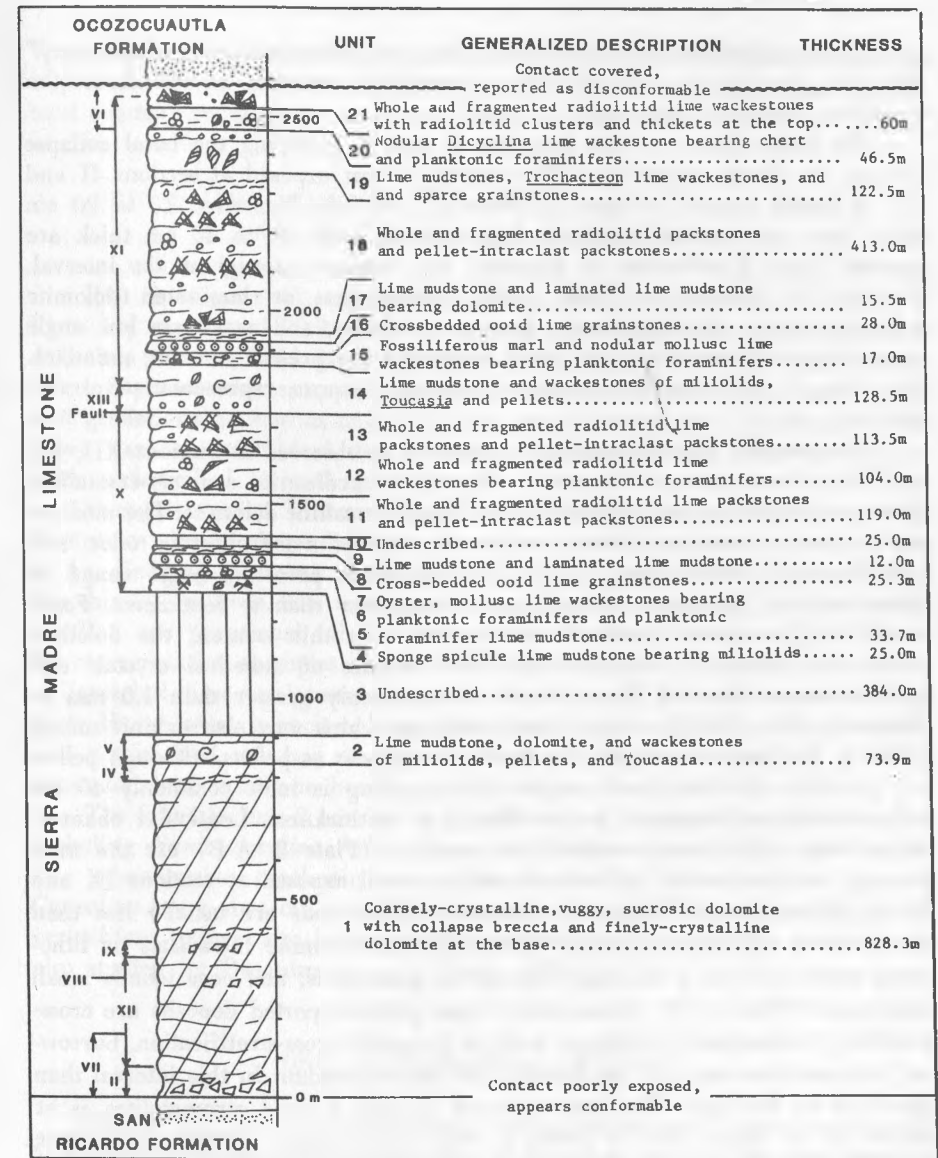


FIGURE 4.—Generalized graphic section of the Sierra Madre Limestone, west-central Chiapas. Roman numerals with arrow bars on left side of column indicate the stratigraphic interval measured at each locality shown on the maps of Study Areas A and B (Figure 1 and Plate 1).

medium-crystalline tan to gray dolomite or is coarsely-crystalline white "sparry" dolomite. Dedolomite characteristic of collapse breccias, is absent in the localities previously mentioned.

The lower 150 m of the dolomite in unit 1, including the basal collapse breccia, are finely crystalline. This interval is best exposed at sections II and VII in Study Area B (Figure 1, Plate 1). Vaguely laminated 10 to 20 cm thick beds are common, although homogeneous beds up to 40 cm thick are present. Vugs, a millimeter in diameter, are common throughout the interval. Vertical "v" desiccation cracks, algal stromatolites or laminated dolomite exhibiting large planar fenestrae, burrow structures, and very rare low angle cross-strata with relict rounded shell fragments are present but not abundant. See Plate 2, D-E for photographs of selected features representative of this interval.

The dolomite interval from 150 m to 785 m observed at sections XII, IX, and IV in Study Area B (Figure 1, Plate 1) is medium to coarsely-crystalline dolomite interbedded with sparse beds of finely-crystalline dolomite. The medium and coarsely-crystalline dolomite is sucrosic, exudes a petroliferous odor, and exhibits fossil moldic, vuggy, and intercrystalline porosity. Vugs range in diameter from less than one millimeter to greater than a centimeter. Fossil molds of high-spined gastropods are common. In thin section, the dolomite consists of medium to coarsely-crystalline mosaics of anhedral crystals and euhedral zoned rhombs. The rhombs are commonly greater than 1.0 mm in diameter with a dark core and clear outer rim which may also exhibit zoning (Plate 3, E). In hand sample, the dark cores appear as pellets, although pellets are probably not the genetic origin. The bedding is most commonly 40 cm to 1 m thick and ranges to greater than 2 m in thickness. Lenticular channel-shaped beds with sharp-scoured lower contacts (Plate 3, A-B) are the most common in this interval of the unit and are well exposed at sections IX and IV in Study Area B (Figure 1, Plate 1). These beds are usually less than 30 cm thick and contain at the base polymictic dolomite intraclasts or lithoclasts, molds of 1 to 2 cm long high-spined gastropods, and occasionally small pelecypods (Plate 3, D). Occasionally, these grain-supported deposits are cross-stratified. Sedimentary structures, such as low-angle cross-stratification, burrowing, stromatolites and thin laminations are more abundant in this interval than elsewhere in the unit. The best exposure of well defined stromatolites is at section IV in Study Area B (Plate 4, A-B). One sample (sample IX-4, Plate 4, C) of thinly laminated dolomite with laminations and anhydrite was collected in the lower 200 m of this interval, associated with evaporite collapse breccia.

The upper 38.3 m of unit 1 observed at section V in Study Area B (Figure 1, Plate 1) are gray finely-crystalline dolomite with sparse medium to coarsely-crystalline dolomite. Bedding ranges from 0.5 to 1 m in thickness.

Vugs and sucrosic textures are common where coarsely-crystalline dolomite is present. Wispy laminations, burrows, mottling and rare fenestrae are the most common sedimentary structures (Plate 4, D-E).

UNIT 2: LIME MUDSTONE; DOLOMITE; AND MILIOLID, PELLET, AND REQUIENIID LIME WACKESTONE

Unit 2 (Figure 4), exposed at section V in Study Area B (Figure 1, Plate 1), consists of 73.9 m of alternating lime mudstones, finely-crystalline dolomite, pellet miliolid lime wackestones, and requieniid rudist lime wackestones. Representative examples of these lithologies are shown on Plate 5. The unit gradationally overlies unit 1 and the upper contact (and maximum thickness) was not established due to lack of exposure in an estimated 384 m thick undescribed interval (unit 3).

Strata at section V superficially resemble broad lenticular bioherms and biostromes due to karst-dissolution weathering and covered intervals (Plate 5, A). Bedding thickness ranges from 0.5 m to greater than 2 m with very few thin 10 cm beds. The most common sedimentary structures are burrowing, mottling and occasional tubular, irregular, and planar fenestrae (see Plate 6 for representative examples of fenestrae). Rare features are a 30 cm thick bed of intraclast lime packstone (sample V-34, Plate 5, E) with rounded large (5 to 10 cm long) intraclast, low-angle cross-strata in miliolid lime grainstones, and a thin (0.3 m) bed of dark brown lime mudstone underlying a thinly laminated lime mudstone bearing organic matter and planar fenestrae.

The fauna in unit 2 consists almost entirely of requieniid rudists; miliolids including *Nummoloculina heimi* Bonet, *Triloculina* sp., and *Quinqueloculina* sp.; other sparse benthonic foraminifera including *Valvulammina* sp. and *Cuneolina*; rare oysters; and the solenoporacean alga *Thaumatoporella parvo-vesiculifera* Raineri also known as *Polygonella*. Samples from this locality were also studied by Bronnimann (*in* Chubb, 1959).

UNIT 3: UNDESCRIBED INTERVAL

Unit 3 is an unmeasured interval between well-exposed outcrops at section V in Study Area B and at section X on the north bank of the Río Venta in Study Area A (Figure 1, Plate 1). The unit is poorly exposed along the Pan American Highway 190 southwest of Ocozocauhtla. The estimated thickness of unit 3 is 384 m, as determined in Appendix.

UNIT 4: SPICULAR LIME MUDSTONE TO WACKESTONE

Unit 4 (Figure 4, Plate 1) consists of 25 m of light colored monaxon spicule lime mudstones to wackestones (Plate 7, D-E) with sparse pellets and miliolids exposed at section X in Study Area A (Figure 1, Plate 1). Allochems show no preferential orientation due to intense bioturbation. Bedding is thick (1.0 to 2.5 m) at the base and is thinner (0.2 to 0.5 m) at the top of the unit. Tubular fenestrae with geopetal structures are common near the base and are cemented by first-generation coarse blocky calcite with no isopachus rim. A stromatolite and an intraclast dolomitic lime packstone were collected from probably displaced beds in an interval of heavy karst dissolution weathering and rubbly exposure. The upper contact is obscured by a 7 m interval of cover and rubble, but appears to be gradational into unit 5.

UNIT 5: PLANKTONIC FORAMINIFER BEARING MOLLUSK
FRAGMENT LIME WACKESTONE

Unit 5 is 10 m thick (Figure 4, Plate 1) and consists of oyster and mollusk fragment lime wackestone with echinoid fragments, planktonic foraminifers, and calcispheres. Photographs of representative lithologies are shown in Plate 8. Beds are from 0.5 to 1.0 thick and are completely homogeneous from intensive bioturbation. Some burrows are preserved as tubular fenestrae, filled by medium to coarsely-crystalline equant calcite cement. All shell material is fragmented without rounding or sorting. Oyster fragments are heavily bored but not micritized. Other molluscan materials are small (0.5 to 2 mm) fragments of gastropods and pelecypods completely recrystallized to medium to coarsely-crystalline equant calcite. The mud matrix is thoroughly pelleted. The upper contact is gradational into unit 6.

UNIT 6: PLANKTONIC FORAMINIFER LIME MUDSTONE TO WACKESTONE

Light-colored planktonic foraminifer lime mudstone to wackestone comprises unit 6 (Figure 4, Plate 1). The unit is no more than 4 m thick and only one sample (Plate 8, E) was collected. Beds are 0.5 to 1.0 m thick and are thinly laminated with occasional burrows disturbing the thin laminae. The contact with unit 7 is apparently gradational.

UNIT 7: PLANKTONIC FORAMINIFER BEARING OYSTER,
MOLLUSK FRAGMENT LIME WACKESTONE

Unit 7 (Figure 4, Plate 1) is 19.7 m thick and primarily consists of oyster and mollusk fragment lime wackestone with echinoid plates and spines, and calcispheres which constitute most of the matrix. Representative examples of the lithology are shown in Plate 8. The upper 9.7 m of this unit is a covered interval. Beds range from 0.5 to 1.5 m in thickness and are thoroughly bioturbated with some surface mottling. Whole and fragmented oysters up to 10 cm long are partially silicified and weather distinctively against the carbonate matrix. Unsorted and unabraded gastropod and pelecypod mollusk fragments are recrystallized to coarsely-crystalline equant calcite. All mollusks are heavily bored but are not micritized. Beds directly below the covered interval have a pelleted matrix and a distinctive fauna including solitary corals, spongiomorph hydrozoans (calcsponges), and the large solenoporacean algae *Gymnocodium* sp. and *Macroporella* sp. The upper contact with unit 8 is probably gradational, but is obscured by a 9.7 m thick interval of rubbly beds.

UNIT 8: WORN SKELETAL FRAGMENT, OOID LIME GRAINSTONE

Unit 8 primarily consists of ooid, worn skeletal fragment lime grainstones, but the upper and lower beds are lime packstones (Figure 4, Plate 1). Photographs of representative samples are shown in Plates 9 and 10. The unit is 25.3 m thick and is physically distinctive in the outcrop due to trough cross-strata which weather with a nodular appearance. A reddish-orange color is imparted to many of these beds by hematite and siderite. The basal bed is 1.5 m thick and is a reddish-orange lime packstone with grainstone lithoclasts and abraded coral fragments. Also present are large, 30 cm high, whole, upright, colonial corals and large, high-spined gastropods. Cross-stratification is absent. The grainstones in the lower part of the unit are composed of 15 to 25 percent oolites, grapestones, well-sorted and rounded fragments of echinoids, radiolite rudists, and gastropods and pelecypod fragments which are preserved as micrite envelopes with the shell material replaced by medium crystalline equant calcite. Bedding in these grainstones is 30 to 60 cm thick trough cross-strata. The grainstones higher in the unit lack oolites, contain more grapestones and heavily micritized whole gastropods (*Actaeonella*) and grade into gastropod packstones. Bedding is 0.2 to 1.5 m thick with internal low-angle cross-stratification. Three primary cement fabrics, shown in Plate 10, were observed in the grainstones; thick, often pendulant rim cements; syntaxial overgrowths around echinoid fragments exhibiting competitive growth fabric with earlier rim cements; and medium crystalline equant-mosaics which replace gastropods

and pelecypods and fill remaining pore space. A fourth cement observed only in the upper grainstones-packstones was clear, coarsely-crystalline equant calcite with numerous inclusions, completely filling pore space, associated with calcedony replacing gastropods and crystalline filling some pore spaces. Unit 8 underlies unit 9 with a gradational contact.

UNIT 9: LIME MUDSTONE; PELLET LIME PACKSTONE; AND
LAMINATED LIME MUDSTONE

Unit 9 (Figure 4, Plate 1) is 12 m thick and consists of lime mudstone, pellet lime packstone, and alternating pellet lime packstone and lime mudstone as millimeter thick laminations. Bedding is 0.5 to 1.5 m thick and is occasionally lenticular. The fauna in the mudstones is primarily restricted to ostracods, except at the base of the unit where the foraminifers *Valvulamina* sp. and very rare *Planomalina* sp. (a planktonic form) are present and at the top, where stromatolites and 2 to 3 cm wide oncolites with gastropods and bored lithoclasts as nuclei were common (Plate 7, C). Unit 9 is separated from unit 11 by an estimated 25 m thick undescribed interval.

UNIT 10: UNDESCRIBED INTERVAL

Unit 10 is an undescribed interval which was inaccessible between two section traverses at section X (Figure 1, Plate 1). The thickness of this interval was estimated as 25 m as described in Appendix.

UNIT 11: PELLET-INTRA-CLAST LIME PACKSTONE; RADIOLITID
FRAGMENT LIME PACKSTONE; AND STROMATOLITES

Unit 11 (Figure 4, Plate 1) is 119 m thick and consists of alternating beds of pellet-intraclast lime packstone, bioclastic radiolitic fragment lime packstones and vaguely laminated stromatolites. Photographs of representative lithologies are shown in Plates 11, 12, and 13. Whole radiolitics occur only occasionally in this unit and none were found in growth position. The radiolitic fragments in the packstones are usually slightly rounded, moderately sorted, heavily bored, micritized, and encrusted by *Thaumatoporella* sp. or *Girvanella* sp. (Plate 11, A). The algal encrustations appear as heavy white rims around the fossils in the outcrop. Intergranular spar cement is generally greater than the percentage of lime mud. Beds of the bioclastic radiolitic fragment lime packstones (Plate 12, C) are characterized by crude, low angle,

10 to 40 cm thick cross-bedding with the crude foresets largely disturbed by bioturbation. The beds most commonly have sharp bases and fine upward to pellet-intraclast grainstone, packstone, or lime mudstone. The stromatolites (Plate 13) lack abundant irregular and planar fenestrae, and exhibit vague and discontinuous thin laminations. The thin laminations are broken by numerous thin laminations of pellet-intraclast packstone to grainstone. The intraclasts associated with the stromatolites are irregular lumps of composite pellets and are small rip-ups of the algal mats. Small high-spired gastropods commonly occur in thin skeletal packstones associated with the stromatolites. The fauna in the unit is restricted to radiolitic rudists, rare requieniid rudists, gastropods including *Nerinea*, blue-green and solenoporacean algae, and microfauna including ostracods, *Valvulamina*, miliolids, and *Cuneolina*. Bedding is very regular throughout the unit and appears flaggy where well-exposed. Beds are 20 to 40 cm thick, except at the base of the unit where several beds of pellet-intraclast packstone are up to 1.5 m in thickness. Other significant sedimentary structures (Plate 13) are gypsum pseudomorphs and celestite which also occurs as the cement. Unit 11 grades into unit 12 without a physically distinct contact.

UNIT 12: PLANKTONIC FORAMINIFER BEARING RADIOLITID
AND PELLET LIME WACKESTONE

Unit 12 (Figure 4, Plate 1) is comprised of alternating beds of pellet lime wackestones and whole and fragmented radiolitic lime wackestone exhibiting a vaguely pelleted (grumeleuse; Cayeux, 1935) matrix. The 104 m thick unit is differentiable from unit 11 in the outcrop by the absence of stromatolites and greater abundance of whole radiolitics which lack heavy micritization and algal encrustation. The fauna is similar to the assemblage in unit 11, but is more varied and includes echinoid fragments and planktonic foraminifera, predominantly *Planomalina* sp. Bedding ranges from 10 to 50 cm in thickness throughout the unit and it is gradational into overlying unit 13.

UNIT 13: PELLET-INTRA-CLAST LIME PACKSTONE; RADIOLITID
FRAGMENT LIME PACKSTONE AND STROMATOLITES

Unit 13 (Figure 4, Plate 1) consists of alternating pellet lime packstone, pellet-intraclast lime packstone, whole and fragmented radiolitic lime packstone, occasional stromatolites, and requieniid lime wackestones. Fine to medium dolomite rhombs were common but rarely exceeded 30 percent of a sample. Representative lithologies are shown in Plates 11 and 12. A minimum thickness

of 113.5 m of the unit was measured; maximum thickness was not determined because the top of the unit is faulted. The estimated minimum throw of the fault is 115 m, as determined by the fault contact between units 13 and 16, an ooid grainstone. Unit 13 is lithologically similar to unit 11 and is differentiated from unit 12 by the occurrence of stromatolites, requieniid-*Toucasia?* sp. wackestones, heavy micritization and algal encrustation of rudistids, and by the absence of echinoid fragments, although rare planktonic foraminifers are present. Other common fauna in unit 13 are benthonic foraminifera including miliolids, *Cuneolina* sp., and *Valvulammina* sp., the solenoporacean algae *Thaumatoporella* sp. and occasional blue-green algae as stromatolites and oncolites. Beds are commonly 20 to 40 cm thick, although occasional beds of radiolitic lime wackestones and pellet-intraclast lime packstones are as thick as 0.8 to 1.5 m.

UNIT 14: LIME MUDSTONE, MILIOLID AND REQUIENIID LIME WACKESTONE AND STROMATOLITES

Unit 14 consists of alternating beds of varied lithologies, predominately: pellet-intraclast lime packstone, miliolid and pellet-intraclast grainstones, stromatolites, lime mudstones, and miliolid and requieniid wackestones (see Figure 4 and Plate 1 for the stratigraphic position and Plates 5 and 6 for representative lithologies). The unit is 128.5 m thick and was measured at excellent exposures in sections XIII and XI in Study Area A (Figure 1, Plate 1). Section XIII was chosen to avoid the previously mentioned large fault and other complex folds in an unsuccessful effort to determine the lower contact with unit 13. Beds in the lower 20 m of unit 14 are cyclical repetitions of 1 to 2 m thick beds of pellet-intraclast packstones (spar averages up to 50% of the cement), capped by thin 10 to 20 cm beds of cross-bedded miliolid and pellet-intraclast grainstones or stromatolites. The remainder of the unit also exhibits lithologic variation, but is predominately wackestones of miliolids, pellets, or requieniids; laminated mudstones; and stromatolites with planar and irregular fenestrae. Burrowing and bioturbation is heavy in the mudstones and wackestones. Irregular branching and "U-shaped" burrows with geopetal structures are commonly preserved as tubular fenestrae which are filled by coarsely-crystalline calcite cement (Plate 6, A-C). A 10 cm thick caliche horizon (Plate 5, C) and lithoclasts occurred within this unit.

The solitary sample of caliche resembles a pustular algal mat as described by Logan (1974). Petrographic analysis of the "pustular" laminations were inconclusive; however, the other laminations were identified as a dense laminoid crust (terminology after Multer and Hoffmeister, 1968; and Reeves, 1976),

The crust exhibits petrographic criteria established by Harrison and Steinen (1978) for recognition of caliche such as: dense, non-spongiostrome, finely laminated micritic fabric; laminations ranging from a few tenths of a millimeter to several millimeters in thickness; laminations variable in color from purple to brown to gray and cream-colored, but variations in the color are due only to concentrations of iron oxide rather than compositional variations; laminations thin over microtopographic highs and thicken into microtopographic lows; and desiccation features and fenestral pores are lacking.

The fauna in the unit is a restricted assemblage of gastropods, sparse pelecypods, *Toucasia?* sp., miliolids, ostracods, algal stromatolites oncolites, and *Thaumatoporella*-stromatolite boundstones. However, it is diverse in the upper 15 m of the unit and includes abundant oysters (usually preserved as fragments), solitary corals, and sponge spicules. Unit 14 underlies unit 15 with an abrupt but conformable contact.

UNIT 15: NODULAR MOLLUSK LIME WACKESTONE AND FOSSILIFEROUS MARL

Unit 15 (Figure 4, Plate 1) consists of alternating fossiliferous marls and nodular lime mudstones to packstones bearing rare ammonites and planktonic microfauna, including abundant calcispheres and foraminifera as shown in Plate 8. The 17.0 m thick unit is well exposed along a primitive logging road at section XI in Study Area A (Figure 1, Plates 1 and 14, A). The basal 7 m of unit 15 are hard, indurated, cream-colored lime mudstone-wackestone with planktonic foraminifera and abundant oyster fragments and are separated from a stromatolite in unit 14 by no more than one meter of vertical stratigraphic section. Microfauna was preserved only in indurated nodules of lime mudstone to wackestone. Various washing procedures performed by L. E. Waite failed to produce recognizable microfauna from the marl units. The marl does contain abundant, well-preserved, easily collectable echinoids, large gastropods and pelecypods. Two poorly preserved ammonites were also collected. Petrographic studies of the wall structure of the pelecypods and gastropods from the marl and nodular limestones indicate the fossils are recrystallized with the original wall structure replaced by neomorphic bladed calcite and medium to coarsely-crystalline equant calcite with abundant hematite after pyrite. The hematite imparts a red to yellow color to the unit. The contact with the overlying unit, unit 16, is gradational.

UNIT 16: WORN SKELETAL FRAGMENT, OOID LIME GRAINSTONE

Unit 16 (Figure 4, Plate 1) is primarily comprised of worn skeletal fragment, ooid grainstones. The 28 m thick unit is well exposed at section XI in Study Area A in the north flank of an anticline (Figure 1, Plates 1 and 14, A). The unit is also in fault contact with unit 13 at section X in this same study area. The basal 8 m of unit 16 consist of nodular, worn skeletal fragment lime packstone which forms a prominent ledge above the marly slope formed by unit 15. Large-scale, 20 to 30 cm thick, trough (?) cross-bedding occurs throughout the grainstone interval and weathers with a distinctive nodular appearance. Allochems are primarily ooids and secondarily of coated, rounded and micritized pelecypod and gastropod fragments with minor echinoid fragments, benthonic foraminifera and ostracods. Porosity is occluded by thick rim cements with common pendent fabrics and pore-filling medium crystalline equant-mosaic calcite which also replaces mollusk fragments and some ooids (Plate 10). The upper 2.0 m of the unit are ooid, skeletal fragment lime packstones which gradationally underlie unit 17. Representative examples of the lithologies are shown on Plate 9.

UNIT 17: LIME MUDSTONE AND LAMINATED LIME MUDSTONE

Unit 17 (Figure 4, Plate 1) consists of lime mudstones and laminated lime mudstones bearing ostracods, *Toucasia?* sp. and sparse benthonic and planktonic foraminifera (see Plate 7, A-B for representative samples). The 15.5 m thick unit is well exposed above the grainstones of unit 16 and forms the dip slope of the northern flank of an anticline at section XI (Plate 14, A). Sparse burrows, finely-crystalline dolomite (to 20%) and planar fenestrae are present in samples from the characteristically thin-bedded (10 to 20 cm thick) laminated mudstones. The upper contact with unit 18 is gradational and was arbitrarily chosen at the first occurrence of radiolitid rudists.

UNIT 18: RADIOLITID FRAGMENT LIME PACKSTONE AND WACKESTONE; PELLET-INTRA-CLAST LIME PACKSTONE AND STROMATOLITES

Unit 18 (Figure 4, Plate 1) consists of extremely varied lithologies (see Plates 11, 12, and 13 for representative examples), predominantly bioclastic radiolitid fragment lime packstones, pellet and pellet-intraclast lime packstones, whole requieniid (*Toucasia?* sp.) and radiolitid lime wackestones, and abundant stromatolites. The measured 413 m thickness of the unit may be in considerable

error due to unseen structural complexities in the broad syncline at section XI in Study Area A (Figure 1, Plate 1) where the unit was measured. Many samples were collected from float blocks in the absence of bedding. Where in place, beds are poorly exposed due to heavy karst weathering, flat terrain, and low structural dip. However, large blocks of the unit, displaced from construction of a logging road, afford glimpses of the rapid and complex lithologic changes in the unit (Plate 12, A and C). Bioclastic radiolitid fragment packstones, similar to those in units 11 and 13, are characterized by moderate sorting, slight rounding of 0.5 to 1.5 cm fragments, occasional whole radiolitids, spar cement comprising up to 50 percent of the matrix, and coarse cross-lamination disturbed by bioturbation. Fragments are most often heavily bored, micritized, and compacted with grain penetration and dissolution common. The radiolitid fragment packstone beds fine upwards and average 20 cm in thickness. Grainstones are not common in the unit but when present, overlie radiolitid fragment packstones as a fining upward sequence and are also associated with pellet-intraclast packstones. The grainstones are comprised of pellets, intraclasts and algal-coated gastropods. Primary laminations are poorly preserved throughout the unit suggesting vigorous bioturbation. However, laminated lime mudstones are common in intervals with abundant stromatolites. Lithologies and sedimentary features associated with intervals of abundant laminated lime mudstones and stromatolites are requieniid lime wackestones, burrowed lime mudstones, fine to medium dolomite rhombs, celestite, gypsum pseudomorphs, centimeter-size lithoclasts, irregular and planar fenestrae, and vertical (polygonal?) desiccation cracks. Many of these features are shown in Plate 13. In contrast to evaporite minerals and desiccation features, sponge spicules, solitary corals and echinoid fragments also occur in this unit. Rare planktonic foraminifera (Plate 11, F) occur throughout the unit in all lithologies, including fenestral laminated mudstones and stromatolites (see Plate 11, F). Other common faunas are benthonic foraminifers including miliolids, *Cuneolina* sp. and *Valvulamina* sp., *Nerinea* sp. and other gastropods, algal rhodalites, oncrites, and *Thaumatoporella* sp., which also forms boundstones when associated with blue-green algae. The upper contact of unit 18 is gradational with unit 19.

UNIT 19: LIME MUDSTONE AND PELLET LIME WACKESTONE

Unit 19 primarily consists of lime mudstone and pellet lime wackestones with pellet-intraclast packstones, *Thaumatoporella*-stromatolite boundstones, and thin grainstones which are common near the top of the unit. The 122.5 m thick unit was measured near the axis of a broad syncline at section XI in Study Area A (Figure 1, Plate 1). Bedding was in place but poorly exposed.

The lime mudstones, wackestones, and packstones of unit 19 are cream-colored, porcellaneous, and fractured with manganese oxides and "horsetail" stylolites; they are very distinctive in the field. The grainstones (Plate 15, F) are thin to medium-bedded, 10 to 30 cm thick, and are comprised of heavily micritized, recrystallized, rounded-mollusk fragments, intraclasts, benthonic foraminifers, and *Acicularia* (a dasycladacean alga). Ooids are absent. Siderite spherulites are very common and replace mollusk grains. Cements consist of a very thin (6 to 10 microns), poorly developed, first-generation, equant rim cement and a second-generation cement of coarsely-crystalline equant calcite with numerous dark inclusions which fill intergranular pore spaces, tectonic fractures, and replaces recrystallized mollusk fragments. The cement and diagenetic features are illustrated in Plate 15, D. Siderite and hematite impart a pale, reddish-orange color to many grainstone beds. The fauna in the unit is unique and varied and was collected in primarily thick-bedded wackestones with a sparse pellet matrix. Fauna includes large radiolitid rudists; *Toucasia?* sp.; gastropods including large *Trochacteon* sp. occurring in 1 to 1.5 m thick lime wackestone to packstone biostromes (Plate 15, E-F); benthonic foraminifera including miliolids, *Valvulamina* sp., and *Cuneolina* sp.; the solenoporacean algae *Pycnoporidium* sp. and *Thaumatoporella* sp.; rhodalites; and *Thaumatoporella*-stromatolite boundstones. Occurring only near the base of the unit are sparse calcispheres, solitary corals, echinoid fragments, and sponge spicules. The upper contact with unit 20 is abrupt, but appears conformable and is best exposed in a dry stream bed at the base of measured section VI in Study Area A (Plates 1 and 14, B).

UNIT 20: NODULAR *DICYCLINA* BEARING, PELLET LIME WACKESTONE
WITH PLANKTONIC FORAMINIFERS AND CHERT NODULES

Unit 20 is characterized by yellowish to reddish-brown nodular *Dicyclina* sp. pellet lime wackestones bearing planktonic foraminifers (Plate 8, E) and blue chert nodules. The 46.5 m thick unit was measured near the axis of a broad syncline at section XI and on the north flank of an anticline at section VI in Study Area A (Figure 1, Plate 1) where it is better exposed. Unit 20 weathers to form rubbly slopes and featureless valleys with abundant blue chert nodules with a white patina and lime wackestone nodules 4 to 25 cm in diameter. Occasional nodular beds, 10 to 40 cm thick, are exposed in the rubbly slopes and valleys. The fauna in the lime wackestone nodules is a diverse assemblage of planktonic foraminifers, benthonic foraminifers including *Dicyclina schlumbergeri* Munier-Chalmas which is uniquely abundant in unit 20, *Cuneolina* sp., *Valvulamina* sp., *Rhapydionina dubia* De Castro, *Bioconcava* sp., and several biserial and uniserial forms. Also present are calcispheres,

sponge spicules, echinoid fragments, solenoporacean algae, gastropods including *Nerinea schiosensis* Pirona, rare radiolarians and solitary coral fragments, and abundant fragments of gastropods, pelecypods, and rudists. Most rudist fragments are less than 1.0 cm in length and are heavily bored, micritized, and slightly rounded. The unit is intensely bioturbated, although vague stratification is present in samples with particularly abundant fine-shell debris. Unit 20 corresponds to the lower "Caliza Sin Nombre" of Castro-Mora and coworkers (1975). The upper contact with unit 21 is gradational and occurs where nodular beds, though increasingly lumpy, are overlain by thick beds of unit 21 which forms a distinctive limestone cap over a rubbly slope (Plate 14, B and D).

UNIT 21: WHOLE RADIOLITID, PELLET LIME WACKESTONES
AND WHOLE RADIOLITID BIOSTROMES

Unit 21 consists primarily of pellet, whole-radiolitid lime wackestones. The 60 m thick unit was measured at section VI in Study Area A (Figure 1, Plate 1) where it is well exposed along the north limb of an anticline. The entire thickness of the unit may be exposed along the axis of a broad syncline at section XI in Study Area A; however, only the lower 45 m were measured in the poor rubbly exposure. Unit 21 is characterized by the first appearance of large (10 to 15 cm wide, 30 to 40 cm long) radiolitid rudists with complex polygonal cell walls (subfamily Sauvagesiinae). Using the terminology of Kauffman and Sohl (1974), the radiolitids occur in growth position as solitary individuals, associations, and clusters in beds 0.3 to 1.0 m thick with abundant rudist debris. Particularly abundant in the upper 15 m of the unit are laterally extensive, 10 cm thick, densely-packed, single-generation, single-species thickets of *Distefanella*(?) which are laterally equivalent to clusters of *Sauvagesia* (?). The thickets and clusters are shown in Plate 12, E-F. Multiple-generation, high-diversity coppices, banks, and biostromes were not observed in the study area. Chubb (1959) identified *Distefanella lombricalis* d'Orbigny, *Sauvagesia* sp., *Radiolites* sp. and several species of *Durania* in equivalent beds along the Pan American Highway, Tuxtla-Sumidero road, Tuxtla Suchiapa-Villa Flores road and the Berriozábal road. Beds laterally equivalent to and overlying the radiolitid associations and clusters are primarily composed of heavily-bioturbated mollusk fragment, pellet lime wackestones and packstones. The mollusk fragments are rudists, pelecypods and gastropods which are most commonly small (1 mm to 2 mm long), and are heavily bored and micritized but not rounded or abraded. Several mollusk fragments are encrusted by oncolite coatings. Other fauna in the unit is sparse, but diverse. Fauna found only at the base of the unit was of stromatoporoids, colonial corals, and hollow,

cylindrical, 2 mm long vertebrae spines (?). The corals were highly abraded and the stromatoporoid occurred with both highly rounded and abraded fragments of echinoids, mollusks, and stromatoporoid as well as delicate costate pelecypods. Elsewhere in the unit, fauna includes solitary corals, echinoid fragments, oyster fragments, solenoporacean algae including *Solenopora* sp. and *Thaumatoporella* sp., sponge spicules, calcispheres, radiolarians, planktonic foraminifers, and benthonic foraminifers including *Cuneolina* sp., sparse *Dicyclina* sp., *Valvulammina* sp., *Rhapydionina* sp. miliolids, biserial forms and uniserial forms.

The upper contact with the Piedra Parada member of the Ocozocuaula Formation was not observable due to a 5 m thick covered interval, but is reported to be disconformable by Chubb (1959) and Castro-Mora and coworkers (1975). At section VI in Study Area A, the Piedra Parada member consists of a medium-grained yellowish-brown sandstone, in contrast to a sandy limestone of the Piedra Parada member described by Bronnimann (*in* Chubb, 1959) which is densely packed with planktonic foraminifers and *Inoceramus* prisms.

ENVIRONMENTAL INTERPRETATION OF LITHOFACIES

The Sierra Madre Limestone, as measured and described in the study area of west-central Chiapas, is comprised of eight major lithofacies, representing four periods of prolonged platform deposition interrupted by three brief periods of open marine deposition (Figure 5). The eight lithofacies identified in the 19 described lithologic units and their interpreted environments of deposition are as follows: dolomite and collapse breccia lithofacies (unit 1) representing a hypersaline platform interior environment; lime mudstone, and lime wackestone of pellets, miliolids and requieniid rudists lithofacies (units 2, 14) representing a platform interior lime mud environment; lime mudstone and laminated lime mudstone lithofacies (units 9, 17) representing a tidal mudflat environment; worn skeletal fragment, ooid lime grainstone lithofacies (units 8, 16) representing an ooid sand shoal environment; pellet-intraclast lime packstone and radiolitid lime packstone lithofacies (units 11, 13) representing a restricted interior lagoon environment; planktonic foraminifer-bearing lime mudstone to wackestone and radiolitid lime packstone lithofacies (units 12, 18, 19, 21) representing an open interior lagoon environment; planktonic foraminifer-bearing nodular mollusk lime wackestone lithofacies (units 5, 7) representing an open marine shelf environment; and planktonic foraminifer lime mudstone to wackestone lithofacies (unit 6) representing a basinal to deep open marine shelf environment.

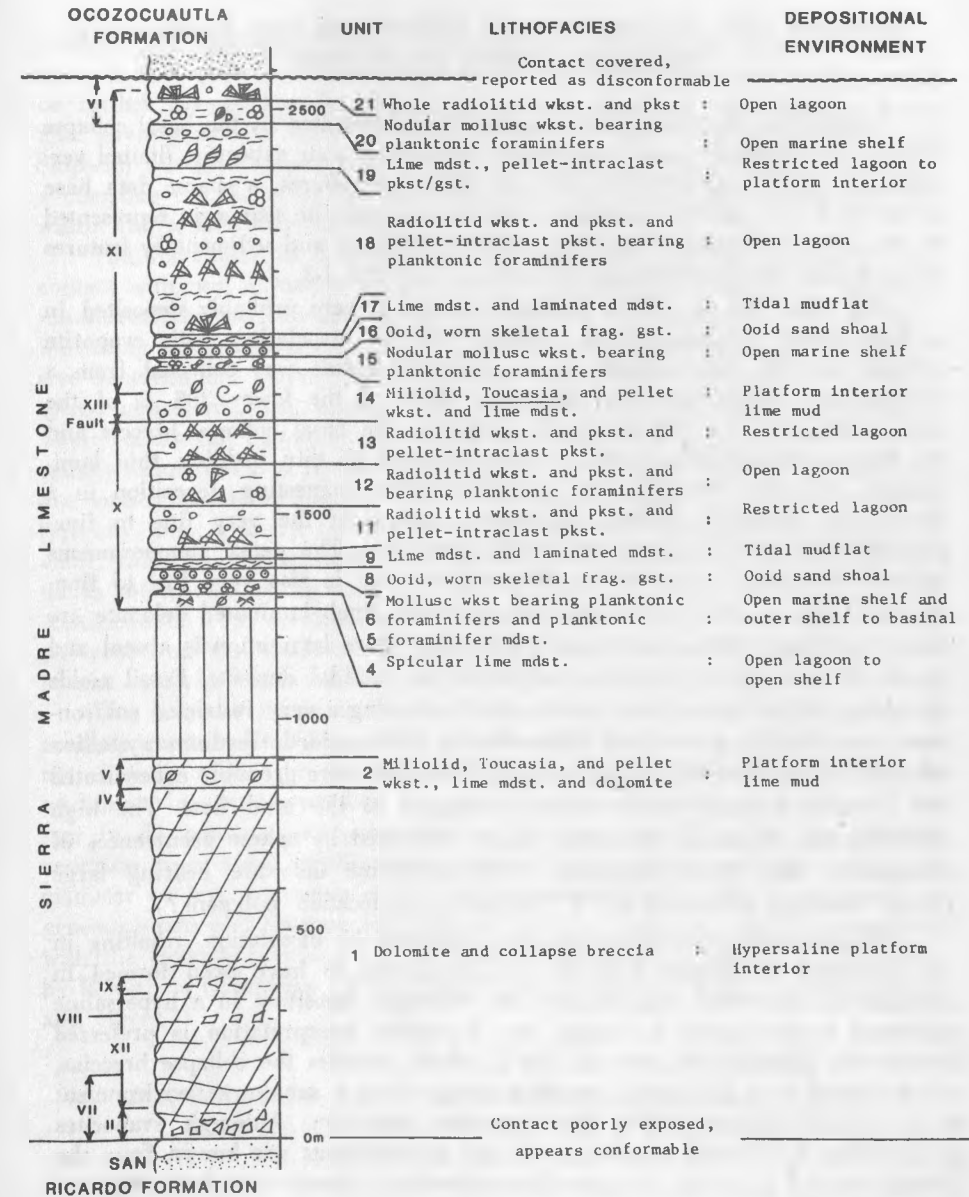


FIGURE 5.—Generalized graphic section with lithofacies and depositional environments in the Sierra Madre Limestone, west-central Chiapas.

DOLOMITE AND COLLAPSE BRECCIA LITHOFACIES: THE HYPERSALINE
PLATFORM INTERIOR ENVIRONMENT

Interpreting the depositional environment represented by the basal collapse breccia and dolomite (unit 1) is tenuous because of poor exposure, limited vertical and lateral successions of beds in the best exposures, a sparse data base in the thick unit, and the inability to observe the evaporite sequences represented by the collapse breccias (Figure 5). Selected lithologic and sedimentary features characteristic of this lithofacies are shown on Plates 1-3.

The basal 355 m of the dolomite in unit 1 were probably deposited in a hypersaline environment as indicated by the association with evaporite collapse breccias. One sample of an anhydrite nodule was collected from a fine-grained, thinly laminated dolomite. Much of the lower 355 m of the unit, particularly the 100 m directly overlying the basal collapse breccia and the beds in the collapse breccia, is characterized by thin bedding, thin laminations and very fine and fine-grained dolomite suggesting deposition in a low-energy intertidal mudflat environment. Much of the very fine to fine-grained dolomite is probably penecontemporaneous. The penecontemporaneous dolomite forming in modern mudflat environments is also very fine to fine-grained rhombs. Interbedded with thinly-bedded, finely-laminated dolomite are thin to medium-bedded, fine-grained dolomites where lamination is absent and sparse burrows occur which are interpreted as subtidal deposits. Fossil molds are absent in the lower 150 m of the unit, indicating a very restricted environment probably as a result of hypersalinity. Thin-bedded, medium-crystalline dolomites of abraded shell fragments and intraclasts were probably concentrated and abraded in small tidal channels marginal to the mud flats. The high intertidal and supratidal environments are indicated by sparse occurrences of stromatolites and thinly-laminated, finely-crystalline dolomite bearing large planar fenestrae and vertical "V" fractures (desiccation polygons?).

The evaporite sequences which were removed by dissolution, resulting in the formation of collapse breccias, are interpreted to have been formed in intertidal to supratidal zones of sabkhas, although deposition in a hypersaline restricted lagoon cannot be ruled out. A sabkha interpretation is preferred because the dolomite sequence of unit 1, which includes the collapse breccias, is interpreted as a low energy mudflat along which a sabkha subenvironment is a common modern analog for evaporite deposition. Although evaporites precipitating in subtidal hypersaline lagoon environments are known from the geologic record, no evaporites other than ephemeral deposits have been observed forming in a Holocene lagoon open to a marine environment (see Dzensus-Litovsky and Vasil'yev, 1973; and Friedman, 1980 for a discussion of possible analogs). The sabkha environment may have been established along a coastline or along

locally broad supratidal exposures in a large interior lagoon where a coastline was not well defined. The implication of these two sabkha environments will be further discussed under "Geologic interpretations of sequential lithofacies and environments". See Evans and coworkers (1964, 1969), Kendall and Skipwith (1968), Purser (1973) and McKenzie and coworkers (1980) for a complete discussion of the distribution of facies, hydrology and deposition within the sabkha environment.

The remainder of the dolomite unit above the collapse breccias to the contact with unit 2 cannot be adequately explained in terms of a low-energy mudflat-sabkha environment. Bedding is medium to massive, up to 2 m thick, indicating less frequent interruption or more homogeneity resulting from intensive bioturbation. Burrow structures and fossil molds, particularly of high-spired gastropods, are common. The gastropods were probably algal grazers. Thinly laminated dolomites interpreted as stromatolites are common, but are usually thin, from 2 to 10 cm thick. Frequently associated with the stromatolites are lenticular channel-shaped beds interpreted as tidal channels. The beds typically have a sharp lower convex downward contact, indicating erosional scour, and a basal grain-supported deposit of intraclasts or lithoclasts and fossil molds interpreted as lag deposits. Several examples exhibited low-angle cross stratification. The environment of deposition was probably not considerably different from the shallow subtidal platform interior environment represented by the overlying lime mudstone and pellet wackestones of unit 2.

The dolomite fabric in the upper part of unit 1 is not typical of penecontemporaneous finely-crystalline dolomite. It is clearly a secondary product not directly related to the depositional environment. The sucrosic texture, medium to coarsely-crystalline mosaics and euhedral zoned rhombs up to 0.4 mm in diameter, strong petroliferous odor, high porosity and permeability resulting from fossil moldic vugs, intercrystalline vugs and vugs 1 mm in diameter or less, pervasive dolomitization through homogeneous and inhomogeneous strata and fracture filling white "sparry" dolomite, which is associated with the collapse breccias, are all features attributed to burial dolomitization by Wong and Oldershaw (1981), Mattes and Mountjoy (1980), Loucks (1977) and others.

LIME MUDSTONE; PELLET, MILIOLID AND REQUIENIID RUDIST
LIME WACKESTONE LITHOFACIES: THE PLATFORM
INTERIOR LIME MUD ENVIRONMENT

Alternating beds of thick-bedded lime mudstone, finely-crystalline dolomite, and lime wackestones composed of pellets, miliolids and *Toucasia?* sp., represented by units 2 and 14 (Figure 5), were probably deposited in a low energy

platform interior lime mud environment. Selected lithologies, diagenetic features, and fauna characteristic of this lithofacies are shown on Plates 5 and 6. Modern platform carbonate mud environments are found in the interior of the Great Bahama Bank and Florida Bay in areas of little tidal or wave-generated turbulence, maximum salinity, and at depths averaging less than 4 m but ranging from 0 to 7 m (Cloud, 1962; Purdy, 1963; Multer, 1977).

The thick-bedded lime mudstones and wackestones of requieniid rudists, pellets and miliolids which characterize the lithofacies are shallow subtidal deposits which are heavily bioturbated and occasionally exhibit burrow structures or color mottling. Sparsely occurring miliolid lime grainstones were probably deposited in tidal channels or as storm deposits. Sample V-34 (Plate 5, E), a lime packstone with large intraclasts, is probably also a storm deposit. The thick successions of subtidal deposits alternate with thin successions of three to four 10 cm thick beds of intertidal to supratidal deposits. Evidence of low energy intertidal to supratidal deposition are stromatolites, thinly-laminated mudstones, irregular and planar fenestrae (bird's-eye fabric) dessication cracks, mudstone lithoclasts commonly with a weathering patina and an oxide rim, one 10 cm bed of caliche, and possible marsh deposits.

Two broad groups of stromatolites were recognized in the intertidal zone (see Plate 6). The first group exhibits a spongiostrome fabric characteristic of stromatolites but the thin laminations are poorly developed and discontinuous, planar fenestrae are absent, irregular fenestrae are sparse, and burrow structures are common. Using the classification of Ginsburg and coworkers (1970), the group has a low exposure index indicating deposition in the lower intertidal zone with stromatolites subject to subaerial exposure less than 50 percent of the time, heavy grazing by gastropods, and higher tidal energy. The second group occurs infrequently and is typified by regular millimeter laminations, large irregular and planar fenestrae, vertical dessication cracks, and lack of burrows. The group has a high exposure index and was deposited in the intertidal zone with subaerial exposure occurring as great as 90 percent of the time.

Supratidal deposits are rare in this lithofacies but are represented by lithoclasts, caliche and marsh deposits. This is in apparent contradiction to modern tidal flat environments in the Bahamas, where the supratidal and marsh zones are the largest area of the tidal flat complex. The small (1 cm long or less), weathered, iron stained lithoclasts were probably formed by subaerial exposure on a mudflat. Early lithification on mudflats is accomplished by periodic wetting and drying and subsequent intensive CO₂ degassing leading to early cementation. All lithoclasts were reworked and found in subtidal deposits. The sample of caliche (Plate 5, C), collected near the top of unit 14 at section XI, was identified as a dense laminoid crust. Laminoid caliche

crusts form aggradationally and only on bare rock in the absence of soil zones (Multer *et al.*, 1968; Reeves, 1976). Samples of dark brown discrite and a dark brown finely laminated lime mudstone bearing organic matter are interpreted as marsh deposits. The samples are similar to Holocene marsh deposits described by Shinn and coworkers (1969) which are sediments consisting of pelleted lime silt or mud, locally dark with admixtures of organic matter generally in distinct laminae and smelling of H₂S. These samples were collected from one 0.3 m thick bed which was overlain by a light colored, medium bedded, burrowed pellet lime mudstone deposited in the subtidal zone.

Early diagenetic fenestral fabrics are common features of this lithofacies (see Plate 6). Fenestrae are defined by Tebbutt and coworkers (1965) as: "primary or penecontemporaneous gap(s) in a rock framework, larger than the grain-supported interstices. Fenestra(e) may be an open space in the rock, or it may be completely or partially filled by secondarily induced sediment or cement. The distinguishing characteristic of fenestra(e) is that the spaces have no apparent support in the framework of the primary grains forming the sediment". Three primary fenestral fabrics were observed: tubular; irregular (vugs or spar-filled blebs); and laminoid or planar, as described by Tebbutt and coworkers (1965), Logan (1974) and Shinn (1968a). All three fabrics occur in Holocene to present-day carbonate sediments where they form in shallow subtidal, intertidal, and supratidal environments (Ginsburg and Hardie, 1975; Shinn, 1968a).

Tubular fenestrae (Plate 6, A-C) are more common in this lithofacies than planar or irregular fenestrae. Tubular fenestrae appear as spar-filled burrows, usually partially filled by internal sediment consisting of micrite, pellets, angular intraclasts (produced from burrowing?), and miliolids. They are circular in cross section and oriented vertical to subvertical and most commonly unbranched, although they may be horizontal or "U" shaped. The tubular fenestrae are primarily large and small (classified as coarse and fine after Logan, 1974). Large tubular fenestrae are 3 to 5 mm wide, and 3 cm to more than 5 cm long. Small tubular fenestrae are less than 1 mm wide and over a centimeter long. Tubular fenestrae occur with irregular fenestrae but are absent in samples with planar fenestrae. They occur primarily in thick-bedded, heavily-bioturbated, cream-colored mudstones and wackestones bearing a restricted fauna of requieniids, miliolids, gastropods and ostracods indicative of the shallow subtidal environment. Less frequently, they occur in the intertidal zone in stromatolites, and in pellet-intraclast packstones to grainstones capped by grainstones or stromatolites which are interpreted as shoal deposits. These shoal cycles were observed only at the base of section XIII in Study Area A, and are interpreted as transitional into the lagoonal environment of unit 13.

In Holocene sediments, tubular fenestrae are formed by plant roots and burrows in shallow subtidal to supratidal environments (Shinn, 1968a). Ginsburg and Hardie (1975) described burrows in tidal flats of the Bahamas which are exposed above high tide over 70 percent of the time, allowing for early cementation. Shinn (1968b) described crustacean burrows in supratidal to shallow subtidal lime mud sediments which, though commonly infilled by sediment, have remained open and uncompacted for a thousand years or more. Grover and Reed (1978) described tubular fenestrae from the Ordovician which precludes a plant root origin. Tubular fenestrae in units 2 and 14 are interpreted to have formed in shallow subtidal to lower intertidal sediments based on modern and ancient analogs, lithologies in which they are found, and their proximity to (but not included in) beds with definite upper intertidal and supratidal aspects.

Irregular and planar fenestrae (Plate 6, D-F) characterize the lithologies deposited in the high intertidal and supratidal zones. Irregular fenestrae are irregular, elongate to spherical in shape; 0.3 to 2 mm in diameter (classified as fine to medium irregular fenestrae after Logan, 1974), although most are less than 1 mm. Irregular fenestrae are not oriented with bedding planes, except when they coalesce and become similar to planar fenestrae. They occupy 5 to 15 percent of the rock volume but comprise up to 35 percent of the rock volume in solenoporacean algae—blue green algae boundstones. Planar fenestrae (bird's-eye structures) occur infrequently. They are parallel to bedding, typically 0.1 to 1 mm high and 1 to 2 cm long (fine to medium as classified by Logan, 1974). Irregular fenestrae occur with both planar and tubular fenestrae; however, planar fenestrae were never observed in the same bed with tubular fenestrae.

Irregular and planar fenestral fabrics occur in thin-bedded laminated mudstones, dolomites and stromatolites. Common sedimentary features associated with the fenestral fabrics are fine-to-coarse vertical desiccation cracks, geopetal structures of micrite, iron-oxide streaks, micrograding, millimeter lamination and leached gastropods and miliolids. Irregular fenestrae also occur associated with burrowing.

Irregular and laminoid fenestrae are thought to form by shrinkage from desiccation, trapped gas from the decay of algal organic matter, and by burrowing activity (Tebbutt *et al.*, 1965; Logan, 1974). Shinn (1968a) observed in Holocene and present-day sediments that irregular and laminoid fenestrae are preserved mainly in the supratidal environment, sometimes in the intertidal environment, but never in the subtidal environment. Voids superficially resembling irregular and laminoid fenestrae were actually interconnected and tubular (tubular fenestrae) and were directly attributable to burrowing or to root holes. Shinn's (1968a) laboratory experiments showed that irregular fenestrae

were formed primarily by trapped gas bubbles in intertidal and supratidal sediments. No particular origin for the gas was speculated on. Planar fenestrae were also duplicated in laboratory experiments by simple desiccation of a mud slurry; blue-green algae, hypersaline water, or diagenetic alteration were not controlling factors. Other workers (Illing, 1959; Folk, 1959; R. D. Perkins, 1963; Laporte, 1967; Grover and Read, 1978) also interpreted irregular and planar fenestrae as forming in the high intertidal and supratidal zones as a result of desiccation and trapped gas bubbles. As previously stated, Ginsburg and coworkers (1970) observed that fenestral pores did not form in algal mats until they were subaerially exposed for at least 75 percent of the time.

Irregular and planar fenestrae in the Sierra Madre Limestone are interpreted to have formed in sediments deposited in the high intertidal and supratidal zones based on the lithologies in which they occur, associated sedimentary features, and modern and ancient analogs. Irregular fenestrae also occur in the subtidal and intertidal zones as a result of burrowing. Tubular fenestrae do not occur with planar fenestrae; because of the hostility of the supratidal environment to burrowing organisms.

The fossil assemblage in this lithofacies is a restricted assemblage consisting of miliolids, ostracods, solenoporacean algae, *Toucasia?* sp., and sparse oysters and gastropods. This faunal assemblage is typical of Cretaceous interior platform mudstone deposits reported by Coogan and coworkers (1972) in the El Abra Limestone of Mexico and by B. F. Perkins (1969, 1974) in the Glen Rose of Texas. High salinity resulting from low circulation rates in the platform interior environment is interpreted to be the primary environmental control in restricting the diversity in this lithofacies. This assemblage may be analogous to the assemblage in the interior of Florida Bay and the Great Bahama Bank which consists of miliolid and peneropoid foraminifera, ostracods, green algae, the burrowing crustacean *Callianassa*, a low-abundance, low-diversity assemblage of pelecypods, and polychaete worms which are largely responsible for creating mud pellets. Although the faunal assemblages in the two modern examples are not completely analogous as discussed by Coogan (1977a), both assemblages occur in low energy, shallow, platform interior lime mud environments and are typically restricted as a result of high seasonal salinity fluctuations due to seasonal rainfall and poorly circulated waters. Gorsline (1963), Ginsburg (1964) and Broecker and Takahashi (1960) discuss the hydrology and salinity variations in Florida Bay and on the Great Bahama Bank.

LIME MUDSTONE AND LAMINATED LIME MUDSTONE LITHOFACIES:
THE TIDAL MUDFLAT ENVIRONMENT

The lime mudstone and laminated lime mudstone lithofacies represented by units 9 and 17 (Figure 5) is interpreted to have been deposited in a low energy subtidal lime mud and intertidal to supratidal mudflat environment. Characteristic lithologies and diagenetic features of this lithofacies are shown in Plate 7, A-C. As shown in Figure 5, this lithofacies overlies the ooid lime grainstone lithofacies and underlies the radiolitic fragment lime wackestone lithofacies. Consequently the environment of deposition is interpreted to have formed directly leeward of the ooid sand complex and seaward of a broad interior lagoon. The ooid sand shoal complex is interpreted to have formed a barrier to open marine circulation, behind which a low energy mudflat environment could be established. In Holocene environments, the seaward shallow subtidal and intertidal mudflat environment is developed leeward of islands of earlier lithified lime sand beach-rock and dunes, as described by Harris (1977) behind the Joulter Cays in the Bahamas and by Bathurst (1975) along the island system of Abu Dhabi.

This lithofacies consists of thick-bedded lime mudstones and pellet wackestones and packstones alternating with thin-bedded sequences of laminated mudstones and stromatolites. Also present are dolomitic lime mudstones. The thick-bedded sequences are interpreted to have been deposited in the shallow subtidal zone and lack sedimentary structures due to heavy bioturbation. The thin-bedded sequences of thinly laminated lime mudstone and stromatolites, which bear desiccation features such as planar fenestrae, were deposited on intertidal to supratidal mudflats. Dolomitic lime mudstones occur in both subtidal and supratidal sequences. The fine to medium-size dolomite rhombs, which may comprise up to 50 percent of the rock, are probably penecontemporaneous.

The fauna in this lithofacies consists primarily of ostracods and blue-green algae with sparsely occurring planktonic foraminifers washed in from the seaward open marine environment, benthonic foraminifers, gastropods, and requeniid rudists. The assemblage is probably restricted because of frequent subaerial exposure rather than hypersalinity.

WORN SKELETAL FRAGMENT, OOID LIME GRAINSTONE LITHOFACIES:
THE OOID SAND SHOAL ENVIRONMENT

The cross-bedded, worn, coated skeletal fragment, ooid lime grainstone lithofacies, constituted by units 8 and 16, was deposited as ooid shoals in a prograding high-energy ooid sand complex marginal to open marine circulation. As shown in Figure 5, this lithofacies overlies the planktonic foraminifer-

bearing nodular mollusk lime wackestone lithofacies and underlies the lime mudstone and laminated lime mudstone lithofacies. Consequently, this lithofacies is interpreted to have been deposited in a high energy zone marginal to open marine circulation and served as an effective barrier to leeward circulation. Selected lithologic and diagenetic features are shown in Plates 9 and 10. Holocene ooid sand complexes, particularly those in the Bahamas, also primarily form at shelf margins and can be subdivided into four primary depositional environments: the mobile ooid sand belt; the seaward skeletal sand with ooids; the leeward stabilized sand flat; and lithified oolite islands. See Ball (1967) and Harris (1977) for a detailed discussion of depositional processes and the distribution of lithologic textures and sedimentary structures within the subenvironments of Bahamian ooid sand complexes.

The vertical stratigraphic sequence in this lithofacies is interpretable as a prograding depositional environment similar to the Holocene model described by Harris (1977) at Joulter Cays. The texture, rock composition, grain size, and the presence or absence of cross-bedding in the lithofacies, typified by unit 16, uniquely subdivides the lithofacies into subfacies analogous to the subenvironments of the Holocene ooid sand complex (Figure 6).

Fine abraded skeletal fragment packstones, with up to 20 percent ooids at the base of the lithofacies, are analogous to the seaward environment comprised of skeletal sand with ooids (Figure 6). This unit is in gradational contact with the underlying open marine unit comprised of whole and fragmented skeletal wackestones with planktonic microfauna and calcispheres. The lowest sample (XI-43 in Figure 6) of the abraded skeletal fragment packstone unit exhibits a distinct bimodal texture of fine (to 0.3 mm) abraded mollusk fragments and larger (to 3 cm) unabraded whole and fragmented pelecypods, gastropods, echinoid plates and oysters. The other samples of this unit lack a bimodal texture and are well sorted, comprised of abraded skeletal fragments similar in size and composition to the overlying ooid grainstones but lack abundant ooids. The ooids present are poorly preserved, dark, and probably heavily micritized. The cement is cloudy microspar characterized by an indistinct contact with the grains and presumably resulted from the neomorphism of lime mud. Preferential grain orientation, cross-bedding and other sedimentary features are lacking, presumably from intense bioturbation. Ooids are interpreted to have been introduced into the skeletal sands by seaward prograding tidal bars as described by Ball (1967), which were subsequently reworked by marine currents and intensive bioturbation.

The well-sorted, cross-bedded ooid lime grainstone interval (Figure 6) is interpreted to be analogous to the mobile ooid sand belt environment. This grainstone interval overlies the abraded skeletal fragment lime packstones with a rapid lithology change and a probable scoured contact. The lowest sample

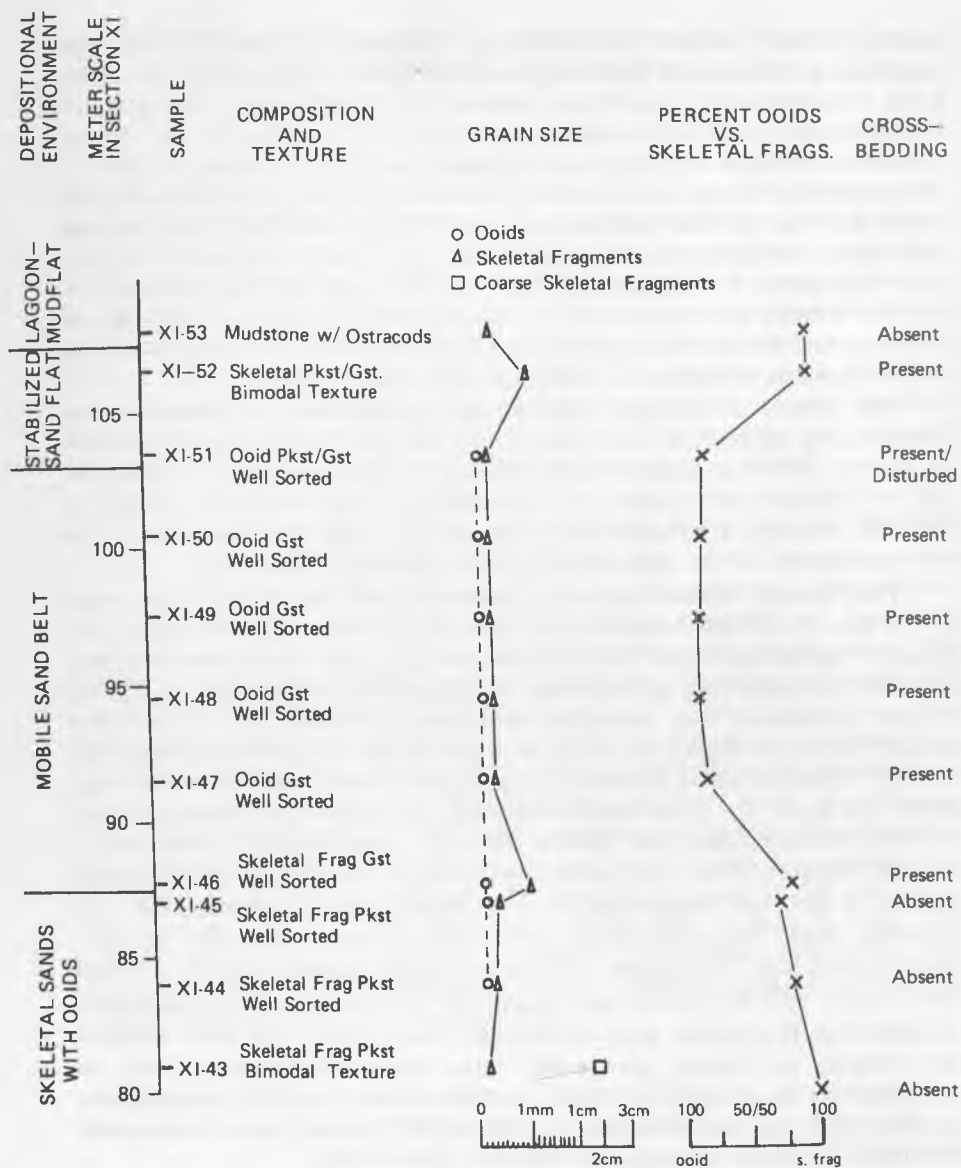


FIGURE 6.—Subenvironments interpretable on the basis of allochem composition, texture, grain size, and primary sedimentary structure in the ooid, worn skeletal grainstone lithofacies represented by unit 16.

(XI-46 in Figure 6) on this interval consists of very coarse sand size (1.2 mm mean) pelecypod fragments and lacks abundant ooids. Many of the pelecypod fragments are similar to pelecypods in the underlying interval and previous lithofacies. All the shells are replaced by medium crystalline equant calcite and are preserved as micrite envelopes which primarily result from intensive boring by endolithic blue green algae. The sample is interpreted as the basal lag of a tidal channel in which shells of the underlying unit were concentrated in as a result of scour into the underlying unit.

The remaining ooid grainstones are cross-bedded and well sorted with ooids comprising at least 80 percent of the allochems. The cross-bedding is characterized by 10 to 15 cm thick beds with low angle foreset laminae. The laminae are not disturbed by bioturbation indicating a lack of fauna adapted to the mobile substrate. The cross-bedding is interpreted to have formed by bedforms (dunes?) migrating across the mobile ooid sand belt. Bimodal directions of cross-bedding characteristic of the Holocene environments were not observed in the field but may be present.

Early cementation as a result of subaerial exposure of ooid shoals is indicated throughout this interval by thick isopachus rim cements of granular microspar which are characteristic of intertidal and shallow subtidal beach-rock deposits as described by many authors including Land (*in* Bricker, 1971), and vadose zone cement fabrics represented by poorly preserved meniscus cements (Dunham, 1971) and gravitational or "pendulant" cements (Muller, 1971). The poor preservation of the vadose zone cements is probably a result of deep burial resulting in the dissolution and interpenetration of grain contacts, grain dissolution as a result of ground water diagenesis and masking of the cement fabrics by later cementation. The remaining pore space in the grainstones is cemented by medium crystalline equant calcite, described by Longman (1980) and others as indicating meteoric phreatic zone ground water diagenesis. The cement also replaces many ooids, particularly those along coarser foreset laminae, and all pelecypod and gastropod fragments. The fresh-water phreatic zone can be established in an otherwise saline system by subaerial exposure. The Ghyben-Herzberg theory (the "iceberg principle") reveals that for each meter the water table rises above sea level, 40 m of fresh groundwater can be formed below it.

The size and structure of the ooids throughout this lithofacies and the absence of massive-scale cross-bedding indicate that the lithofacies was deposited under relatively low energy. The ooids are fine sand size, average 0.18 mm in diameter and range from 0.13 to 0.24 mm. They characteristically lack multiple concentric coatings, have radial calcite crystals with the *c* axis perpendicular to the nucleus, and are similar in structure to ooids described from Great Salt Lake by Kahle (1974) and from Laguna Madre by Rusnak

(1960). Laboratory syntheses of ooids by Davies and coworkers (1978) suggest that ooids with radial internal structure form under quiet water conditions, whereas Bahamian type ooids with multiple concentric layers form under higher energy conditions. Friedman (1977) and Bathurst (1975) related a decrease in the size of Bahamian-type ooids to a decrease in the energy of the depositional environment. Abraded skeletal fragments in this lithofacies are slightly larger than the ooids, ranging from 0.3 to 0.7 mm in diameter, but are still within the size range to serve as nuclei for Bahamian-type ooids. Evidently they were too large to serve as nuclei in this lower energy environment of deposition.

The interval interpreted as analogous to the stabilized ooid sand flat environment is represented by only two samples (XI-51 and 52 in Figure 6). The interval gradationally overlies the ooid grainstones and grades upward into heavily bioturbated mudstones bearing ostracods which is the lowest sample in the lime mudstone and laminated lime mudstone lithofacies previously described. The primary characteristics of the stabilized ooid sand flat environment are heavy bioturbation, mud matrix, decreased ooid content, and algal encrustation. However, both samples believed analogous to the environment are laminated. The well-sorted ooid grainstone to packstone (sample XI-51 in Figure 6) is probably only marginal to the stabilized ooid sand environment, because it is only partly bioturbated with much of original foreset lamination preserved. The cement is microspar and is indistinct with the grains and may represent neomorphosed lime mud. The whole and fragmented gastropod packstone/grainstone (sample XI-52 in Figure 6) probably represent a tidal deposit within the stabilized grain flat. The sample exhibits a bimodal texture comprised of thick laminations of gastropod packstone and gastropod grainstone. The gastropods are small, to 4 mm wide, probably algal grazers and are heavily micritized and coated with algae. Hematite after pyrite (?) is common and would indicate a reducing environment similar to H₂S-rich sediment of a modern stabilized sand flat.

RADIOLITID LIME WACKESTONE AND PACKSTONE AND PELLET-INTRA-CLAST LIME PACKSTONE LITHOFACIES: LAGOONAL ENVIRONMENTS

Units 4, 11, 12, 14, 18, 19, and 21 represent two lithofacies which are sufficiently similar to be discussed in one section. The lithofacies are interpreted as deposits in a large complex interior lagoon environment. The predominant lithologies are whole and fragmented radiolitid lime wackestones and packstones and pellet-intraclast lime wackestones and packstones. Lime mudstones, laminated lime mudstones, requieniid lime wackestones and stromatolites

occur less frequently. The many lithologies, diagenetic features, and faunal assemblages characteristic of these lithofacies are shown on Plates 11, 12 and 15. The lithofacies are extremely thick, second in thickness to the basal dolomite lithofacies, and are characterized by rapid lithologic changes which are probably not laterally continuous and will probably not be useful for stratigraphic correlation. The variety of lithologic textures in the lagoonal environment is exemplified by units 11, 12, 13 and 18 (Figure 7). The units interpreted as representing lagoonal environments are subdividable into two primary lithofacies and subenvironments: open and restricted. Units 4, 12, 18 and 21 are interpreted as open lagoonal environments with units 12 and 18 used as examples. Units 11 and 13 are interpreted as restricted lagoonal environments and are the examples shown in Figure 7. Strata interpreted as representing the open lagoonal environment are differentiated from those of the restricted lagoonal environment by the sparse but relatively uniform occurrence of planktonic foraminifers and echinoid fragments.

The dominant lithologic texture in these lithofacies is pellet-intraclast packstone, with the exception of unit 12 where the wackestone texture is predominant. Nearly all the pellet-intraclast packstones are comprised of at least 10 to 20 percent skeletal fragments of which radiolitid rudists and solenoporacean algae are the most common constituents. Most of the pellets are 0.05 to 0.2 mm in diameter, irregularly elongate to roughly spherical in shape and might be more appropriately termed as peloids, after McKee and Gutschick (1969), because the origin of the particles is not known. They appear both as uniform particles of cryptocrystalline calcite and with a mottled appearance suggesting they are aggregates of smaller fecal(?) pellets. Grains larger than 0.2 mm were generally, unquestionably intraclasts comprised of composite grains of peloids or skeletal grains and peloids. Smooth, uniform ellipsoid shapes attributed to fecal pellets by various authors, including Shinn (1968b), Garrett (1977), Enos and Perkins (1977, p. 71), and Wanless and coworkers (1981), were sparse.

The peloids are interpreted to have formed by three primary modes: by intensive micritization of skeletal grains from boring endolithic algae, as fecal pellets, and by initial grain aggregation from blue-green algae and subsequent mechanical grain degradation of aggregates. All three modes of formation require well circulated water with low turbulence, stable substrates and water depths less than 12 to 15 m.

All stages of micritization were observed on skeletal grains in these lithofacies. The degree of micritization ranged from a thin rim a few microns thick to near obliteration of the grain where the skeletal structure was preserved only in the center of the grain. Even though micritization is commonly heavy, intensive micritization of skeletal grains is not interpreted to be a primary

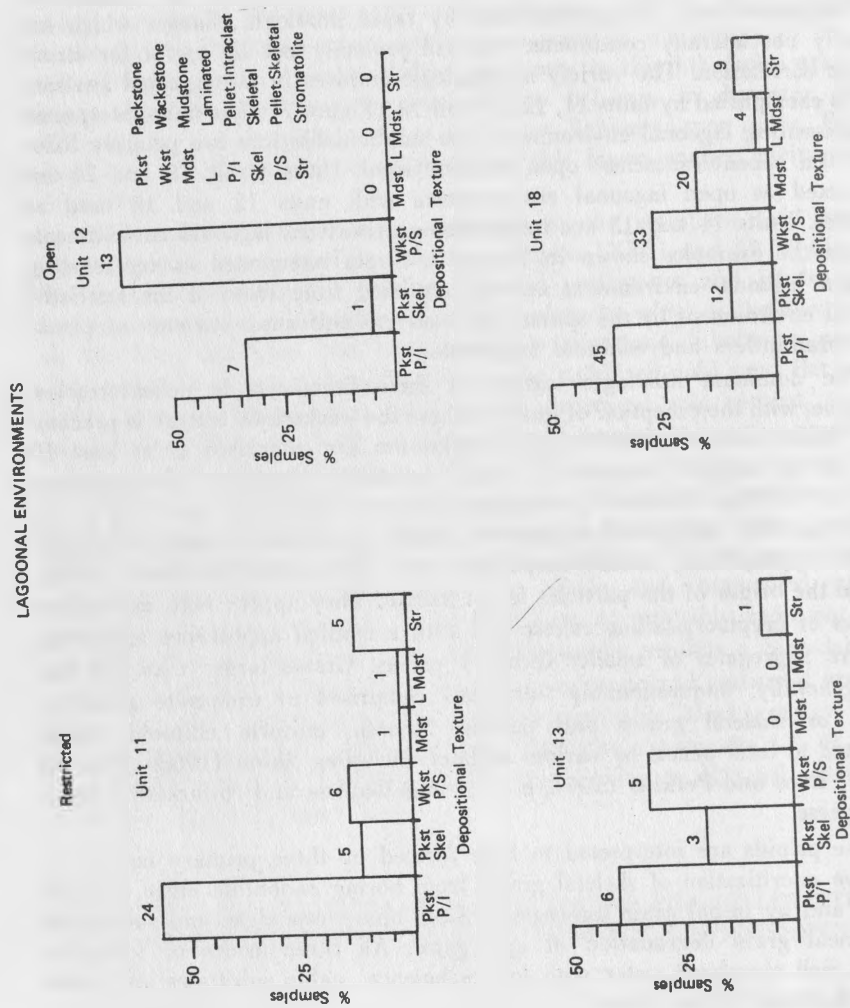


FIGURE 7.—Contrast in the distribution of depositional textures in representative units of open lagoonal deposits (units 12, 18) versus restricted lagoonal deposits (units 11, 13).

mode of peloid formation, because of the low abundance of nearly obliterated grains and the significantly larger size of skeletal fragments than the peloids. The extensive micritization does imply a unique physical environment. Intense micritization in Bahamian sediments is the result of endolithic blue-green algae (Purdy, 1963; Bathurst, 1966). The intense micritization largely occurs in a well-defined environment termed the grapestone facies (Purdy, 1963), or also the pelletoidal lime sand facies after Wanless and coworkers (1981). Multer (1977) observed that the primary control in the environment of deposition was "a high rate of water flow over the surficial sediments" to remove mud and preserve pore space, but with insufficient energy to allow grain mobility. These energy requirements are met behind the reef trend in water depths ranging from 10 to 15 m to 3 m which are within the depth limits for photosynthesis required by boring endolithic blue-green algae.

Many of the peloids in the packstones were probably formed as irregularly-shaped fecal pellets similar to those described by Ginsburg (1957), as suggested by the heavy bioturbation in most of the strata. In Holocene sediments pellets with the highest preservation potential are those formed by infaunal sediment feeders of which gastropods and polychaete worms are primarily important (Shinn, 1968b; Bathurst, 1975; Garrett, 1977; Multer, 1977). Without diagenetic hardening, the pellets compact within the first 20 cm of burial resulting in obscure pellet-grain boundaries. Pellet hardening is the result of rim micritization and early cementation at the sediment/water interface (Bathurst, 1975; Wanless *et al.*, 1981). These conditions are also characteristic of the Bahamian grapestone facies as previously discussed.

Grain aggregation resulting from blue-green algal sediment binding is interpreted to be a primary mechanism of peloid formation. Peloids could form by two processes of aggregation; whereby smaller allochems are bound together to form larger composite allochems similar to Bahamian grapestones as described by Windland and Matthews (1974), or whereby broad areas similar to subtidal *Schizothrix* algal mats described by Gebelein (1969) are eroded and mechanically degraded into smaller particles. Although grain aggregation similar to the formation of Bahamian grapestones is probably very common, the process cannot be demonstrated by simple petrographic examination. Evidence is strong for the mechanical break-down of subtidal algal mats, however.

Evidence for algal sedimentation binding is relatively common in these lithofacies as shown by the abundance of stromatolites with higher exposure indices (Figure 7). Unfortunately, there are no definite criteria to distinguish shallow subtidal algal bound sediments from low intertidal algal mats with a low exposure index. Due to the extent of the environment, subtidal algal binding as in the Bahamian grapestone facies, was probably more important

than intertidal processes. In contrast to intertidal stromatolites, subtidal algal bound sediments comprise a very small percent of an entire bed and do not exhibit regular thin laminations, fenestral fabric, or desiccation features. Vague discontinuous laminations occur when the sediment is not disturbed by heavy bioturbation and superficially appear as micrograded fining upward sequences sparsely distributed in a bed comprised of pellet-intraclast packstone. The laminations are up to 1.5 mm in thickness and are comprised of lime mud and small peloids ranging from 0.05 to 0.1 mm in diameter. Evidence that the sediment comprising the laminations is algal bound is two-fold. First, the laminations consistently span large intergranular pore spaces. Lime mud would have settled into the pore spaces if deposited as a fining upward sequence. Secondly, the laminations are cohesive after being eroded, either during episodic higher turbulence or by bioturbation. Once eroded, the laminations behave as intraclasts and readily break down into smaller-size particles. Presumably with continual reworking the intraclasts degrade into peloid-size particles. It is doubtful that intraclasts, other than the eroded algal-bound laminations, would degrade into the significant quantity and uniformity exhibited by the peloids in comprising the packstones.

Skeletal packstones are also characteristic of these lithofacies (Figure 7). The skeletal fragments are primarily comprised of unabraded whole and fragmented radiolitid rudists with sparse gastropods and pelecypod fragments. Beds of skeletal packstones are characterized by a sharp lower contact, crude lamination, fining upwards into pellet-intraclast packstones to grainstones, poor to moderate sorting, and sparry calcite comprising up to 75 percent of the cement (see Plate 11, A and C). The skeletal packstones are most commonly 5 to 15 cm thick and range rarely up to 40 cm thick (Plate 12, A and C). These features suggest that the packstones are storm deposits similar to those described by Ball and coworkers (1967), Perkins and Enos (1968) and Kresia (1981). The lack of lamination in the overlying pellet-intraclast packstones-grainstones suggests that the deposits are heavily bioturbated during the typically non-turbulent water conditions in the lagoon. Recent paleogeographic maps by Scotese and coworkers (in preparation) indicate that southern Mexico lay between 20° - 25° north latitude during the Albian-Cenomanian. These latitudes are within the latitudes characterized by hurricanes in the Holocene.

Radiolitid rudists are the single most characteristic feature of strata interpreted as lagoonal deposits. As previously discussed, the radiolitids do not primarily occur in growth position and are storm deposits. In the four units dominated by radiolitid rudists (units 11, 12, 13, and 18; excluding unit 21), which constitute 749.5 m of measured section, on only one small sample (XI-60, Plate 12, D) of a cluster were the radiolitids in growth position. The cluster consists of 24 individuals of the same species and two to three generations.

Kauffman and Sohl (1974) recognized and described diverse lagoonal assemblages of radiolitid rudists in primarily Upper Cretaceous exposures throughout the Caribbean. The inner lagoon foreslope assemblage described by Kauffman and Sohl (1974) has many similarities to assemblages observed in the units interpreted as lagoonal in the Sierra Madre Limestone. The inner lagoon foreslope assemblage is comprised primarily of rudists with common corals, stromatoporoids and algae. The rudists are characteristically small, erect and form small clusters and thickets. The clusters or thickets are dominated by a single genus and rarely exceed two generations as a result of episodic scouring and high-energy wave and current activity associated with tropical storms. Consequently radiolitid rudists were preserved as irregularly distributed, thin-bedded calcarenites with scattered *in situ* radiolitid clusters and thickets. Other paleoenvironmental interpretations include good water circulation, stable to semistable substrate, abundant food, light and subtidal water depths ranging to 3 m.

The upper 15 m of unit 21 are characterized by the unique occurrence of 10 cm thick, laterally continuous, single generation, single species, radiolitid thickets. The thickets are laterally equivalent to clusters of large radiolitids exhibiting polygonal cell wall structures in transverse section (Sauvagesiinae) which are characteristic of Upper Cretaceous genera and one Cenomanian genus (Coogan (1977b)). The marked difference between the radiolitids of unit 21 and other units, particularly unit 18, is interpreted to be an evolutionary adaptation of the rapidly radiating radiolitid rudists. However, there is also a difference in the depositional environment of unit 21. The absence of laminated mudstones, stromatolites, heavy micritization and clusters and the abundance of grumeleuse structure, suggest a deeper water, less turbulent environment of deposition.

Strata interpreted as representing deposition in an open lagoonal environment are differentiated from those interpreted as deposited in a restricted lagoonal environment by the sparse but uniform occurrence of planktonic foraminifers and echinoid fragments. The presence of planktonic foraminifers indicates relatively close proximity to open marine circulation and that the seaward barrier to the lagoon, the ooid sand complex, was not completely effective in preventing washover from and access to open marine circulation. The planktonic foraminifers are found in all lithologies including intertidal stromatolites and their presence alone does not indicate deposition at bathyal depths. Based on the paleoecology of Holocene echinoids, as discussed by Moore (1966) and Tasch (1973), the presence of echinoids implies normal tropical marine salinities (32 to 38 ‰). The presence of sponge spicules and solitary corals also implies near-normal salinities and well circulated water.

The contrast of depositional texture of units 12 and 18 (Figure 7) indicates

that the lithology of a unit interpreted as an open lagoonal environment may be similar to units interpreted as restricted, as in unit 18, or the lithology may be dissimilar, as is unit 12. The increase in the lime wackestone texture and the subsequent decrease in the lime packstone texture in unit 12 (which is similar to unit 21) is accompanied by a decrease in algal encrustation and grain micritization and an increase in grumeleuse structure. These differences are best interpreted as a result of an increase in the water depth in the lagoonal environment. A water depth greater than 15 m would probably result in insufficient light penetration to allow photosynthesis of blue-green algae, thus limiting algal encrustation and micritization which is also necessary for pellet hardening and preservation of pellet structure. An increase in water depth would also decrease the effectiveness of current winnowing, resulting in more wackestone textures.

Unit 18 is the best example of a complex lagoonal environment characterized by cyclical transitions of strata interpreted as subtidal, intertidal and supratidal deposits. Each subenvironment is defined by a unique combination of depositional textures, lithologies, sedimentary structures, early diagenetic features and fauna. Similar transition also occurs in units 11 and 13.

The lagoonal deposits, as previously described, consist of thin to thick-bedded pellet-intraclast packstones, thick-bedded, heavily-bioturbated skeletal wackestones commonly exhibiting grumeleuse structure, and thin-bedded storm deposits of skeletal packstones primarily comprised of whole and fragmented radiolitid rudists with sparse gastropods. Most of the skeletal material is heavily micritized, bored, encrusted by blue-green algae and solenoporoid algae indicating water depths of less than 10 to 15 m.

The shallow subtidal environment in the complex lagoon environment represented by unit 18 is characterized by thin to thick-bedded, heavily-bioturbated mudstones bearing whole requieniid rudists (*Toucasia?* sp.) and commonly exhibit grumeleuse structure. The lithology is very similar to the units comprising the platform interior mud environment.

The intertidal and supratidal environments are characterized by stromatolites often associated with *Thaumatoporella* which exhibit morphologies characteristic of both high and low indices of subaerial exposure, laminated mudstones exhibiting large planar fenestrae and vertical desiccation cracks, lithoclasts, penecontemporaneous fine to medium dolomite rhombs, celestite and selenite pseudomorphs replaced by celestite and calcite microspar (Plate 13). The evaporite minerals in the intertidal to supratidal sequences are interpreted to have formed on isolated subaerial islands in the open lagoon similar to mud banks and Keys in Florida Bay. Conditions for evaporite precipitation and preservation would have been more favorable during the long dry season characteristic of tropical climates. However, brackish water conditions probably

did not result during the rainy season as in Florida Bay, because there was no large paleogeographic continental land mass to supply fresh water runoff to the adjacent lagoon.

Other lagoonal environments are represented by units 4 and 19. Both units are comprised primarily of lime mudstones and lime wackestones. Both units are interpreted as quiet water lagoon deposits and underlie units interpreted as open marine deposits. However, the two lagoonal deposits represent two distinct subenvironments.

The primary sedimentary features observed in unit 4 were heavy bioturbation, thick to massive bedding, and tubular fenestrae. As discussed previously, tubular fenestrae are primarily associated with shallow subtidal and intertidal deposits within the platform interior mud environment. However, because they are the result of burrowing activity, they are not environmentally restricted and were observed (rarely) in unit 5 which are interpreted as open marine deposits. The primary allochems in unit 4 are sparse pellets and miliolids and abundant sponge spicules. The unit is interpreted as deeper water open lagoon deposits, primarily because of the abundance of sponge spicules, the stratigraphic position underlying open marine deposits, and the lack of features attributable to other shallow lagoon deposits such as radiolitid rudists, storm deposits, peloids, and abundant algae. Typical shallow water features, including a stromatolite and a dolomitic intraclast packstone, were collected but these unfortunately came from an interval of poor exposure and may be out of sequence. If the stratigraphic position of these samples is true, unit 4 more probably represents a platform interior environment with an anomalously high amount of sponge spicules.

The lithology, sedimentary structures, and fauna of unit 19 are highly varied. Lime packstones of large (to 3 cm) intraclasts or lithoclasts, thin-bedded grainstones interbedded with thin-bedded porcellaneous lime mudstones to pellet wackestones, thick-bedded gastropod (*Trochacteon* sp.) biostromes (Plate 15, E and F), abundant stromatolites, solenoporacean algae, and dasycladacean algae indicate shallow subtidal to intertidal water depths characterized by episodic scour and periods of high turbulence. This unit is interpreted as transitional between a thick, underlying succession of open lagoon deposits (unit 18) and a low energy platform interior lime mud environment.

PLANKTONIC FORAMINIFER BEARING NODULAR MOLLUSK LIME WACKESTONE LITHOFACIES: THE OPEN MARINE ENVIRONMENT

The lithofacies of planktonic foraminifer bearing mollusk lime wackestones represented by units 5, 7, 15, and 20 which comprise less than 4 percent (100 m) of the stratigraphic section, is interpreted to have been deposited in

an open marine shelf environment. The lithologic and diagenetic features characteristic of this lithofacies are shown on Plates 8 and 14. The environment of deposition is interpreted as open marine primarily on the basis of fauna rather than lithology. Although each unit is characterized by a unique faunal assemblage, each contains relatively abundant planktonic foraminifers, calcispheres, and whole or fragmented echinoids indicating normal marine salinity and open circulation. Other fauna, particularly abundant or unique to this lithofacies, are large gastropods including *Tylostomata* sp. and *Nerinea* sp., pelecypods, oysters, ammonites (rare), large solenoporacean algae, sponge spicules, calcisponges, and *Dicyclina schlumbergeri* - a large benthonic foraminifer.

The lithology and sedimentary features exhibited by this lithofacies are also variable. However, the depositional texture is almost exclusively lime wackestone comprised of mollusks and foraminifers (both planktonic and benthonic) and indicates minimal current winnowing and deposition below effective wave base. The skeletal allochems are both whole and fragmented. The fragments are not abraded and are probably the result of intensive bioturbation and weakening from boring rather than turbulent wave currents. The primary non-skeletal allochems are ellipsoidal fecal pellets, pelloids and "micro-pellets", commonly preserved as grumeleuse structure.

As previously noted, grumeleuse structure results from the compaction of unhardened fecal pellets which are primarily produced by infaunal deposit feeders. Conditions favorable to the formation of grumeleuse structure are low circulation rates, abundant intergranular lime mud and/or depths below the limit of photosynthesis for endolithic blue-green algae (15 m). Although circulation was probably good on the inferred open shelf, the depositional texture indicates that the sediments were below effective wave base. This depth must have also exceeded the limits of blue-green algae as indicated by the absence of micritization on skeletal grains.

Bedding in units 15 and 20 is characteristically nodular and marly, resulting from heavy sediment churning by irregular echinoids and crustaceans and from the influx of terrigenous clay and fine sand (observable only in the insoluble residue of unit 15). The most nodular beds occur in unit 15 in which the clay and echinoids are most abundant.

Chert nodules and silicified mollusks were most abundant within and stratigraphically proximal to units interpreted as open marine lithofacies. The chert nodules were only briefly examined in the field. Because the formation of chert nodules is apparently polygenetic and controversial, a comment on its environmental significance would be inappropriate.

Estimating the water depth of an open marine environment, based on evidence from the stratigraphic record, is extremely tenuous but useful. The

best indicators of water depth are photosynthetic algae. Algae utilize different wavelengths of the light spectrum depending on their pigmentation. Depending on a variety of factors, primarily water clarity, the different wavelengths have unique depths of penetration, therefore controlling the maximum depth ranges of the algae. As previously noted, blue-green algae are absent in this lithofacies and are most abundant in water less than 15 m deep. Also absent are dasy-cladacean algae which may extend to depths of 50 m but are abundant in depths less than 15 m (Ginsburg, 1972). Large solenoporacean algae (red algae), particularly abundant in unit 7, are usually found in water less than 95 m deep. Based on the presence of algae, the water depth of the open marine environment was greater than 15 m but less than 95 m.

The stratigraphic relationship is very significant between the mollusk lime wackestone lithofacies representing the open marine shelf environment and the ooid lime grainstone lithofacies representing the shallow platform ooid shoal environment. The gradational vertical lithofacies succession (Figure 6) suggests that the open marine environment passed gradationally along a gentle shelf slope into the shallow carbonate platform environment with skeletal lime sands and ooids deposited in a zone of higher energy between the two environments. A gentle shelf slope is also indicated by the sparse mixing between shallow and deeper water allochems, and absence of slumped or truncated beds, graded beds, and breccia or talus deposits. A steep shelf slope in the Ocozocuaula area would not be expected because the periods of open marine shelf deposition were probably brief and the known platform margin reported by Viniestra-Osorio (1981) was 75 km northwest of the study area.

PLANKTONIC FORAMINIFER LIME MUDSTONE LITHOFACIES: THE BASINAL OPEN MARINE ENVIRONMENT

Unit 6 (Plate 14, F), a planktonic foraminifer lime mudstone to wackestone with ostracods and sponge spicules represents a lithofacies interpreted to have been deposited in a deep outer shelf to basinal environment. As evidenced by the gradational contacts with the overlying and underlying units (5 and 7) interpreted as open marine shelf environments, this environment is inferred to be the basinward equivalent to previous and subsequent shelf environments.

The inferred depth of accumulation of this lithofacies and similar deposits is highly controversial because of the disparity between modern ocean systems and Cretaceous epicontinental shelf seaways. The presence of fine laminations in this lithofacies, disturbed only slightly by burrowing, suggests that the depth was below the range of most benthonic organisms. Benthonic organisms become sparse on modern shelves at a depth of 100 m because of rapidly diminishing

light (Ager, 1963). Recent planktonic foraminifer-rich muds with sparse benthonic organisms accumulate in ocean systems in hundreds of meters of water. Loucks (1977) used a non-uniformitarian approach and interpreted planktonic foraminifer wackestones in the Pearsall Formation to have been deposited in waters only slightly deeper than 20 m (60 feet). If the maximum depth interpretation of the units overlying and underlying unit 6 is correct, unit 6 was probably deposited in water depths exceeding 100 m.

GEOLOGIC INTERPRETATIONS OF SEQUENTIAL LITHOFACIES AND ENVIRONMENTS

The following interpretation of the geologic history of the Ocozocauitla region is based on only one partially incomplete composite measured section with relatively poor biostratigraphic control and a meager collection of previous studies to provide regional framework. However, in light of the absence of more detailed geologic reporting the writer hopes this study will provide a good reference point for continuing research and understanding of the basin evolution of southern Mexico.

By the end of the Neocomian, tectonism associated with the formation of the Gulf of Mexico was quiescent throughout southern Mexico. In west-central Chiapas basinal subsidence, denudation of the Chiapas massif and a marine transgression resulted in a facies change from predominately fluvial deposition characteristic of the Todos Santos Formation to marginal marine deposition characteristic of the San Ricardo Formation. The diverse lithologies in the San Ricardo Formation, ranging from tidal flat and supratidal evaporites to siliclastic and sandy carbonate marine deposits, indicate a widely fluctuating strandline along a low-relief arid coastal plain.

Continued denudation, transgression over the hinterland and coastal submergence led to a facies change from lithologies comprising the San Ricardo Formation deposited in a clastic dominated marginal marine environment to the dolomite and collapse breccia (unit 1) comprising the basal Sierra Madre Limestone deposited in a carbonate and evaporite dominated marginal marine environment. As previously noted, a disconformable contact between the San Ricardo Formation and the Sierra Madre Limestone has been interpreted on the basis of inconclusive faunal evidence. If the contact is disconformable, the lower dolomite and evaporite sequences of the Sierra Madre Limestone represent a coastal supratidal sabkha resulting from a transgressive shoreline over an erosional surface at the top of the San Ricardo Formation. This interpretation obscures the apparent genetic similarity between the upper San Ricardo Formation and the lower Sierra Madre Limestone and is not preferred until firm faunal or stratigraphic evidence is established.

Deposition kept pace with subsidence and a eustatic sea level rise throughout the Aptian and most of the Albian. During this time dolomite, some evaporite, pellet miliolid wackestones and requieniid rudist wackestones (units 1 and 2) were deposited in a low-energy quiet water platform interior environment. Much of these facies were pervasively dolomitized during deep burial.

Late Albian through early Cenomanian age strata comprise an unmeasured and undescribed interval of the composite measured section. Preliminary observations from the subsequent work by Guillermo Moreno, graduate student at the University of Texas at Arlington, indicate a possible open marine interval in this age strata.

During the mid-Cenomanian, the deposition rate did not keep pace with subsidence coupled with a eustatic rise in sea level. Consequently, deeper water conditions were established on the platform, carbonate production decreased rapidly and the platform was inundated rapidly and open marine conditions prevailed. Oyster-mollusk wackestones with echinoid fragments and planktonic microfauna (unit 5) were deposited on the broad open marine shelf. Planktonic foraminifer wackestones (unit 6) were deposited during the mid-Cenomanian when the previous platform was completely inundated and subsiding rapidly. The water depth may have exceeded 100 m at this time.

The previous facies sequence is schematically illustrated in Figure 8 and is interpreted as time transgressive (Figure 9). This implies that the facies were laterally equivalent through time, although the transition from carbonate platform to marine shelf was probably rapid. An exception is the planktonic foraminifer wackestone which is interpreted as a time-rock (chronostratigraphic) unit, having been extensively deposited over the shelf platform area during a limited time span. The facies sequence is probably a result of both basinal subsidence and eustatic sea level rise. The time of maximum inundation is apparently synchronous to the maximum global eustatic sea level rise described by Vail and coworkers (1977) as a result of rapid oceanic spreading in the Atlantic.

Based on global eustatic sea level curves, a rapid eustatic sea level fall in the mid-Cenomanian may have resulted in the exposure of the carbonate platform, dramatically decreasing the biological and depositional productivity of the platform prior to the marine transgression (Figure 9). Consequently, the following eustatic rise coupled with subsidence, resulted in a rapid transgression and the establishment of open marine conditions. As the depositional rate surpassed the combined rates of subsidence and sea level rise, a shallow carbonate platform rapidly prograded across a gently sloping open shelf. Planktonic foraminifer bearing oyster-mollusk wackestones (unit 7, Figure 9) were deposited on the open marine shelf.

The vertical sequence of facies resulting from the prograding platform is

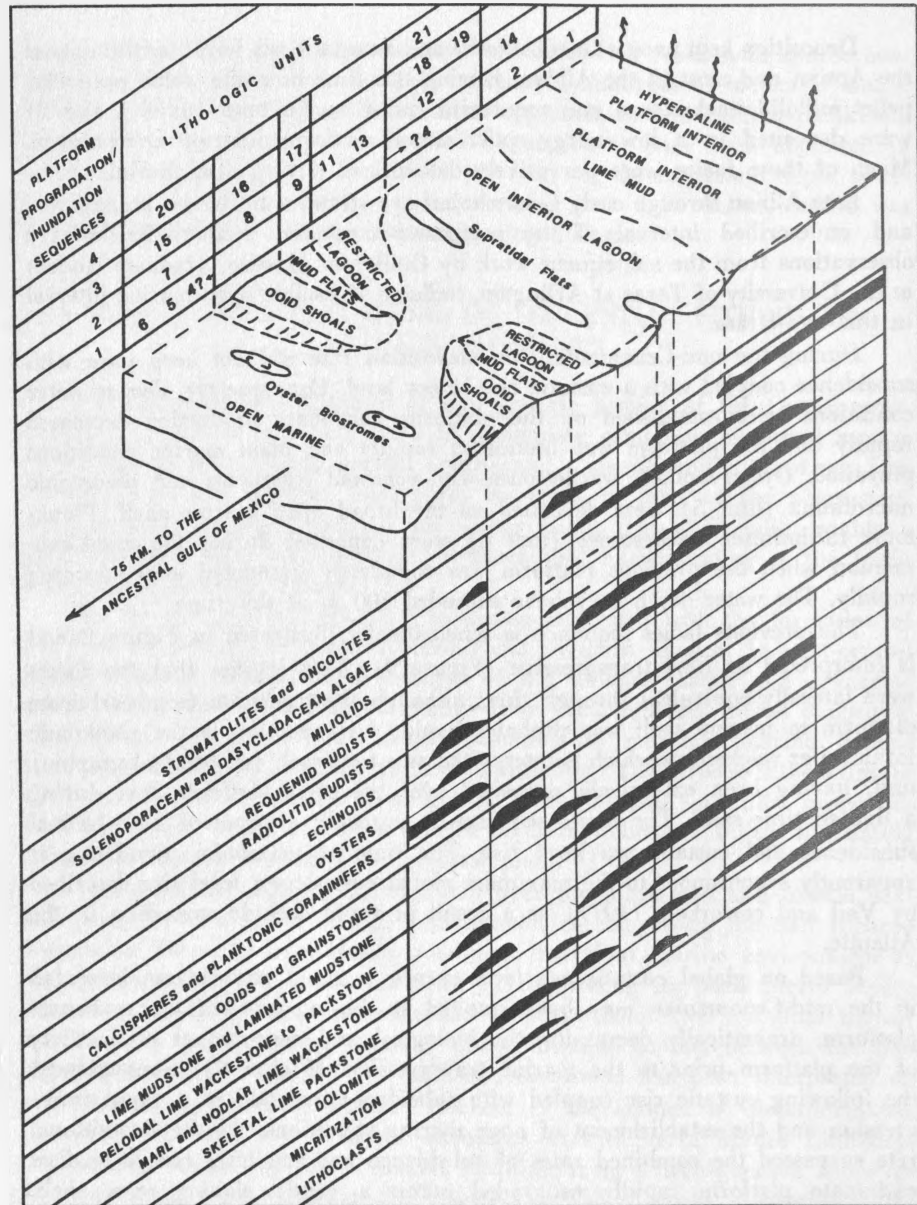


FIGURE 8.—The three dimensional depositional model inferred from the succession of lithofacies in the Sierra Madre Limestone of west-central Chiapas.

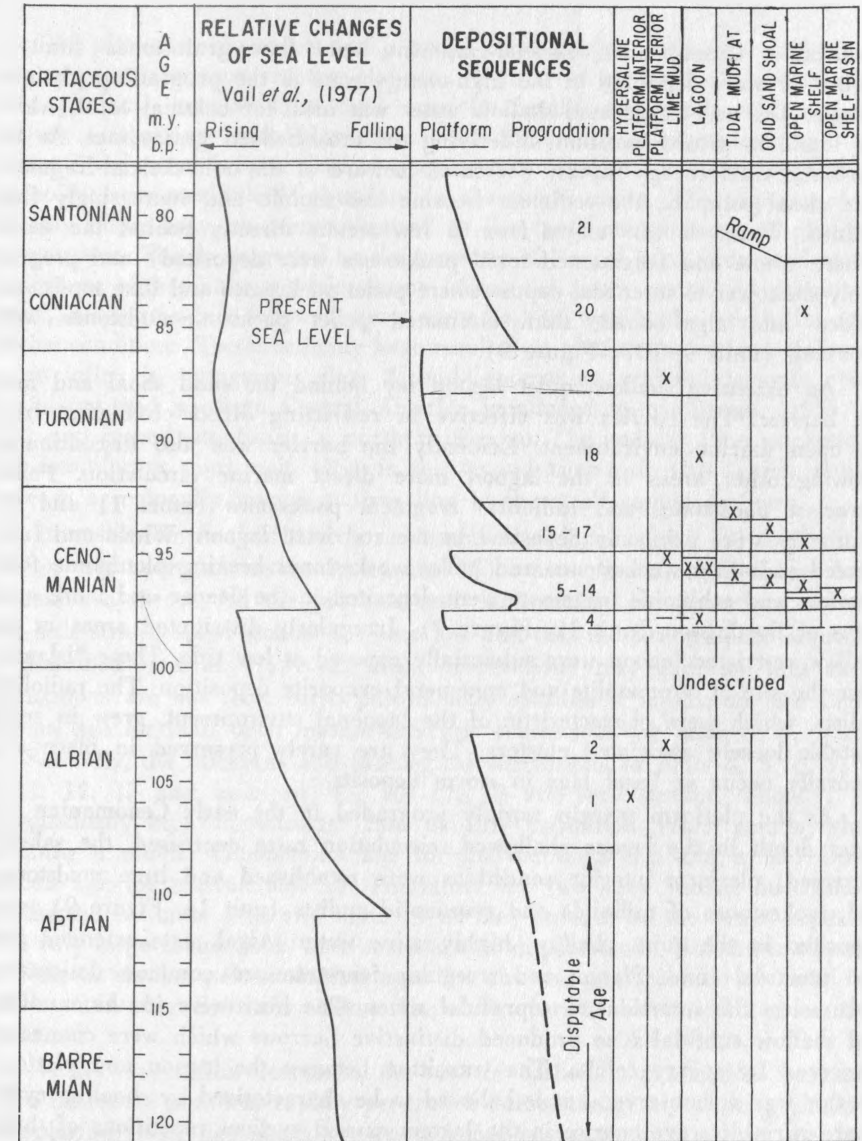


FIGURE 9.—Illustration of the predictable and orderly time-transgressive succession of lithofacies and depositional environments interpreted from the lithologic units of the Sierra Madre Limestone composite measured section, west-central Chiapas

predictable. Cross-bedded, skeletal-fragment, ooid lime grainstones (unit 8, Figure 9) were deposited in the high-energy zone at the prograding platform margin. The well-oxygenated shallow water was ideal for colonial corals which are found in growth position underlying the cross-bedded grainstones. As the wave and tidal energy rapidly decreased leeward of the ooid-skeletal-fragment, sand shoal complex, the sediment became less mobile and increasingly fine-grained. Water depths ranged from a few meters directly behind the shoals (where whole and fragmented fossil packstones were deposited) and progressively shallower to intertidal depths where pellet packstones and lime mudstones graded into algal-bound, thinly-laminated pellet packstone-mudstones were deposited (units 9, 10?; Figure 9).

An extensive shallow, quiet lagoon lay behind the sand shoal and mud flat barrier. The barrier was effective in restricting direct circulation from the open marine environment. Evidently the barrier was also discontinuous allowing other areas in the lagoon more direct marine circulation. Pellet-intraclast packstones and radiolitid fragment packstones (units 11 and 13, Figure 9) were primarily deposited in the restricted lagoon. Whole and fragmented radiolitid wackestones and pellet wackestones bearing planktonic foraminifers and echinoids fragments were deposited in the deeper and more open areas of the lagoon (unit 12, Figure 9). Irregularly distributed areas in the shallow restricted lagoon were subaerially exposed at low tide. These "islands" were the site of stromatolite and ephemeral evaporite deposition. The radiolitid rudists, which were characteristic of the lagoonal environment, grew in small unstable loosely associated clusters. They are rarely preserved in place and generally occur as basal lags in storm deposits.

As the platform margin rapidly prograded in the early Cenomanian the water depth in the lagoon shallowed, circulation rates decreased, the salinity increased, platform interior conditions were established and lime mudstones, and wackestones of miliolids and requieniid rudists (unit 14, Figure 9) were deposited in the quiet, shallow, highly-saline water. Algal mats extended into the intertidal zone. Planar and irregular fenestrae are common desiccation features in the intertidal to supratidal zones. The burrowers in the mudflats and shallow subtidal zone produced distinctive burrows which were commonly preserved by sparry calcite. The transition between the lagoon and platform interior was not observed but is believed to be characterized by shoaling cycles where variable wave energy in the lagoon caused cyclical repetitions of thick-bedded packstones and thin-bedded grainstones.

In the middle to late Cenomanian the Chiapas massif was subaerially exposed resulting in a strong influx of terrigenous clays covering the carbonate platform. The influx of clays was enough to decrease carbonate productivity on the platform. Consequently the subsidence rate exceeded the deposition

rate, the platform submerged and a broad open marine shelf was established. The rapid submergence of the platform resulted in an abrupt facies change from platform interior lime mudstones to fossiliferous marls and nodular mollusk wackestones with planktonic microfauna and calcispheres (unit 15, Figure 9) deposited in a shallow open marine shelf environment. Irregular echinoids were particularly abundant in the marly zones. The importance of the clay influx may be overemphasized as the fundamental cause of platform submergence. This is suggested by the presence of 7 m of hard, indurated oyster wackestone with planktonic microfauna below the marly zones. As previously stated, a eustatic fall followed by a eustatic rise would also result in open marine conditions. Tectonism may have resulted in platform subsidence followed by an influx in terrigenous clay. A mid-Cenomanian regional tectonic event in Chiapas and northern Central America is alluded to by Dengo (1975, p. 311) and is well-established in northern Mexico. The nodular lime wackestone and fossiliferous marl unit (15) is the second time-rock unit which should serve as a regionally mappable time line in the stratigraphic section.

It must be emphasized that the succession from lagoon (unit 13) to platform interior and open marine (units 14 and 15) was separated by a thrust fault of unknown throw. All the previous and forthcoming interpretations assume that little stratigraphic section has been lost and that the stratigraphic sequence as described is true. However, three observations may indicate that these assumptions are not true. First, paleontology ascribes a middle to late Cenomanian age for both open marine intervals represented by units 5, 6, 7 and 15. Secondly, the thickness and lithological successions of units 4, 5, 6, 7, 8, 9, 11, 12, 13 and units 14, 15, 16, 17, 18 are very similar. Thirdly, an unrealistically high depositional rate of 210 m/million years results when ascribing a middle Cenomanian age for marine units 5-7 and a late Cenomanian age for marine unit 15. Therefore, the two very similar successions represented by units 4-13 and units 14-18 may in fact be the same, repeated by a very large thrust fault with considerable displacement. Unfortunately, the problem of similar paleontological ages for the two marine intervals was not known until after the field season. Hopefully, further work will resolve this problem.

As the clay influx decreased, the rate of carbonate production increased and a carbonate platform rapidly prograded across the gently sloping, shallow, open-marine shelf, depositing a second facies sequence identical to the first progradational sequence. Cross-bedded ooid and skeletal fragment grainstones (unit 16, Figure 9) were deposited in the highest energy zone marginal to the open marine environment. Parts of the ooid sand shoals were subaerially exposed and cemented into beach-rock. Directly behind the shoal complex the water turbulence was minimal and the environment of deposition graded into

a low-energy tidal flat. Thin-bedded, dolomitic, thinly-laminated lime mudstones and stromatolites (unit 17, Figure 9) were deposited on the tidal flats. Lime mudstones bearing requieniid rudists, ostracods and sparse foraminifers (also unit 7) were deposited in the shallow subtidal area between the mobile sand shoal complex and the tidal flats.

A broad shallow lagoon environment lay leeward of the ooid sand shoal and tidal flat complex. The presence of planktonic foraminifers and echinoid fragments in the lagoonal deposits comprised of pellet-intraclast packstones and radiolitid packstones and wackestones (unit 18, Figure 9) indicates that the lagoon was characterized by open and good circulation. Good circulation was probably due to open access to the shelf environment through discontinuities through the ooid shoal and tidal flat complex. Gastropods and radiolitid rudists were the dominant fauna in the lagoon. Episodic storms toppled the small rudist clusters and deposited both radiolitids and gastropods as basal lags in storm deposits. Lime mudstones and *Toucasia?* sp. wackestones (also unit 18) were deposited in areas where circulation was apparently restricted by broad supratidal exposures. Stromatolites were deposited in the intertidal zones and thinly-laminated dolomitic lime mudstones with planar fenestrae indicate areas of supratidal tidal exposure. Stable platform conditions continued from the late Cenomanian through the Turonian.

By the late Turonian a platform interior environment was again being established. Lime mudstones, pellet wackestones to packstones, stromatolites and occasional thin-bedded grainstones (unit 19, Figure 9) were deposited in the low-energy shallow water environment. The lithologies appear porcellaneous. Gastropods with sparse *Toucasia* sp. and radiolitids were the dominant fauna.

Before thick accumulations of platform interior sediments could be deposited, the platform was once again submerged. In the early Coniacian *Dicyclina* sp. pellet wackestones bearing planktonic foraminifers and calcispheres (unit 20, Figure 9) were deposited on the open marine shelf abruptly overlying the previous platform interior sediments. The bedding is characteristically nodular resulting from heavy bioturbation, principally from echinoids. Nodular chert is also abundant. This unit defines the third time-rock unit in the stratigraphic section. This unit and the overlying limestones form the "Caliza Sin Nombre" which has been recognized as a mappable unit throughout Chiapas (Castro-Mora *et al.*, 1975).

The transition between the open marine shelf deposits and the overlying shallower water carbonates is not defined by a facies deposited in a zone of high energy and effective wave and current energy. The transition is characteristic of a gentle carbonate ramp rather than a prograding platform margin. The possibility also exists that the locality studied happened to represent an area between a laterally discontinuous higher energy environment. The facies

deposited in the shallower water open ramp environment consists primarily of whole radiolitid and pellet wackestones (unit 21, Figure 9). Many of the large radiolitid clusters and thickets are preserved in growth position. Storm deposits are largely absent. Other mollusks, echinoids and benthonic foraminifers are abundant. Planktonic foraminifers are sparse.

The duration of ramp or lagoonal deposition is not established as a result of poor biostratigraphic control. Carbonate deposition was continuous into the Santonian (Castro-Mora *et al.*, 1975; Waite, 1983). Widespread carbonate deposition ended by the Campanian. During the Campanian the entire region, including the Chiapas massif, was uplifted, resulting in a regional unconformity and terrigenous clastic fluvial deposition.

CONCLUSIONS

1. The Sierra Madre Limestone is approximately 3,430 m thick southwest of Ocozocuahtla, as shown by subsequent work (see footnote on p. 11).
2. The age of the formation is known to be at least Albian-Turonian with the lower and upper age limits disputably ranging from late Neocomian to Santonian.
3. Eight major cyclic lithofacies sequences are identifiable representing four periods of platform deposition and progradation interrupted by three major marine inundations.
4. A thick, basal Sierra Madre Limestone, late Neocomian? to Albian lithofacies succession, represents a transgressive sequence of hypersaline and normally saline platform interior environments. Basal collapse breccias in the hypersaline platform interior deposits indicate the former presence of evaporites.
5. Latest Albian and earliest Cenomanian age strata were not sampled due to inaccessibility in the field area.
6. Early Cenomanian to middle Cenomanian and middle Cenomanian to Turonian lithofacies successions were deposited on a rapidly prograding platform in platform edge ooid sand shoal, tidal mudflat, interior lagoon, and platform interior environments. Platform progradation was initiated when the platform deposition rate exceeded subsidence and eustatic sea level rise. It is possible that these two successions are in fact the same, and represent repeated section by a large thrust fault.
7. Planktonic foraminifer-bearing, nodular, mollusk fragment lime wackestones were deposited in an open marine shelf environment during the middle Cenomanian, late Cenomanian, and Coniacian.
8. Platform inundations during the middle Cenomanian, late Cenomanian, and Coniacian occurred during rapid eustatic sea level rise, probably following

a sea level fall and platform exposure. Argillaceous marl and quartz grains in late Cenomanian strata suggest that clastic input contributed to the inundation of the platform by inhibiting carbonate productivity.

9. Coniacian to Santonian age strata are characterized by whole radiolitic, pellet lime wackestones and radiolitic biostromes. The absence of both the higher energy ooid grainstone lithofacies and shallow water fauna and sedimentary structures indicates the existence of a carbonate ramp rather than of a platform.

REFERENCES CITED

- AGER, D. V., 1963, Principles of paleoecology: New York, McGraw-Hill, 371 p.
- ANDERSON, T. H., BURKART, BURKE, CLEMONS, R. E., BOHNENBERGER, O. H., AND BLOUNT, D. N., 1973, Geology of the western Altos Cuchumatanes, northwestern Guatemala: *Geol. Soc. America Bull.*, v. 84, p. 805-826.
- BALL, M. M., 1967, Carbonate sand bodies of Florida and the Bahamas: *Jour. Sed. Petrology*, v. 37, p. 556-591.
- BALL, M. M., SHINN, E. A., AND STOCKMAN, K. A., 1967, The geologic effects of Hurricane Donna in south Florida: *Jour. Geology*, v. 75, p. 583-597.
- BATHURST, R. G. C., 1966, Boring algae, micrite envelopes and lithification of molluscan biosparites: *Geol. Jour.*, v. 5, p. 15-32.
- , 1975, Carbonate sediments and their diagenesis: New York, Elsevier, 191 p.
- BLAIR, T. C., 1981, Alluvial fan deposits of the Todos Santos Formation of central Chiapas: Arlington, Univ. Texas at Arlington, M. Sc. thesis, 134 p. (unpublished).
- BLOUNT, D. N., AND MOORE, C. H., JR., 1969, Depositional and non-depositional carbonate breccias, Chiantla quadrangle, Guatemala: *Geol. Soc. America Bull.*, v. 80, p. 429-441.
- BÖSE, EMIL, 1905, Reseña acerca de la geología de Chiapas y Tabasco: *Inst. Geol. México, Bol.* 20, p. 5-100.
- BRICKER, O. P., ED., 1971, Carbonate cements: Baltimore, Johns Hopkins Press, 376 p.
- BROECKER, W. S., AND TAKAHASHI, T., 1960, Calcium carbonate precipitation on the Bahama Banks: *Jour. Geophys. Research*, v. 71, p. 1575-1602.
- BUFFLER, R. T., WATKINS, J. S., SHAUB, F. J., AND WORZEL, J. L., 1980, Structure and early geologic history of the deep central Gulf of Mexico basin: in *The origin of the Gulf of Mexico and the early opening of the central North Atlantic Ocean—a symposium*. Baton Rouge, Louisiana State Univ., p. 3-16.
- BURCKHARDT, CHARLES, 1930, Étude synthétique sur le Mésozoïque mexicain: *Soc. Paléont. Suisse, Mém.* 49-50, 280 p.
- BURKART, BURKE, AND CLEMONS, R. E., 1972, Late Paleozoic orogeny in northwestern Guatemala: Margarita, Venezuela, *Conferencia Geológica del Caribe*, 6, p. 210-213.
- CASTRO-MORA, JOSÉ, SCHLAEPFER, C. J., AND MARTÍNEZ-RODRÍGUEZ, EDUARDO, 1975, Estratigrafía y microfácies del Mesozoico de la Sierra Madre del Sur, Chiapas: *Bol. Asoc. Mex. Geólogos Petroleros*, v. 27, p. 1-103.
- CAYEUX, LUCIEN, 1935, Les roches sédimentaires de France; roches carbonatées (calcaires et dolomies): Paris, Masson, 413 p.
- CHUBB, L. J., 1959, Upper Cretaceous of central Chiapas, Mexico: *Am. Assoc. Petroleum Geologists Bull.*, v. 43, p. 725-755.
- CLEMONS, R. E., ANDERSON, T. H., BOHNENBERGER, O. H., AND BURKART, BURKE, 1974, Stratigraphic nomenclature of recognized Paleozoic and Mesozoic rocks of western Guatemala: *Am. Assoc. Petroleum Geologists Bull.*, v. 58, p. 313-320.
- CLOUD, P. E., JR., 1962, Environments of calcium carbonate deposition west of Andros Island, Bahamas: U. S. Geol. Survey, Prof. Paper 350, 138 p.
- CONTRERAS-VELÁZQUEZ, HUGO, AND CASTILLÓN-BRACHO, MANUEL, 1968, Domes of Isthmus of Tehuantepec: *Am. Assoc. Petroleum Geologists, Mem.* 8, p. 244-260.
- COOGAN, A. H., 1977a, Bahamian and Floridian biofacies: in Multer, H. G., ed., *Field guide to some carbonate rock environments, Florida Keys and western Bahamas*. Dubuque, Kendall/Hunt Publ. Co., p. 354-358.
- , 1977b, Early and middle Cretaceous Hippuritacea (rudists) of the Gulf Coast: in Bebout, D. G., and Loucks, R. G., eds., *Cretaceous carbonates of Texas and Mexico; applications to subsurface exploration*. Austin, Univ. Texas, Bur. Econ. Geology, Rept. Invest. 89, p. 32-70.
- COOGAN, A. H., BEBOUT, D. G., AND MACCIO, CARLOS, 1972, Depositional environments and geologic history of Golden Lane and Poza Rica trend, Mexico, an alternative view: *Am. Assoc. Petroleum Geologists Bull.*, v. 56, p. 1419-1447.
- DAVIES, P. J., BUBELA, B., AND FERGUSON, J., 1978, The formation of ooids: *Sedimentology*, v. 25, p. 703-730.
- DENCO, GABRIEL, 1975, Paleozoic and Mesozoic tectonic belts in Mexico and Central America: in Nairn, A.E.M., and Stehli, F. G., eds., *The ocean basins and margins; Volume 3, the Gulf of Mexico and the Caribbean*. New York, Plenum Press, p. 283-323.
- DUNHAM, R. J., 1962, Classification of carbonate rocks according to depositional texture: in *Classification of carbonate rocks — a symposium*. Am. Assoc. Petroleum Geologists, Mem. 1, p. 108-121.
- , 1971, Meniscus cement: in Bricker, O. P., ed., *Carbonate cements*. Baltimore, Johns Hopkins Press, p. 297-300.
- DZENS-LITOVSKY, A. I., AND VASIL'YEV, G. V., 1973, Geologic conditions of formation of bottom sediments in Karabogaz-Gol in connection with fluctuations in Caspian sea level: in Kiekland, D. W., and Evans, R., eds., *Marine evaporites, origin, diagenesis, and geochemistry*. Stroudsburg, Pa., Dowden, Hutchinson & Ross, p. 9-16.
- ENOS, PAUL, AND PERKINS, R. D., 1977, Quaternary sedimentation in south Florida: *Geol. Soc. America, Mem.* 147, 148 p.
- EVANS, G., KINSMAN, D. J. J., AND SHEARMAN, D. F., 1964, A reconnaissance survey of the environment of Recent sedimentation along the Trucial Coast, Persian Gulf: in Van Straaten L. M. J. U., ed., *Deltaic and shallow marine deposits*. Amsterdam, Elsevier, p. 129-135.
- EVANS, G., SCHMIDT, V., BUSH, P., AND NELSON, H., 1969, Stratigraphy and geologic history of the sabkha, Abu Dhabi, Persian Gulf: *Sedimentology*, v. 12, p. 145-159.
- FOLK, R. A., 1959, Practical petrographic classification of limestones: *Am. Assoc. Petroleum Geologists Bull.*, v. 43, p. 1-38.
- FRIEDMAN, G. M., 1959, Identification of carbonate minerals by staining methods: *Jour. Sed. Petrology*, v. 29, p. 87-97.
- , 1977, The Bahamas and southern Florida; a model for carbonate deposition: in Multer, H. G., ed., *Field guide to some carbonate rock environments, Florida Keys and western Bahamas*. Dubuque, Kendall/Hunt, p. 388.
- , 1980, Dolomite is an evaporite mineral; evidence from the rock record and from sea-marginal ponds of the Red Sea: in Zenger, D. H., Dunham, J. B., and Ethington, R. L., eds., *Concepts and models of dolomitization*. Soc. Econ. Paleontologists and Mineralogists, Spec. Publ. 28, p. 69-80.

- GARRETT, P., 1977, Biological communities and their sedimentary record: in Hardie, L. A., ed., Sedimentation on the modern carbonate flats of northwest Andros Island, Bahamas. Johns Hopkins Univ., Studies Geology 22, p. 124-158.
- GEBELEIN, C. D., 1969, Distribution, morphology and accretion rate of Recent subtidal algal stromatolites, Bermuda: Jour. Sed. Petrology, v. 39, p. 49-69.
- GINSBURG, R. N., 1957, Early diagenesis and lithification of shallow water carbonate sediments in south Florida: in LeBlanc, R. J., and Breeding, J. G., eds., Regional aspects of carbonate deposition. Soc. Econ. Paleontologists and Mineralogists, Spec. Publ. 5, p. 80-99.
- , 1964, South Florida carbonate sediments: Miami, Geol. Soc. America, Annual Meeting, Guidebook Field Trip 1, 72 p.
- , 1972, South Florida carbonate sediments: in Sediments II; marine geology and geophysics. Miami, Univ. Miami, Rosenstiel School of Marine and Atmospheric Science.
- GINSBURG, R. N., BRICKER, O. P., WANLESS, H. R., AND GARRETT, P., 1970, Exposure index and sedimentary structures of a Bahama tidal flat: Geol. Soc. America, Abstracts with Programs, v. 2, p. 744 (abstract).
- GINSBURG, R. N., AND HARDIE, L. A., 1975, Tidal and storm deposits, northwestern Andros Island, Bahamas: in Ginsburg, R. N., ed., Tidal deposits; a casebook of Recent examples and fossil counterparts. New York, Springer-Verlag, p. 201-208.
- GORSLINE, D. S., 1963, Environments of carbonate deposition, Florida Bay and Florida Straights: in Bass, R. O., and Sharps, S. L., eds., Shelf carbonates of the Paradox Basin. Denver, Four Corners Geol. Soc., Annual Field Conference, 4, p. 130-143.
- GROVER, G., JR., AND REED, J. F., 1978, Fenestral and associated diagenetic fabrics of tidal flat carbonates, Middle Ordovician New Market Limestone, southwestern Virginia: Jour. Sed. Petrology, v. 48, p. 453-473.
- GUTIÉRREZ-GIL, ROBERTO, 1956, Bosquejo geológico del Estado de Chiapas: México, D. F., Internat. Geol. Cong., 20, Libro-guia de la excursión C-15, p. 9-32.
- HARRIS, P. M., 1977, Depositional environments of Joulter Cays area: in Multer, H. G., ed., Field guide to some carbonate rock environments; Florida Keys and Western Bahamas, Dubuque, Kendall/Hunt, p. 157-162.
- HARRISON, R. S., AND STEINEN, R. P., 1978, Subaerial crusts, caliche profiles, and breccia horizons; comparison of some Holocene and Mississippian exposure surfaces, Barbados and Kentucky: Geol. Soc. America Bull., v. 89, p. 385-396.
- ILLING, L. V., 1959, Deposition and diagenesis of some upper Paleozoic carbonate sediments in western Canada: World Petroleum Congress, 5, Proc., Section 1, paper 2.
- KAHLE, C. F., 1974, Ooids from Great Salt Lake, Utah, as an analogue for the genesis and diagenesis of ooids in marine limestones: Jour. Sed. Petrology, v. 44, p. 30-39.
- KAUFFMAN, E. G., AND SOHL, N. F., 1974, Structure and evolution of Antillean Cretaceous rudist frameworks: Verhandl. Naturf. Ges. Basel, v. 84, p. 399-467.
- KENDALL, C. G., ST. G., AND SKIPWITH, P. A. D'E., 1968, Holocene shallow-water carbonate and evaporite sediments of Khor al Bazam, Abu Dhabi, southwest Persian Gulf: Am. Assoc. Petroleum Geologists Bull., v. 53, p. 841-869.
- KRESIA, R. D., 1981, Storm generated sedimentary structures in subtidal marine facies with examples from the Middle and Upper Ordovician of southwestern Virginia: Jour. Sed. Petrology, v. 51, p. 823-848.
- LAPORTE, L., 1967, Carbonate deposition near mean sea-level and resultant facies mosaic; Manlius Formation, Lower Devonian of New York State: Am. Assoc. Petroleum Geologists Bull., v. 51, p. 73-102.
- LOGAN, B. W., 1974, Diagenesis in Holocene-Recent carbonate sediments: in Logan, B.

- W., Hoffman, P., and Gebelein, C. D., eds., Evolution and diagenesis of Quaternary carbonate sequences, Shark Bay, western Australia. Am. Assoc. Petroleum Geologists, Mem. 22, p. 195-249.
- LONGMAN, M. W., 1980, Carbonate diagenetic textures from nearsurface diagenetic environments: Am. Assoc. Petroleum Geologists Bull., v. 64, p. 461-487.
- LÓPEZ-RAMOS, ERNESTO, 1975, Carta geológica del Estado de Chiapas (second edition): México, D. F., Univ. Nal. Autón. México, scale: 1:500,000.
- LOUCKS, R. G., 1977, Porosity development and distribution in shoal-water carbonate complexes - subsurface Pearsall Formation (Lower Cretaceous), South Texas: in Bebout, D. G., and Loucke, R. G., eds., Cretaceous carbonates of Texas and Mexico; applications to subsurface exploration. Austin, Univ. Texas, Bur. Econ. Geology, Rept. Invest. 89, p. 97-126.
- MANDELBAUM, H., AND SANFORD, J. T., 1952, Table for computing thickness of strata measured in a traverse or encountered in a bore hole: Geol. Soc. America Bull., v. 63, p. 765-776.
- MATTES, B. W., AND MOUNTJOY, E. W., 1980, Burial dolomitization of the Upper Devonian Miette buildup, Jasper National Park, Alberta: Soc. Econ. Paleontologists and Mineralogists, Spec. Publ. 28, 259-297.
- McKEE, E. D., AND GUTSCHICK, R. C., 1969, History of Redwall Limestone of northern Arizona: Geol. Soc. America, Mem. 114, 726 p.
- McKENZIE, J. A., HSU, K. J., AND SCHNEIDER, J. F., 1980, Movement of subsurface waters under the sabkha, Abu Dhabi, UAE, and its relation to evaporite dolomite genesis: in Zenger, D. H., Dunham, J. B., Ethington, R. L., eds., Concepts and models of dolomitization. Soc. Econ. Paleontologists and Mineralogists, Spec. Publ. 28, p. 11-30.
- MOORE, H. G., 1966, Ecology of echinoids: in Boolootian, R. A., ed., Physiology of Echinodermata: New York, Interscience, p. 73-83.
- MORAVEC, D. L., 1983, Study of the Concordia Fault System near Jerico, Chiapas, Mexico: Arlington, Univ. Texas at Arlington, M. Sc. thesis, 155 p. (unpublished).
- MULLER, G., 1971, "Gravitational" cement; an indicator for the vadose zone of subaerial diagenetic environment: in Bricker, O. P., ed., Carbonate cements: Baltimore, Johns Hopkins Press, p. 301-302.
- MÜLLERRIED, F. K. G., 1936, Estratigrafía preterciaria preliminar del Estado de Chiapas: Bol. Soc. Geol. Mexicana, v. 9, p. 31-41.
- MULTER, H. G., 1977, Field guide to some carbonate rock environments; Florida Keys and western Bahamas: Dubuque, Kendall/Hunt Pub. Co., 415 p.
- MULTER, H. G., AND HOFFMEISTER, J. E., 1968, Subaerial laminated crusts of the Florida Keys: Geol. Soc. America Bull., v. 79, p. 183-192.
- PERKINS, B. F., 1969, Rudist faunas in the Comanche Cretaceous of Texas: in Shreveport Geological Society Guidebook, 1969, Spring Field Trip; Comanchean Stratigraphy of the Fort Worth-Waco-Belton Area, Texas, Baton Rouge, Louisiana State Univ., p. 121-137.
- , 1974, Paleogeology of a rudist reef complex in the Comanche Cretaceous Glen Rose Limestone of central Texas: Geoscience and Man, v. 8, p. 131-173.
- PERKINS, R. D., 1963, Petrology of the Jeffersonville Limestone (Middle Devonian) of southeastern Indiana: Geol. Soc. America Bull., v. 74, p. 1335-1354.
- PERKINS, R. D., AND ENOS, PAUL, 1968, Hurricane Betsy in the Florida-Bahama-area geologic effects and comparison with Hurricane Donna: Jour. Geology, v. 76, p. 710-717.
- PURDY, E. G., 1963, Recent calcium carbonate facies of the Great Bahama Bank; I.

- Petrology and reaction groups; 2. Sedimentary facies: *Jour. Geology*, v. 71, p. 334-335, 472-497.
- PURSER, B. H., ED., 1973, *The Persian Gulf; Holocene carbonate sedimentation and diagenesis in a shallow epicontinental sea*: Berlin, Springer-Verlag, 471 p.
- REEVES, C. C., JR., 1976, *Caliche*: Lubbock, Texas, Estacado Books, 233 p.
- RICHARDS, H. G., 1963, Stratigraphy of earliest Mesozoic sediments in southeastern Mexico and western Guatemala: *Am. Assoc. Petroleum Geologists Bull.*, v. 47, p. 1861-1870.
- ROBERTS, R. J., AND IRVING, E. M., 1957, Mineral deposits of Central America: *U. S. Geol. Survey, Bull.* 1034, 205 p.
- RUSNAK, G. A., 1960, Some observations of recent oolites: *Jour. Sed. Petrology*, v. 30, p. 471-480.
- SÁNCHEZ-MONTES DE OCA, R., 1969, Estratigrafía y paleogeografía del Mesozoico de Chiapas: *Inst. Mex. Petróleo, Seminario Expl. Petrol., Mesa Redonda* 5, 31 p.
- SAPPER, KARL, 1894, Grundzüge der physikalischen Geographie von Guatemala: *Petermanns Geog. Mitt., Erg.* 24, n. 113, 59 p.
- , 1899, Über Gebirgsbau und Boden des nördlichen Mittelamerika: *Petermanns Geog. Mitt., Erg.* 27, n. 127, 119 p.
- SCOTSESE, C. R., BAMBACK, R. K., BARTON, C., VAN DER VOO, R., AND ZIEGLER, A. M., In preparation, Mesozoic base maps: The University of Chicago, The University of Michigan.
- SHINN, E. A., 1968a, Practical significance of birdseye structures in carbonate rocks: *Jour. Sed. Petrology*, v. 38, p. 215-224.
- , 1968b, Burrowing in Recent lime sediments of Florida and the Bahamas: *Jour. Paleontology*, v. 42, p. 879-894.
- SHINN, E. A., LLOYD, R. M., AND GINSBURG, R. N., 1969, Anatomy of a modern carbonate tidal-flat, Andros Island, Bahamas: *Jour. Sed. Petrology*, v. 39, p. 1202-1228.
- STEELE, D. R., 1982, Physical stratigraphy and petrology of the Cretaceous Sierra Madre Limestone, west-central Chiapas, Mexico: Arlington, Univ. Texas at Arlington, M. Sc. thesis, 1974 p. (unpublished).
- SWANSON, R. G., 1981, Sample examination manual: Tulsa, Am. Assoc. Petroleum Geologists, p. III-3 to III-9.
- TASCH, P., 1973, Encoded data in living and fossil echinoids: in *Paleobiology of the invertebrates, data retrieval from the fossil record*: New York, John Wiley, p. 672-700.
- TEBBUTT, G. E., CONLEY, C. D., AND BOYD, D. W., 1965, Lithogenesis of a distinctive carbonate rock fabric: University of Wyoming, *Cont. Geology*, v. 4, p. 162-167.
- VAIL, P. R., MITCHUM, R. M., AND THOMPSON, S., 1977, Seismic stratigraphy and global changes of sea level; part 4, global cycles of relative changes of sea level. *Am. Assoc. Petroleum Geologists, Mem.* 26, p. 83-97.
- VER WIEBE, W. A., 1925, Geology of the southern Mexico oil fields: *Pan-Am. Geol.*, v. 44, p. 12-128.
- VINIEGRA-OSORIO, FRANCISCO, 1971, Age and evolution of salt basins of southeastern Mexico: *Am. Assoc. Petroleum Geologists Bull.*, v. 55, p. 478-494.
- , 1981, Great carbonate bank of Yucatán, southern Mexico: *Jour. Petroleum Geology*, v. 3, p. 247-278.
- VINSON, G. L., 1962, Upper Cretaceous and Tertiary stratigraphy of Guatemala: *Am. Assoc. Petroleum Geologists Bull.*, v. 46, p. 425-456.
- WAITE, L. E., 1983, Biostratigraphic and paleoenvironmental analysis of the Cretaceous Sierra Madre Limestone, Chiapas, southern Mexico: Arlington, Univ. Texas at Arlington, M. Sc. thesis, 192 p. (unpublished).

- WALPER, J. L., 1960, Geology of Cobán-Purulhá area, Alta Verapaz, Guatemala: *Am. Assoc. Petroleum Geologists Bull.*, v. 44, p. 1273-1315.
- WANLESS, H. R., BURTON, E. A., AND DRAVIS, J., 1981, Hydrodynamics of carbonate fecal pellets: *Jour. Sed. Petrology*, v. 51, p. 27-36.
- WILSON, H. H., 1974, Cretaceous sedimentation and orogeny in nuclear Central America. *Am. Assoc. Petroleum Geologists Bull.*, v. 58, p. 1348-1396.
- WINDLAND, H. D., AND MATTHEWES, R. R., 1974, Origin and significance of grapestone, Bahama Islands: *Jour. Sed. Petrology*, v. 44, p. 921-927.
- WONG, P. K., AND OLDERSHAW, A., 1981, Burial cementation in the Devonian Daybob Reef Complex, Alberta, Canada: *Jour. Sed. Petrology*, v. 51, p. 507-520.
- ZAVALA-MORENO, J. M., 1971, Estudio geológico del proyecto hidroeléctrico Cañón del Sumidero, Río Grijalva, Estado de Chiapas: *Bol. Asoc. Mex. Geólogos Petroleros*, v. 23, p. 1-92.

APPENDIX

The geometric method outlined by Mandelbaum and Sanford (1952) was used to determine the thickness of strata which were inaccessible or impractical to measure by other means.

The general formula is:

$$T = s (\cos a \sin c \sin d \pm \sin a \cos d)$$

where: s = slope distance

a = slope angle

c = angle between strike and traverse

d = dip angle

+ is used when the slope and dip are opposed.

— is used when the slope and dip are the same direction.

CETENAL maps of a 1:50,000 scale and 20 m contour interval were used to measure distances, angles and slopes.

The structural geology was field checked when possible; when not, regional strike and dip was used.

A. Estimated thickness of unit 1, as calculated along Pan American Highway 190 to section V, unit 2.

1. Interval 1, from contact with San Ricardo

Map distance:	1,850 m
Elevation difference:	20 m
Strike and dip:	N35W, 8°NE; 10°NE (maximum)
Road bearing:	N47W
s	= 1,850 m
a	= .169°
c	= 82°
d	= 8° to 10° (max)
T	= 274 m
T (max)	= 337 m

2. Interval 2, to measured section IX

Map distance: 550 m
 Elevation difference: 0 m
 Strike and dip: N38W, 9°NE, 10°NE (max)
 Road bearing: N68E
 $s = 550$ m
 $a = 0$ m
 $c = 74^\circ$
 $d = 9^\circ, 10^\circ$ (max)
 $T = 81$ m
 T (max) = 91 m

3. Interval 3, measured section IX

$T = 30$ m

4. Interval 4, measured section IX to measured section V

Map distance: 2,050 m
 Elevation difference: 20 m
 Strike and dip: N45W, 12°NE (average)
 Road bearing: N20E
 $s = 2,050$ m
 $a = .558^\circ$
 $c = 65^\circ$
 $d = 12^\circ$
 $T = 405$

5. Dolomite in section V

$T = 37$ m

6. Thickness of unit 2

$T = 827$ m
 T (max) = 900 m

B. Estimated thickness of unit 3.

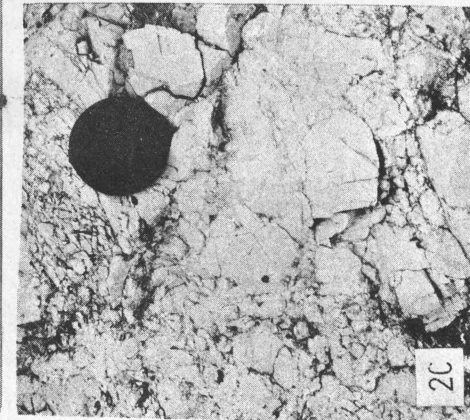
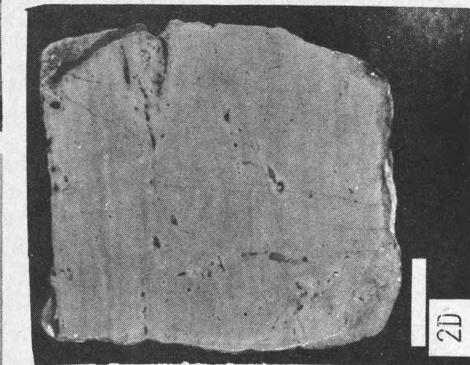
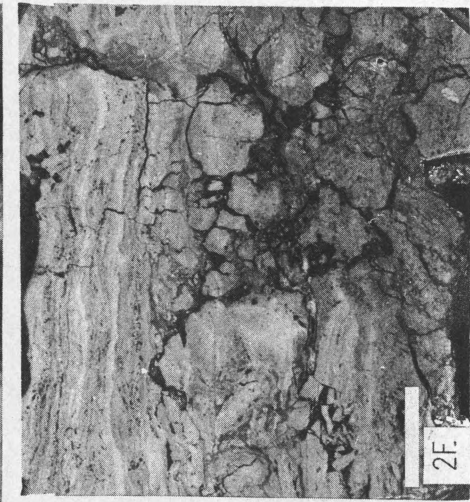
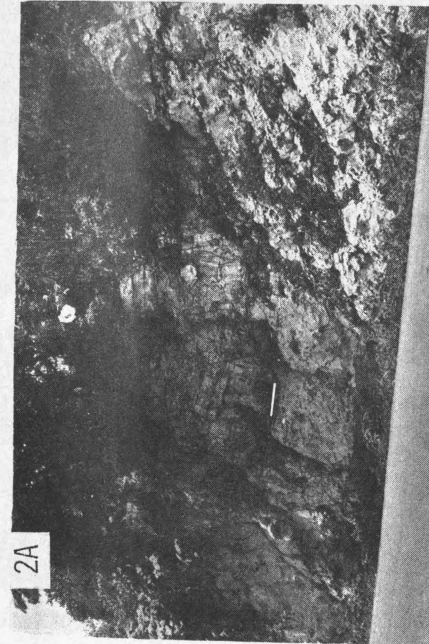
Map distance: 13,850 m
 Elevation difference: 210 m
 Strike and dip: N28W, 8°NE
 Traverse bearing: N55W
 $s = 13,850$ m
 $a = .7440$
 $c = 17^\circ$
 $d = 8^\circ$
 $T = 344$

PLATES 2-15

P L A T E 2

FIELD EXPOSURES AND CHARACTERISTIC TEXTURES OF THE BASAL
COLLAPSE BRECCIA AND DOLOMITE LITHOFACIES

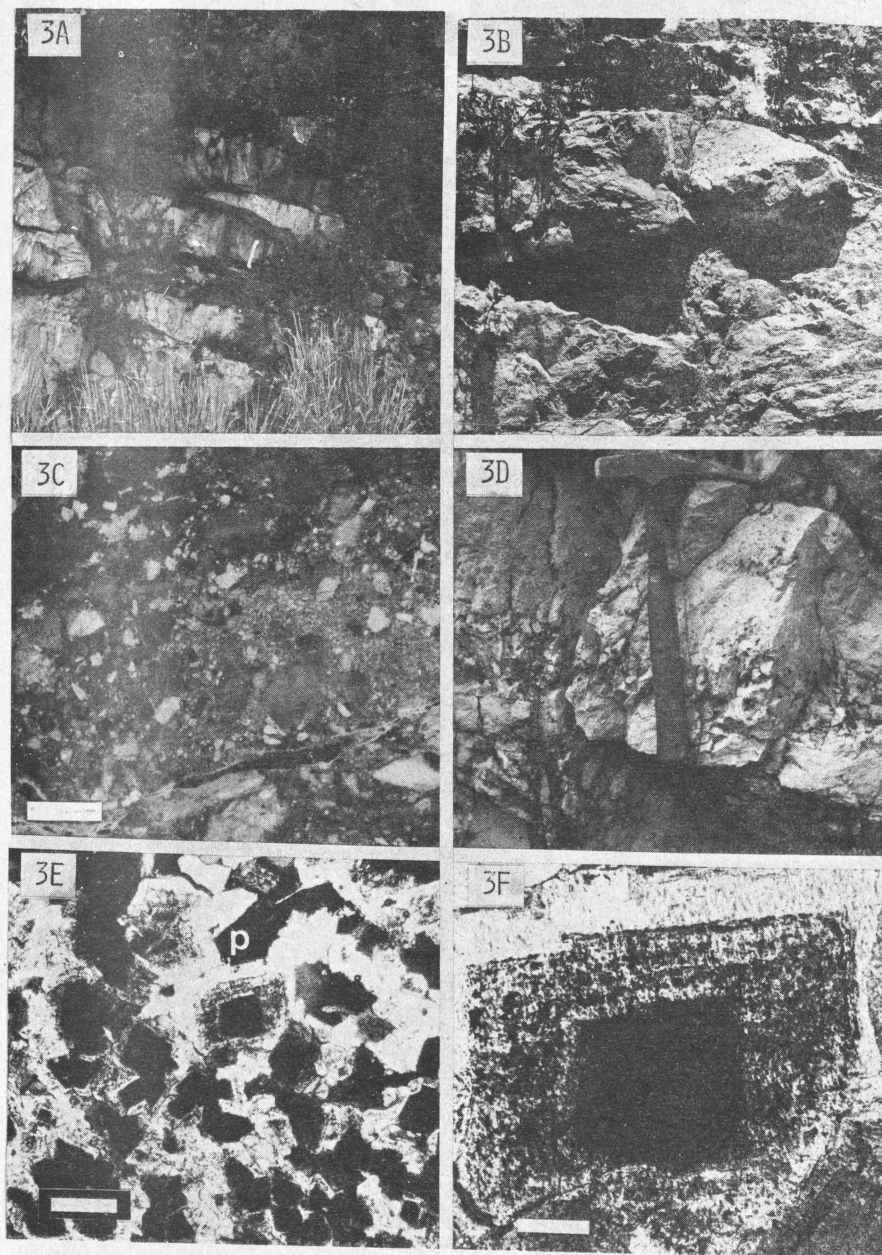
- 2A — Collapse breccia overlying the San Ricardo Formation (to the right, not pictured) along the Federal Highway 190 at section II. The white line (left center) separates a large collapse block of disturbed bedding from the underlying breccia (Plate 2C).
- 2B — Highly porous collapse breccia with "white-sparry" dolomite cement. Float block at section II. Hammer for scale.
- 2C — Collapse breccia directly beneath the disturbed beds shown in 2A. Note the vertical fractures in the clasts and the absence of "white-sparry" dolomite matrix. Camera lens cap for scale.
- 2D — Thinly-laminated, finely-crystalline dolomite, characteristic of the lower 100 m overlying the basal collapse breccia at section VII. Note the tubular and irregular fenestrae. Sample VII-15; 1.0 cm bar for scale.
- 2E — Thinly-laminated, finely-crystalline dolomite exhibiting desiccation fractures, planar fenestrae and brecciation. Brecciation and collapse is probably from the dissolution of evaporites. Float sample from section VII; 1.0 cm bar for scale.



P L A T E 3

CHANNEL DEPOSITS AND DOLOMITE TEXTURES CHARACTERISTIC OF THE
COLLAPSE BRECCIA AND DOLOMITE FACIES

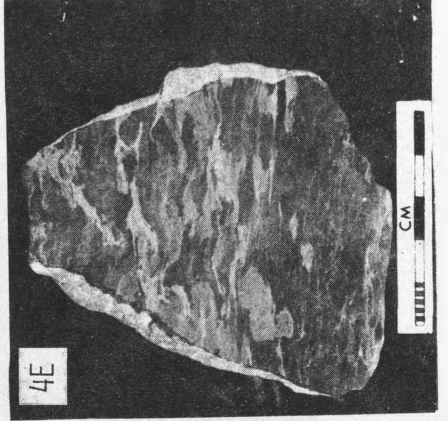
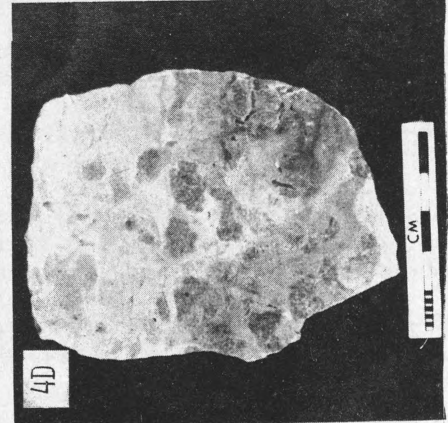
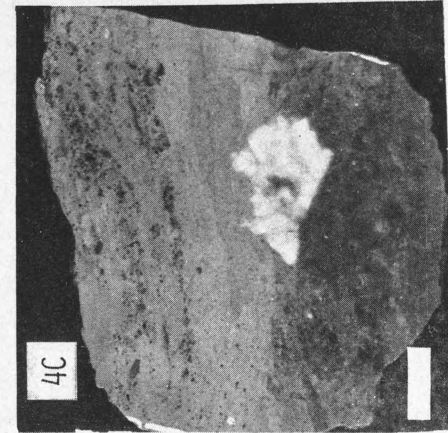
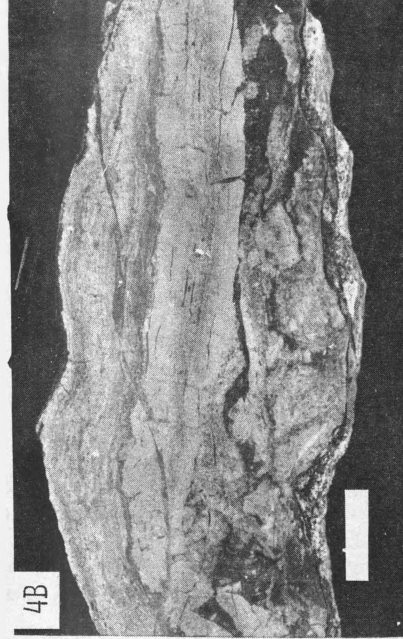
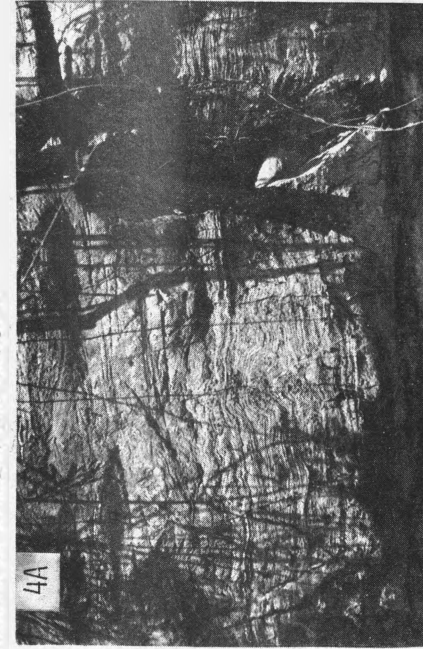
- 3A — A tidal channel at section IX along Federal Highway 190. Note lense shape and scour into the underlying bed. The white bracket highlights the hammer used for scale.
- 3B — A tidal channel at section IV. Note the moss and small plant (left center) growing in the porosity developed from dissolution of a basal shell lag. The bed is approximately 35 cm thick.
- 3C — Angular to subround polymictic lithoclast depositional breccia deposited as a basal lag in a tidal channel, Sample IX-14; 1.0 cm bar for scale.
- 3D — A zone of intraparticle porosity at section IX, developed as a result of dissolution of high spired gastropods and small pelecypods in a shell lag. Hammer for scale.
- 3E — Sample VII-12, representative of the coarsely to very coarsely-crystalline dolomite. The "P" indicates intercrystalline porosity. 1.0 mm bar for scale, XN.
- 3F — Sample VII-12 showing zoning in the dolomite crystals and dark inclusions — probably of calcite. Bar scale is 0.15 mm.

CHANNEL DEPOSITS AND DOLOMITE TEXTURES CHARACTERISTIC OF THE
COLLAPSE BRECCIA AND DOLOMITE FACIES

P L A T E 4

ALGAL STROMATOLITES AND SEDIMENTARY STRUCTURES
CHARACTERISTIC OF THE UPPER INTERVAL IN THE COLLAPSE BRECCIA
AND DOLOMITE LITHOFACIES

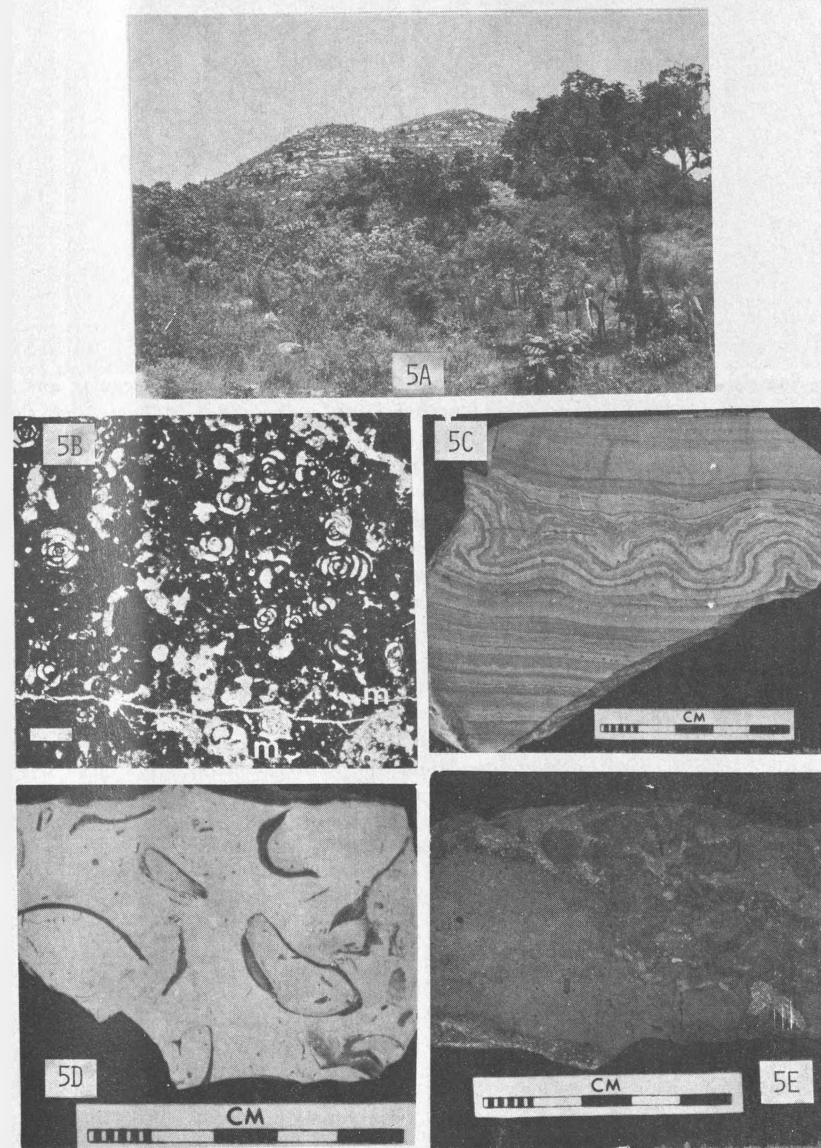
- 4A — Well developed stromatolites at section IV. Hammer for scale.
- 4B — Sample IV-18 collected from the lateral pinchout of Plate 3A. Note the desiccation fractures, planar fenestrae, and brecciation which are overlain by a thin interval of stromatolites. Polished slab; 2.0 cm bar for scale.
- 4C — Sample IX-4 of thinly-laminated, finely-crystalline dolomite overlying medium crystalline dolomite. Note the numerous small vugs and anhydrite nodule disrupting the laminations. Polished slab; 1.0 cm bar for scale.
- 4D — Sample V-12 exhibiting heavy burrowing. Dolomite filling the burrows (light) is finely-crystalline, while dark dolomite matrix is coarsely-crystalline. Polished slab.
- 4E — Sample V-13 exhibiting wispy laminations in dolomite resulting from slight burrowing and differential compaction. Polished slab.



P L A T E 5

FIELD EXPOSURES OF SECTION V AND LITHOLOGIC FEATURES
 CHARACTERISTIC OF THE LIME MUDSTONE, AND PELLET, MILIOLID,
 REQUIENIID RUDIST LIME WACKESTONE LITHOFACIES

- 5A — View of section V as seen looking to the southeast from the road to Cascada El Aguacero (section IV). The beds which look like bioherms are merely a product of weathering.
- 5B — Sample V-57, slightly dolomitic lime wackestone of miliolids and pellets. Dolomite is preferentially replacing miliolids (m). Thin section, plane light; 0.5 mm bar for scale.
- 5C — Laminoid caliche crust. Note the lack of desiccation features, and thinning of laminations over highs and thickening into lows. Polished slab.
- 5D — Sample XIII-14, requieniid (*Toucasia* sp?) lime wackestone. Samples are whole and undisturbed indicating quiet water deposition. Polished slab.
- 5E — Sample V-34, a large intraclast lime packstone exemplifying a storm deposit. Small white "spots" are miliolids. Polished slab.

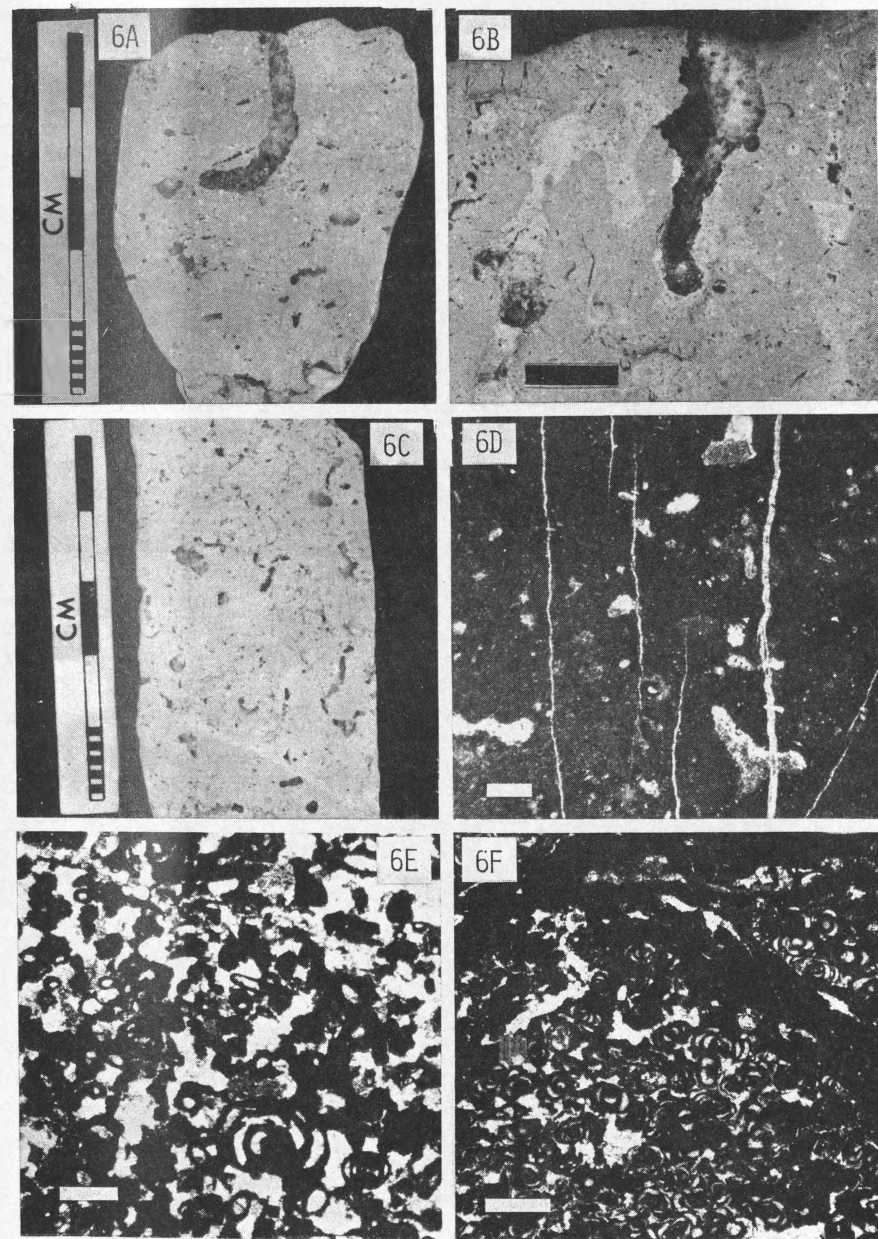


FIELD EXPOSURES OF SECTION V AND LITHOLOGIC FEATURES
 CHARACTERISTIC OF THE LIME MUDSTONE, AND PELLET, MILIOLID,
 REQUIENIID RUDIST LIME WACKESTONE LITHOFACIES

P L A T E 6

FENESTRAL FABRICS

- 6A — Sample XIII-30, pelletal, miliolid lime wackestone with large irregular and "U" shaped tubular fenestrae. The fenestral fabric is the result of burrowing. Polished slab.
- 6B — Sample XIII-26, large tubular fenestrae filled by coarsely-crystalline calcite. Note that the slab is heavily burrowed with the other burrows filled by internal sediment. Small tubular fenestrae are also present. Polished slab; 1.0 cm bar for scale.
- 6C — Sample XIII-28, small sinuous tubular fenestrae which bifurcate. Polished slab.
- 6D — Sample XI-7, lime mudstone with irregular fenestrae exhibiting geopetal structures. Thin section, plane light; 0.5 mm bar for scale.
- 6E — Sample XI-3, algal boundstone with highly irregular fenestral fabric. Tubular structures appear to be solenoporacean algae when well preserved. The entire fabric is knit together by mucilagenous blue green algae. Note the trapped miliolid. Thin section; XN; 0.5 mm bar for scale.
- 6F — Sample XIII-6, algal stromatolite exhibiting planar fenestrae. Note the "bubble" shaped laminations and abundant miliolids bound by the mucilagenous blue green algae. Sample collected from the top of a shoaling cycle characteristic of the base of section XIII. Thin section, plane light; 1.0 mm bar for scale.

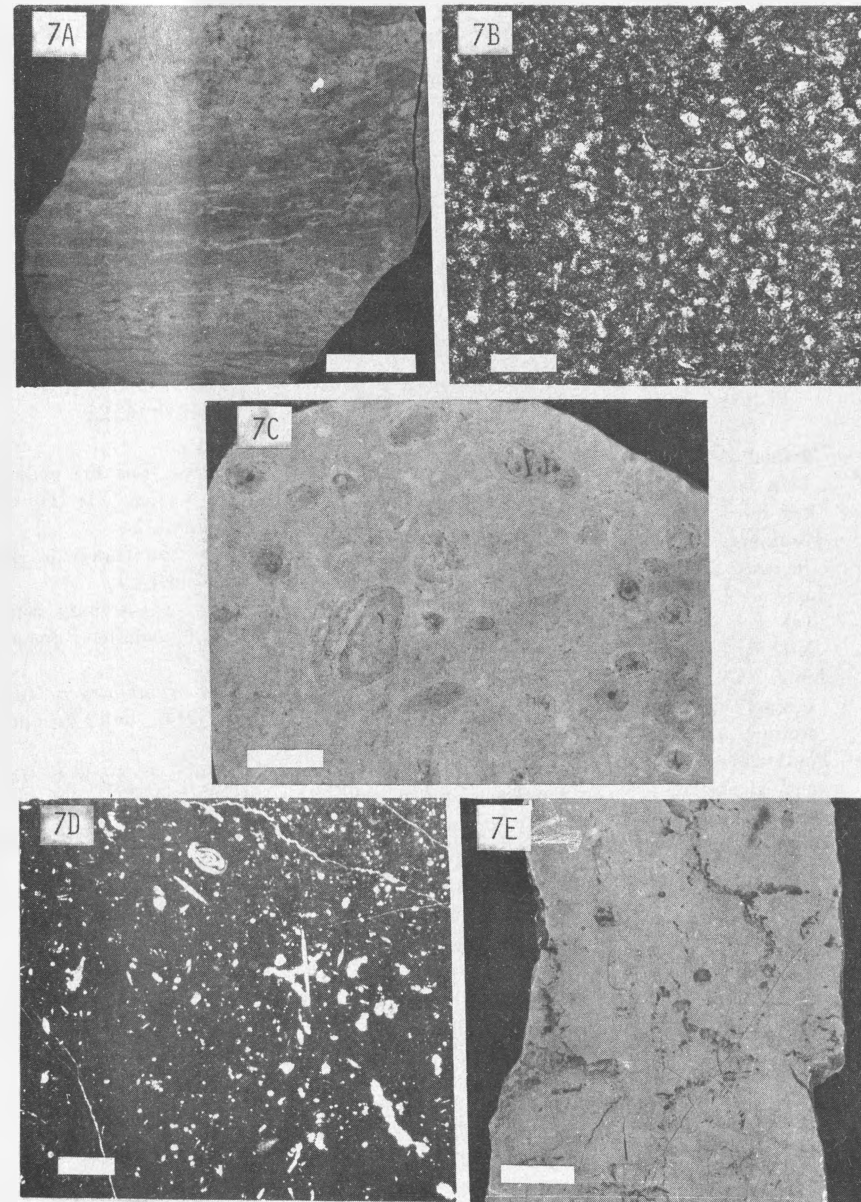


FENESTRAL FABRICS

P L A T E 7

REPRESENTATIVE LITHOLOGIC TEXTURES OF UNIT 4 AND THE LIME
MUDSTONE AND LAMINATED LIME MUDSTONE LITHOFACIES

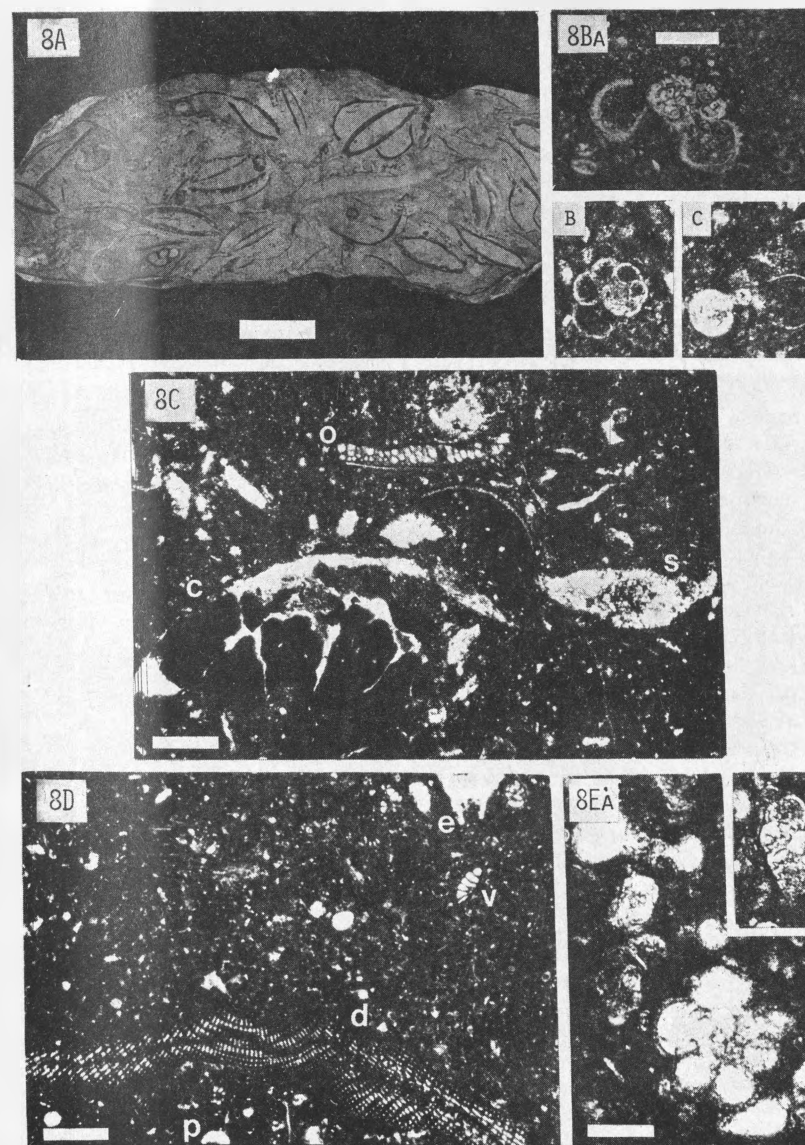
- 7A — Sample XI-59, laminated mudstone grading upward into heavily bioturbated mudstone. Laminations bear celestite. Polished slab; 1.0 cm bar for scale.
- 7B — Sample XI-57, ostracod-bearing finely-crystalline dolomite, typical of penecontemporaneous dolomite in unit 17. Note that the scale is the same as Plate 2E. Thin section, plain light; 0.15 mm bar for scale.
- 7C — Lime wackestone of lithoclasts and high-spired gastropods. Allochems are oncolithically coated and bored. Sample X-33, polished slab; 1.0 cm bar for scale.
- 7D — Miliolid-bearing spicular lime wackestone typical of unit 4. Sample X-2.5, thin section, plain light; 0.5 mm bar for scale.
- 7E — Polished slab of sample X-2.5 illustrating bifurcating tubular fenestrae; 1.0 cm bar for scale.

REPRESENTATIVE LITHOLOGIC TEXTURES OF UNIT 4 AND THE LIME
MUDSTONE AND LAMINATED LIME MUDSTONE LITHOFACIES

P L A T E 8

FAUNA AND LITHOLOGIC TEXTURES OF THE PLANKTONIC FORAMINIFER-BEARING NODULAR MOLLUSK LIME WACKESTONE LITHOFACIES AND PLANKTONIC FORAMINIFER LIME MUDSTONE LITHOFACIES

- 8A — Mollusk lime wackestone of pelecypods and gastropods collected from the nodular beds directly below the marl zone shown in Plate 14C. Section XI; 2.0 cm bar for scale, polished slab.
- 8B — Planktonic foraminifers in sample XI-33, unit 15. Note that the matrix is rich in calcispheres. Thin section; 0.15 mm bar for scale (a, b, and c).
- 8C — Lime wackestone of highly mixed fossil fragments; (o) oyster, (c) solitary coral, (s) solenoporacean algae. The matrix is rich in planktonic foraminifers. Sample X-12, unit 7; thin section; 1.0 mm bar for scale.
- 8D — Lime wackestone with a matrix of "micropellets", *Dicyclina schlumbergeri* (d), echinoid fragments (e), and *Valvulamina* (v). Sample VI-6, unit 20; thin section; 1.0 mm bar for scale.
- 8E — Planktonic foraminifer-bearing lime mudstone, sample X-11, unit 6. Both biserial and globigerinid planktonic forms are present. Thin section; 0.1 mm bar for scale. (Note the difference in size between these planktonics and those in unit 15, Plate 8B).

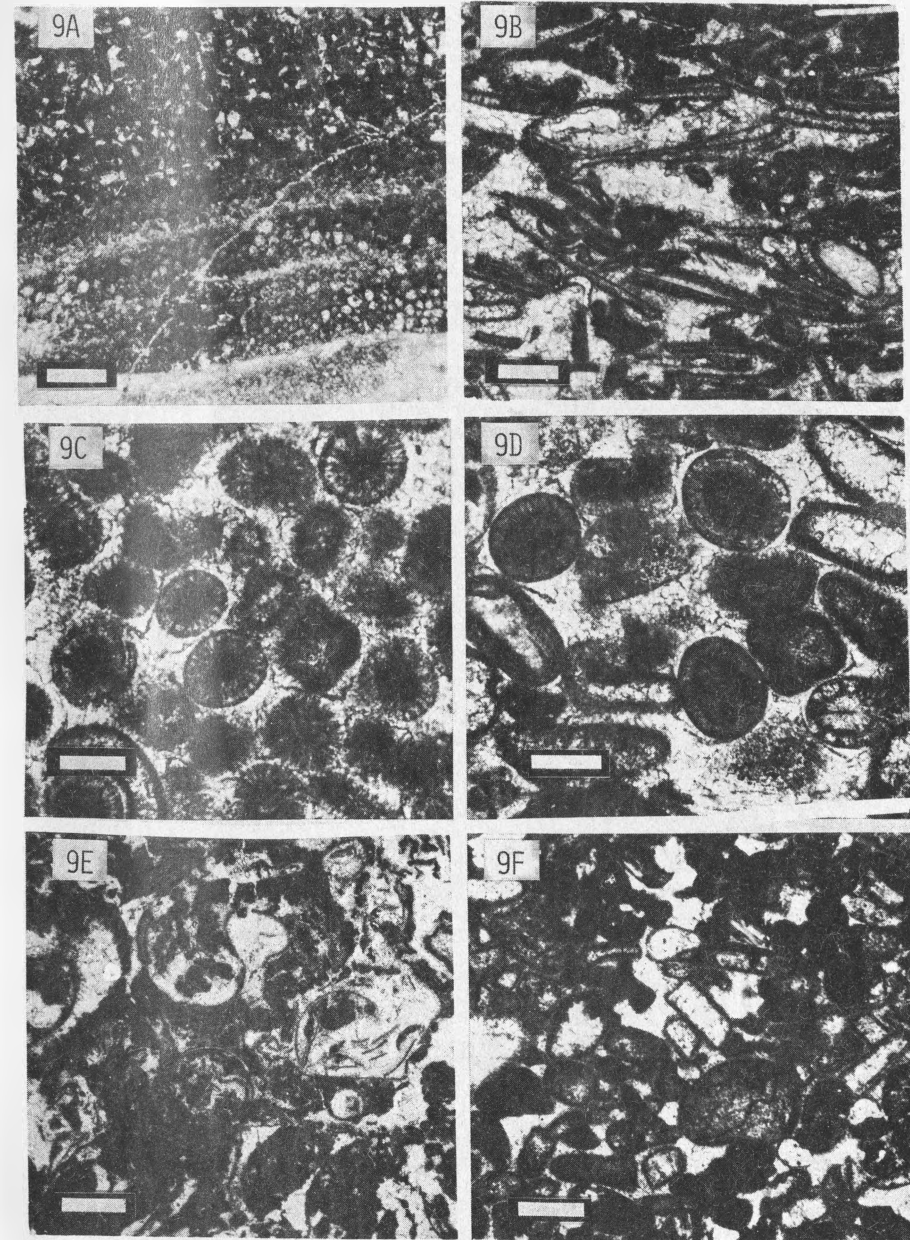


FAUNA AND LITHOLOGIC TEXTURES OF THE PLANKTONIC FORAMINIFER-BEARING NODULAR MOLLUSK LIME WACKESTONE LITHOFACIES AND PLANKTONIC FORAMINIFER LIME MUDSTONE LITHOFACIES

P L A T E 9

TEXTURAL FEATURES IN THE WORN SKELETAL FRAGMENT, OOID LIME
GRAINSTONE LITHOFACIES

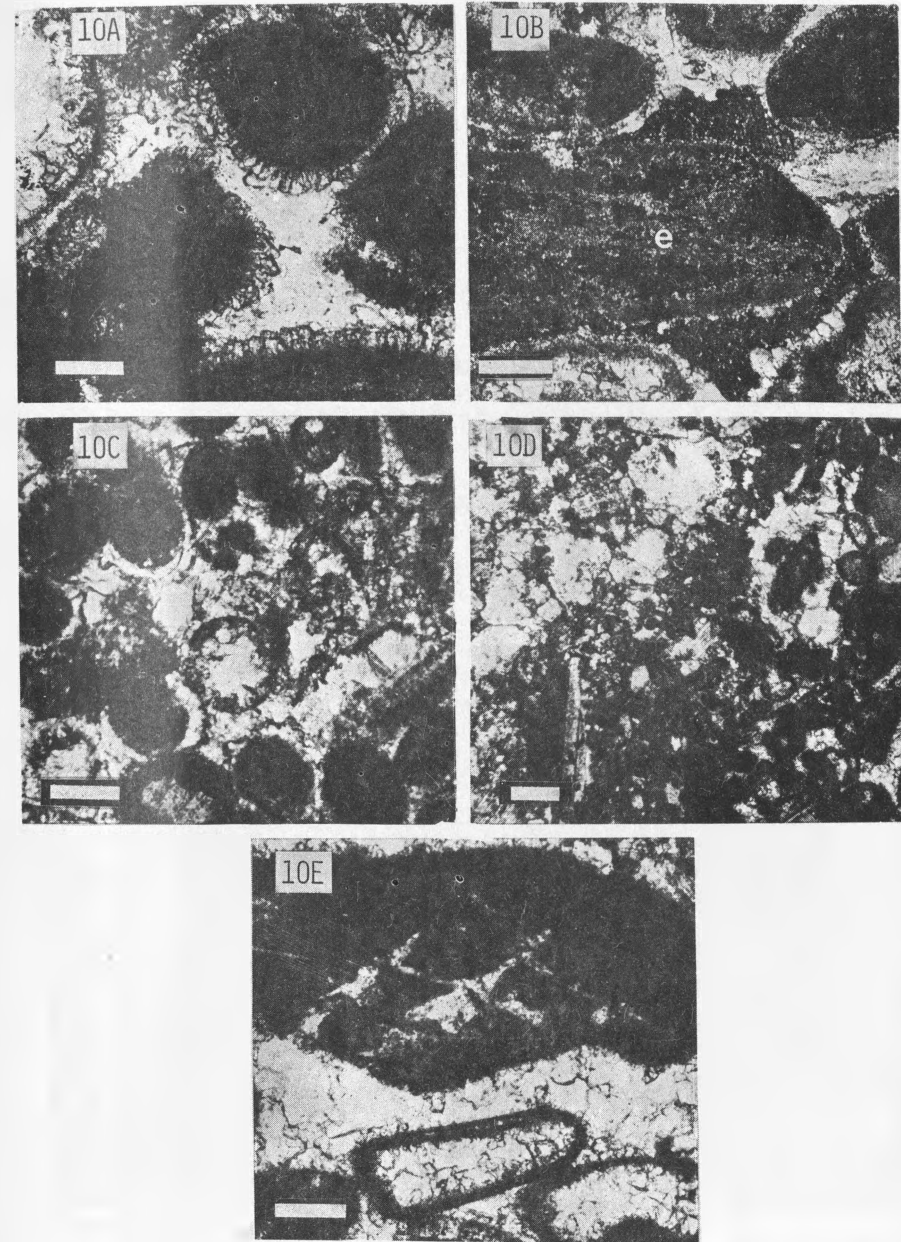
- 9A — Sample XI-43, unit 16, worn skeletal fragment lime packstone. The sample typically has a bimodal texture of fine worn skeletal fragments and large unabraded mollusk fragments, in this case a bored oyster. Thin section, plane light; 0.5 mm bar for scale.
- 9B — Sample XI-46, unit 16, worn skeletal fragment grainstone. Thin section, plain light; 0.5 mm bar for scale.
- 9C — Ooid lime grainstone, sample XI-50, unit 16. Ooids are typically small, lack concentric laminations and have a radial structure. Thin section, plane light; 0.15 mm bar for scale.
- 9D — Ooid lime grainstone, sample X-17, unit 8. Thin section, plane light; 0.15 mm bar for scale.
- 9E — Laminated gastropod lime grainstone-packstone, sample XI-52, unit 16. Gastropods are heavily micritized and coated by blue-green algae. Thin section, plane light; 1.0 mm bar for scale.
- 9F — Sample X-22, unit 8, worn skeletal fragment lime grainstone. Dark grains are completely micritized skeletal grains. Other mollusk grains are replaced by coarsely-crystalline calcite with a well developed micrite envelope.

TEXTURAL FEATURES IN THE WORN SKELETAL FRAGMENT, OOID LIME
GRAINSTONE LITHOFACIES

P L A T E 10

CEMENTATION FABRICS AND DIAGENETIC FEATURES PRIMARILY IN THE
WORN SKELETAL FRAGMENT, OOID LIME GRAINSTONE LITHOFACIES

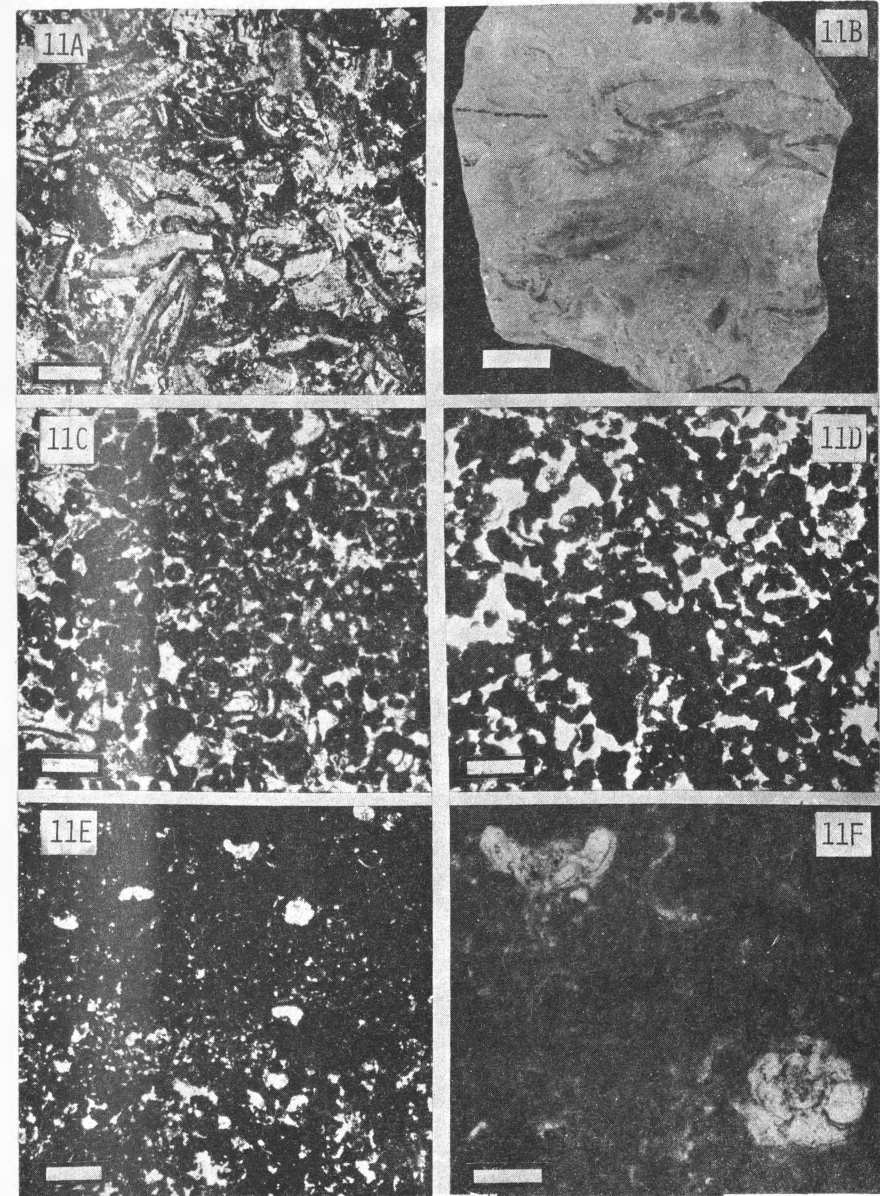
- 10A — Isopachus blocky rim cements with remaining pore space occluded by coarsely-crystalline calcite. Sample X-22; thin section; 0.15 mm bar for scale.
- 10B — Syntaxial rim cement surrounding an echinoid fragment(e). Note the very thin primary rim cements around the peloids possibly indicating very early exposure to phreatic meteoric waters. Sample X-17; thin section; 0.15 mm bar for scale.
- 10C — Partial dissolution and replacement of the ooids by medium and coarsely-crystalline calcite. Sample XI-50; thin section; 0.15 mm bar for scale.
- 10D — Total dissolution of and recrystallization of a grainstone fabric by coarsely-crystalline calcite. Sample X-18; thin section; 0.5 mm bar for scale.
- 10E — Extensive micritization of a radiolitid rudist fragment. Intense phreatic meteoric diagenesis indicated by medium to coarsely-crystalline calcite replacing mollusk fragments and occluding pore space. Enfacial junctions are absent. Sample X-17; thin section; 0.15 mm bar for scale.

CEMENTATION FABRICS AND DIAGENETIC FEATURES PRIMARILY IN THE
WORN SKELETAL FRAGMENT, OOID LIME GRAINSTONE LITHOFACIES

P L A T E 11

TEXTURAL FEATURES AND FAUNA REPRESENTATIVE OF THE RADIOLITID
LIME WACKESTONE AND PACKSTONE, AND PELLET-INTRA-CLAST LIME
PACKSTONE LITHOFACIES

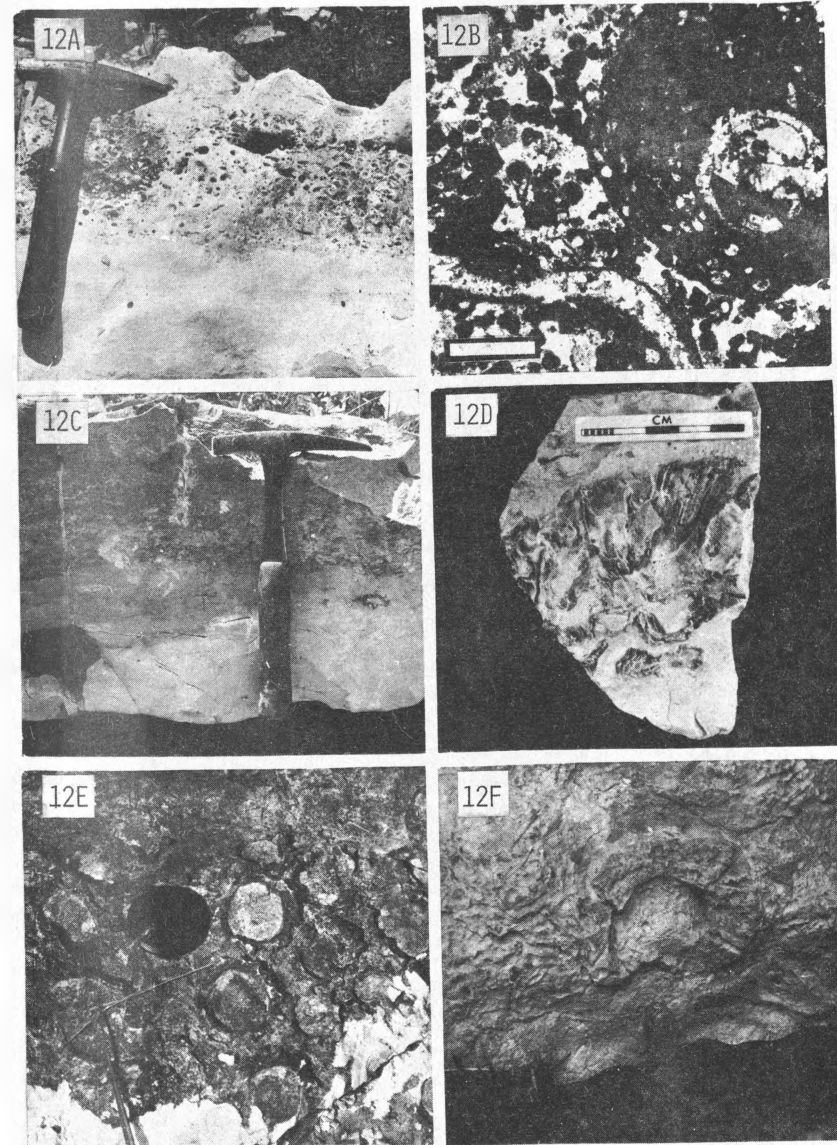
- 11A — Sample XI-91, a radiolitid rudist fragment lime packstone representing the basal lag of a storm deposit. The sample shows infiltrating mud shelter structures and ellipsoidal pellets (upper right) which indicate post depositional bioturbation. The rudist fragments are "over packed" with grain penetration from burial pressure solution. Thin section; 1.0 mm bar for scale.
- 11B — Whole radiolitid lime packstone. Grain supported fabric is also indicated by extensive compaction. Sample XI-126, polished slab; 1.0 cm bar for scale.
- 11C — Sample XI-191, a pellet-intraclast grainstone. The sample represents a fining upward sequence in a storm deposit with a basal lag of radiolitid rudist fragments. Thin section; 0.5 mm bar for scale.
- 11D — Sample XI-205, an intraclast grainstone. Thin section; 0.5 mm bar for scale.
- 11E — Sample XI-73, a planktonic foraminifer-bearing pellet lime wackestone. The sample grades into grainstone (not pictured). Thin section; 0.5 mm bar for scale.
- 11F — Detail of planktonic foraminifers in sample XI-73. These foraminifers occur throughout strata interpreted as open lagoonal deposits. Note the squashed pellets (grumeleuse structure in the matrix). Thin section; 0.5 mm bar for scale.

TEXTURAL FEATURES AND FAUNA REPRESENTATIVE OF THE RADIOLITID
LIME WACKESTONE AND PACKSTONE, AND PELLET-INTRA-CLAST LIME
PACKSTONE LITHOFACIES

P L A T E 1 2

SURFACE EXPOSURES OF STORM DEPOSITS AND RADIOLITID THICKETS
AND CLUSTERS CHARACTERISTIC OF THE LAGOONAL ENVIRONMENT AND
RADIOLITID LIME WACKESTONE AND PACKSTONE AND
PELLET-INTRACLAST LIME PACKSTONE LITHOFACIES

- 12A — Thin bed of oncolithically-coated gastropod lime grainstone (see Plate 11B for detail). Bed is characteristic of a storm deposit; note the sharp lower contact and fining upward sequence which is overlain by whole radiolitid rudists not in growth position. Float block along section XI. Hammer for scale.
- 12B — Oncolithically-coated gastropod grainstone, sample XI-90B. Thin section; crossed nichols; 1.0 mm bar for scale.
- 12C — Thin bed of radiolitid fragment lime packstone characteristic of storm deposits. Float block, section XI. Hammer for scale.
- 12D — Cluster of whole radiolitids in growth position; sample XI-60.
- 12E — Thicket of larger radiolitids in growth position characteristic of the upper 15 m of the Sierra Madre or "Caliza Sin Nombre", section VI; camera lens cap for scale.
- 12F — Large radiolitid rudist no longer in growth position. Large radiolitids in overlying and underlying beds are in growth position. Laterally equivalent beds to 12E, section VI. Pocket knife for scale.

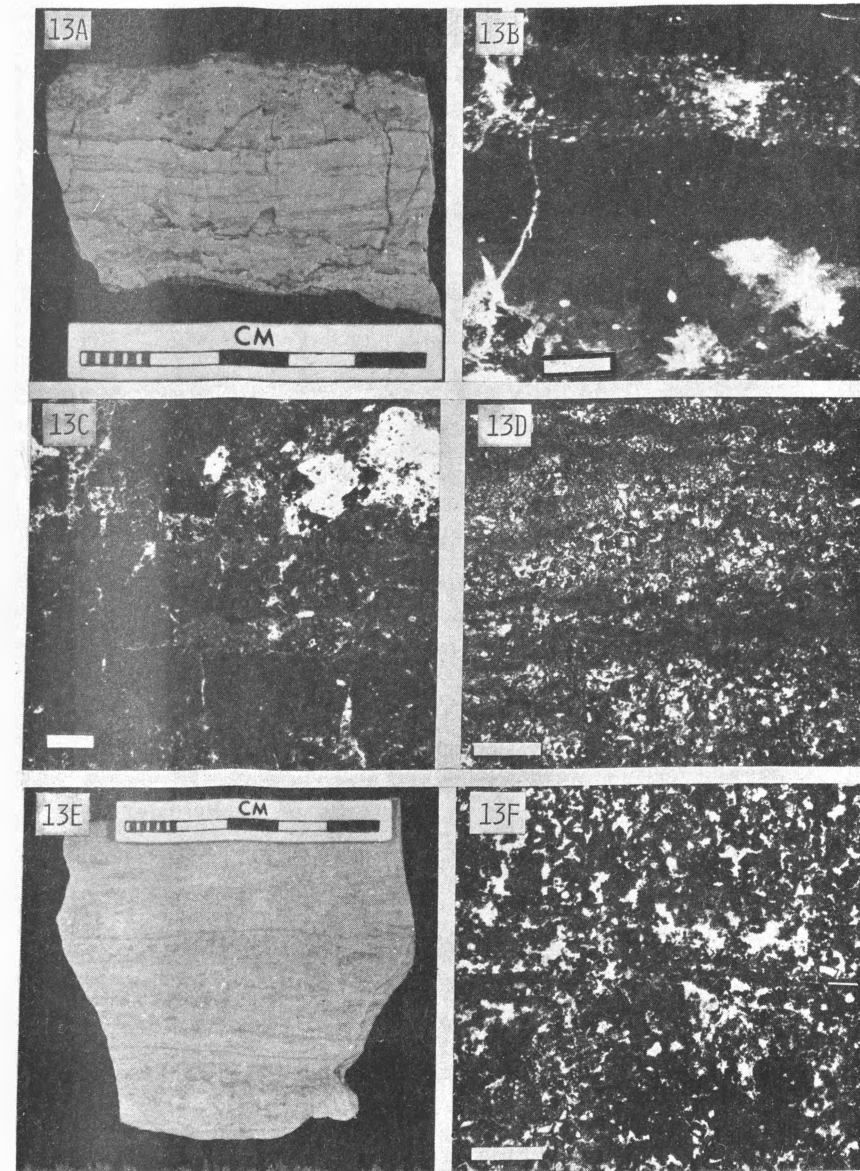


SURFACE EXPOSURES OF STORM DEPOSITS AND RADIOLITID THICKETS
AND CLUSTERS CHARACTERISTIC OF THE LAGOONAL ENVIRONMENT AND
RADIOLITID LIME WACKESTONE AND PACKSTONE AND
PELLET-INTRACLAST LIME PACKSTONE LITHOFACIES

P L A T E 13

ALGAL STROMATOLITES AND ASSOCIATED SUPRATIDAL EARLY DIAGENETIC FEATURES IN THE RADIOLITID LIME WACKESTONE AND PACKSTONE AND PELLET-INTRACLAST LIME PACKSTONE LITHOFACIES

- 13A — Thinly laminated lime mudstone with gypsum pseudomorphs (see detail Plate 11B). Note the discontinuity surfaces overlying and underlying the thin laminations and the desiccation cracks. Sample X-80, representative of the supratidal environment in a sequence of strata interpreted as lagoonal deposits.
- 13B — Selenite gypsum crystallites now replaced by calcite. Detail of the darker laminations in 13A. Sample X-80; thin section; 1.0 mm bar for scale.
- 13C — Celestite or original gypsum from a thinly laminated lime mudstone with early diagenetic desiccation fractures. Sample XI-194; thin section; crossed nichols; 0.5 mm bar for scale.
- 13D — Regular thin lamination in an intertidal stromatolite. Sample X-68; thin section; 1.0 mm scale.
- 13E — Irregular thin laminations of sediment bound by mucilagenous blue-green algae separated by thicker laminations of pellet-intraclast lime packstone to grainstone. Characteristic of lower intertidal and subtidal stromatolites. Sample X-43; polished slab.
- 13F — Detail of a single algal bound lamination (white bar). Note that the lamination spans pores with fining upward sediment perched on the lamination. Sample XI-141; thin section; 1.0 mm bar for scale.

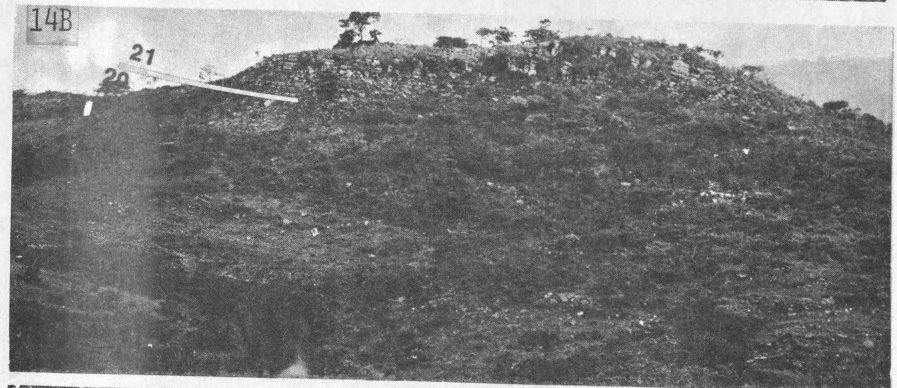
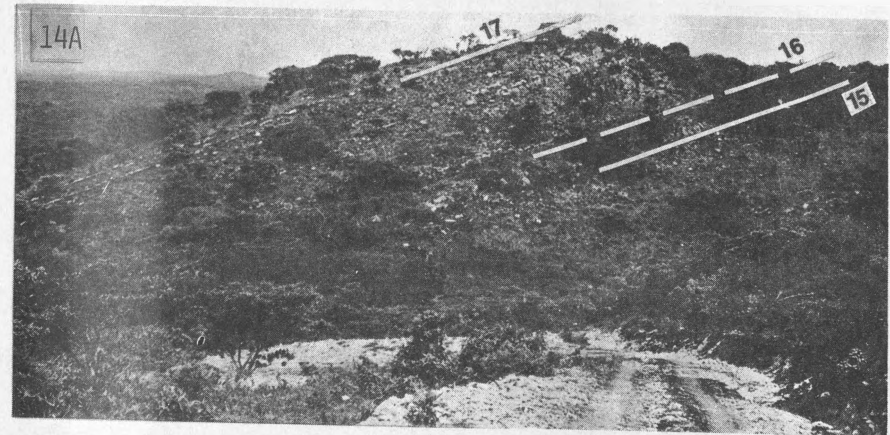


ALGAL STROMATOLITES AND ASSOCIATED SUPRATIDAL EARLY DIAGENETIC FEATURES IN THE RADIOLITID LIME WACKESTONE AND PACKSTONE AND PELLET-INTRACLAST LIME PACKSTONE LITHOFACIES

P L A T E 14

FIELD EXPOSURES OF SECTIONS XI AND VI

- 14A — Field exposures on the north limb of the anticline at sections XI and XIII where units 15, 16, and 17 are well exposed. Unit 15, the nodular mollusk lime wackestone and marl is well exposed on the road and forms the featureless valley; the basal skeletal fragment lime packstone of unit 16 forms the ledge above unit 15; the ooid lime grainstones form the slope where they are capped by unit 17; the thinly laminated — dolomitic lime mudstones of unit 17 form the dip slope of the north flank of the anticline.
- 14B — Field exposures of section VI where unit 20, planktonic foraminifer-bearing, nodular, *Dicyclina* lime wackestone, is capped by unit 21, thick-bedded whole radiolitid lime wackestone.
- 14C — Detail of a marl zone at section XI, Plate 15A. Note the nodularity of the lime wackestone overlying and underlying the marl. Hammer for scale.
- 14D — Detail of the transitional contact between units 20 and 21, section VI, Plate 15A. Hammer for scale.



FIELD EXPOSURES OF SECTIONS XI AND VI

P L A T E 15

FIELD EXPOSURES AND DEPOSITIONAL TEXTURES OF UNIT 21 IN SECTION X AND UNIT 19 IN SECTION XI

- 15A — Stromatoporoid at the base of unit 21, associated with open lagoonal or ramp deposits. Thin section; 1.0 mm bar for scale.
- 15B — Lime wackestone of pellets and *Cuneolina* sp. (a benthonic foraminifer). The association of *Cuneolina*, grumeleuse texture, planktonic foraminifers and echinoderm fragments (present but not pictured) is common in the strata interpreted as open lagoonal deposits. Sample X 86; thin section; 0.5 mm bar for scale.
- 15C — Field exposures along the logging road at section XI. Large float blocks afford glimpses of the bedding and lithology and are not removed far from their original position.
- 15D — Lime grainstone of intraclast and heavily micritized miliolids. Note the siderite spherulites (s) with pseudo uniaxial cross. Sample XI-229 is typical of the thin bedded grainstones in unit 19. Thin section, crossed nichols; 0.5 mm bar for scale.
- 15E — In place bedding of large gastropod lime wackestones to packstones. Note the heavy karst dissolution and low structural dip; near the axis of a broad syncline at section XI. Sample XI-206 was collected from these beds. Hammer for scale (in the shadows, left center).
- 15F — Large gastropod lime wackestone uniquely characteristic of unit 19. Gastropods are *Trochacteon*? Float block, camera lens cap for scale.



FIELD EXPOSURES AND DEPOSITIONAL TEXTURES OF UNIT 21 IN SECTION X AND UNIT 19 IN SECTION XI